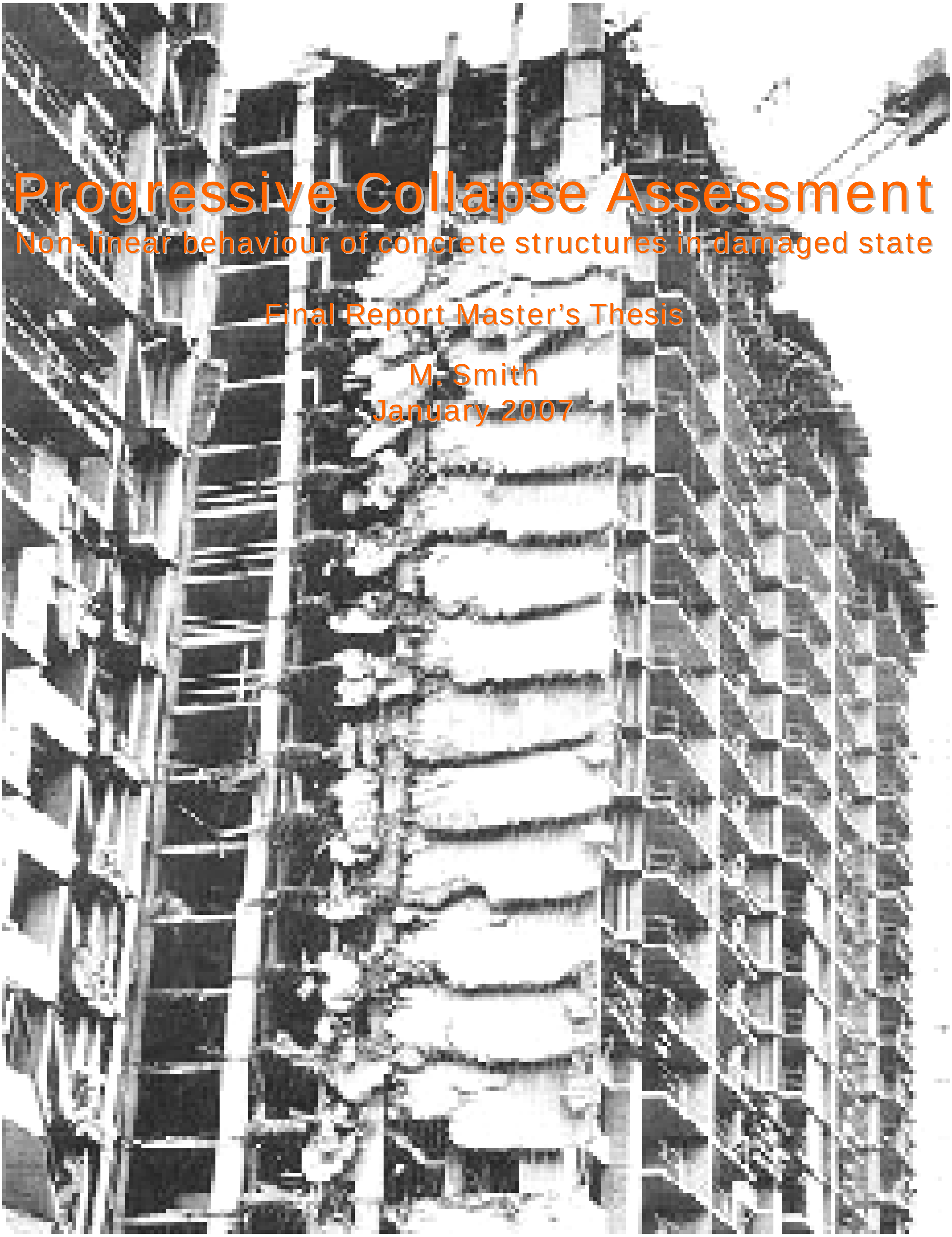

Progressive Collapse Assessment

Non-linear behaviour of concrete structures in damaged state

Final Report Master's Thesis

M. Smith

January 2007

ARCADIS
Infrastructure, environment, buildings

TU Delft
Delft University of Technology

Picture on cover:
Progressive Collapse at the Skyline Plaza,
Fairfax County, Virginia, 1973

Progressive Collapse Assessment

Non-linear behaviour of concrete structures in damaged state

Final Report Master's Thesis

Meint Smith
studentnumber: 1041215
email: meintsmith@hotmail.com

January 26th, 2007

Delft University of Technology
Faculty of Civil Engineering
and Geosciences
Department of Structural
and Building Engineering

Graduation Committee:
Prof. dipl. ing. J.N.J.A.Vambersky
Ir. J.L. Coenders
Ir. A.M. de Roo (ARCADIS)
Prof. ir. A.C.W.M. Vrouwenvelder
Ir. J.W. Welleman

STATUS: FINAL

TU Delft
Delft University of Technology

ARCADIS
Infrastructure, environment, buildings

Preface

This thesis is the final report in my Master's project on Progressive Collapse Assessment of reinforced concrete structures. The thesis comes under the Structural Design Lab, an educational and research body which deals with subjects of innovative structures, the relating (structural) design process and related technologies. It is part of the Structural and Building Engineering Department of Delft University of Technology, faculty of Civil Engineering and Geosciences.

The graduation project is conducted at ARCADIS The Netherlands, at the structural engineering section of the department Buildings and Real Estate in The Hague. This company offered me a place of work and support for which I am thankful.

This final report combines all previous progress reports to one Master's thesis and also replaces these reports. The subject of the graduation project is progressive collapse of building structures and focus is on the structural behaviour of concrete structures in damaged state.

I would like to thank ir. André de Roo at ARCADIS for making it possible to conduct my graduation project at his office. Furthermore I would like to thank ir. Jeroen Coenders at the Structural Design Lab for coming up with the subject and his support. Moreover I would like to express my gratitude to prof. dipl. ing. J.N.J.A. Vambersky, prof. ir. A.C.W.M. Vrouwenvelder and ir. J.W. Welleman for supervising and assessing my graduation project in coöperation with the previous mentioned persons.

Special thanks is owed to dr. ir. Björn Angström for providing me with his PhD thesis on ductility of tie connections in precast structures and dr. ir. Pierre Hoogenboom for standing in for mr. Welleman when he was ill.

Last but opposite to least I would like to thank my wife Tineke for her support and her indefatigable effort to kick me out of bed in the morning.

The Hague, December 2006

Meint Smith

Contents

Abstract

Progressive collapse is a collapse where local failure leads to a disproportionate collapse. Due to a focus on ease of erection in the construction process and more and more optimisation of design through advanced analysis techniques buildings are believed to have become more vulnerable to loads outside the design envelope over the past decades and are thus more vulnerable to progressive collapse.

When a building is subjected to local failure the load resisting behaviour is quite different than the behaviour considered in conventional linear elastic design. To design a building resistant to progressive collapse in a cost efficient and aesthetically attractive way consideration of these non-linear effects is required.

The purpose of this research is to investigate structural non-linear behaviour of building structures and develop design rules or strategies to economically design building structures resistant to progressive collapse. Focus is on RC structures in static loading conditions.

In order to do this first the progressive collapse phenomenon itself was considered. Three design approaches were distinguished: the event control approach aimed at improving the level of protection of a building, the specific local resistance approach aimed at increasing the hardness of a building and the alternate load path approach which aims at improving the robustness of building. The latter approach has been elaborated.

Alternate load paths can be developed roughly in four manners. By arch action, suspension action, Vierendeel action and catenary action. Ductility of the structure and its connections is important to enable these alternate load paths. For arch and catenary action special detailing of structural ties is needed, especially catenary action depends highly on the elongation capacity of these ties.

When Vierendeel action occurs, redistribution of internal moments is an important effect. This effect relies highly on the ductility of the RC structure.

To assess the effect of non-linear effects numerical determination of limit loads was performed for a case study. Three non-linear effects creating an overcapacity compared to linear assessment were distinguished in the case study: strain hardening of the reinforcement steel, moment redistribution and occurrence of torsional moments in hollow core slabs.

The magnitude of these effects depends on the actual reinforcement lay-out

and the structural geometry. For three investigated cases of column removal the non-linear overcapacity was in the order of magnitude of 1.8.

With this overcapacity factor a linear procedure of notional element removal was performed for the entire building. Each column was removed one by one, one at a time and the effects were assessed.

It was concluded that via this approach the design of the studied building can be adjusted adequately and economically to enhance the robustness. The right detailing if of primary importance in enhancement of robustness.

Chapter 1

Introduction

In this chapter the background of the research conducted is sketched and the research itself is outlined.

1.1 Background

Since the terrorist attacks at the Oklahoma Federal Building in 1995 and the World Trade Center in New York in 2001 the phenomenon of progressive collapse has had renewed public attention. The attention of structural engineers to this topic however, dates back to the world famous partial collapse of an apartment complex at Ronan Point, London, UK in 1968 when a gas explosion led to collapse of part of all 22 floors.

Although intuitively most people can imagine what is meant by the expression progressive collapse it seems hard to give a closed definition of this phenomenon. Progressive collapse involves initial local damage leading to a disproportionate collapse, but it is difficult to give a quantitative expression to the terms 'local' and 'disproportionate'.

When looked at progressive collapse from the viewpoint of a structural engineer, probability of progressive collapse can be reduced by designing a building in such a way that it is robust, where robustness is defined as a measure of the performance of a building in damaged state. However, robustness is equally difficult to measure as it is difficult to quantitatively express progressive collapse.

Furthermore robustness should be distinguished from collapse resistance. The probability of progressive collapse can be reduced by more means than just increasing robustness. Also the level of protection and the hardness of a building exert influence on the collapse resistance.

In 1976 it was estimated that approximately 15 to 20 percent of building collapses develop in a progressive manner [Leyendecker & Burnett, 1976]. It should be remarked that progressive collapse is a relatively rare event, also to date. This means that the experience base is also small.

1.2 Problem Analysis

It is widely assumed buildings have become more vulnerable to progressive collapse over the past decades. Two circumstances have contributed to the increased vulnerability of building structures to progressive collapse. First the development and refinement of analysis techniques made possible by the use of the computer and innovations in structural systems have enabled engineers to optimize designs to a greater extent. This has lead to designs with a smaller margin of safety because the structures have become lighter and more flexible making them more vulnerable to loads outside the design envelope.

Secondly designs over the past decades have become more and more focused on ease of erection which might lead to designs with less inherent continuity, also making them more vulnerable to abnormal loads.

Moreover, with the rise of terrorist threat and increasing development of high rise buildings causes of progressive collapse have a higher probability of occurrence and consequences are larger.

1.2.1 Current Situation in Design Practice

In the design practice of structural engineering, until recently not much attention was paid to progressive collapse and if progressive collapse was considered it was mainly considered in a late stage of the design. However in the past few years a growing concern for progressive collapse can be noticed. Current building codes also proof not to be very helpful, since the qualitative and general nature of statements addressing progressive collapse leads to a lot of discussion in engineering practice. Also in the field of building codes recent and future improvements can be seen, for example the approaching introduction of the Eurocode in Europe and introduction of Progressive Collapse Guidelines in the U.S.

Tools able to accurately assess the structural integrity of a building and analyze progressive collapse are complex and time consuming. A method to quantitatively and quickly compare design alternatives for the sensitivity to progressive collapse is currently not available.

One idea for a tool capable of giving an indication of the sensitivity of a building to progressive collapse is to combine a finite element calculation with stochastic variation of the initial failure. However, this tool needs to be developed, more refined and more thoroughly theoretically founded before it can be used in practice.

Especially the modeling of a progressive collapse or the determination of the limit load of structures in damaged state needs attention. When a structure is designed to remain stable in damaged state via conventional analysis method the structure is bound to be extremely over dimensioned. Therefore non-linear behaviour normally not considered in design is likely to be depended on for the stability and strength in damaged state. At present day however there is little experience in praxis with designing in such a way and there is no consensus of how to design a structure in damaged situation.

1.2.2 Problem Definition

To effectively and economically analyze and enhance designs on sensitivity to progressive collapse non-linear effects should be taken into account. To what extend these effects occur should be investigated.

1.2.3 Master's Project Aim

Investigate structural non-linear behaviour of building structures and develop design rules or strategies to economically design building structures resistant to progressive collapse.

1.2.4 Most Important Starting Points

- Focus will be on Reinforced Concrete (henceforth RC) structures.
- Only the static loading cases are considered.

1.3 Thesis Structure Overview

In the next chapter the phenomenon of progressive collapse is discussed. Historical cases, a definition and design approaches come up. In Chapter 3 focus is on the structural behaviour of building structures in damaged state. Chapter 4 is dedicated to advanced analysis of building structures which is needed to assess the behaviour in damaged state, and this is exemplified by a case study. In Chapter 5 the design approach known as the notional element removal method is elaborated. This design approach in combination with the findings of Chapter 4 is used to come up with design solutions for the case study in order to make this building more resistant to progressive collapse. The thesis is concluded with a summary of findings and recommendations on the subject brought forward in the thesis.

Chapter 2

Dealing with progressive collapse

In this chapter the phenomenon colloquially known as progressive collapse is discussed. A brief overview of historical cases commonly associated with progressive collapse is given and current design approaches are dealt with.

2.1 Historical Perspective to Progressive Collapse

A number of cases of collapse often associated with progressive collapse given in Figure 2.1 will be discussed in this section.

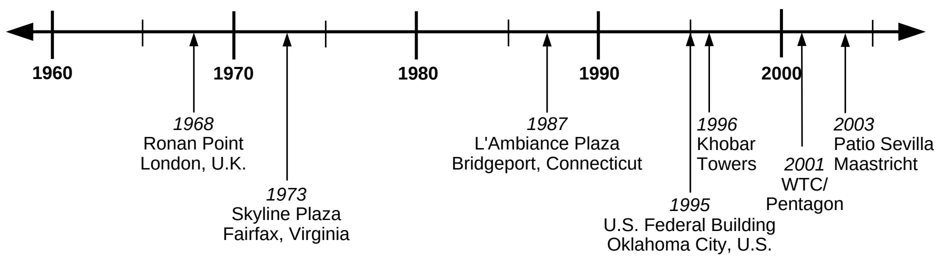

Figure 2.1: A time line of cases associated with progressive collapse.

The first widely known case of progressive collapse and a classical example is the Ronan Point disaster which took place in London in 1968. In this case a gas explosion blew out a concrete panel on the 18th floor. This caused the loss of support of the panels of the above floors. The debris loading from the upper floors eventually lead to successive collapse of all floors below. The 22 story high apartment complex was constructed completely out of pre-cast panels. Interesting about this case is that although poor workmanship is often referred to as one of the possible causes, an inquiry found no violation of building standards. After this disaster a lot of research and discussion about progressive collapse

Figure 2.2: Two similar cases of progressive collapse: Ronan Point (left) and Skyline Plaza (right).

Figure 2.3: Damage to the Alfred P. Murrah building in Oklahoma (left) and the Khobar Towers (right).

took place. Also a lot of changes in building standards in several countries are directly related to this event.

A very similar, but less well-known collapse occurred in 1973 at the Skyline Plaza in Fairfax County, Virginia. This building was still under construction. A premature removal of slab shoring on the 22th floor lead to progressive collapse of all floors above and below. Debris loading from this collapse also caused the progressive collapse of an entire parking garage under construction adjacent to the building. Pictures of both the Ronan Point building as Skyline Plaza just after the collapse are given in Figure 2.2.

In 1987 a collapse of a building under construction in Bridgeport, Connecticut, known as L'Ambiance Plaza occurred. This collapse is directly related to construction failures. The building was designed to be constructed using the 'lift slab system'. Though no consensus exists on what ultimately caused the collapse it is assumed a number of local failures eventually lead to a total collapse of the building.

In 1995 the Alfred P. Murrah Federal building in Oklahoma City was destroyed by a bomb. The explosion shattered one column and damaged two others. This lead to a collapse of approximately 50 percent of the total floor area of the building. See Figure 2.3. The nine story building was designed in the early 1970's. The structural system was an ordinary moment resistant frame of reinforced concrete and had a large transfer girder at the third floor. Research [Corley, 2002] showed that with relatively simple and cost efficient measures to provide a better general continuity and ductility of the structure the damage could have been reduced by about 50 percent.

An example that could be considered as a prevention of progressive collapse is the Khobar Towers bombing in Khobar, Saudi Arabia one year after the Oklahoma bombing. In this case damage was minimized because of restricted access to the building and concrete barriers between the bomb and the building. These measures are assumed to have prevented a total collapse. Figure 2.3 gives a clear view of the damaged building.

The world's attention was again brought to the subject of progressive collapse by the terrorist attacks on September 11th 2001. Two aircrafts were crashed into two towers of the World Trade Center in New York which lead to the total or partial collapse of 10 major buildings. Though it is sometimes discussed if this is an example of progressive collapse, since the towers remained stable for over an hour after the initiating event withstanding the initial load, this event did bring attention to the inherent weakness of buildings when exposed to unexpected or extreme loadings. Less well-known is that this event also showed a lot examples of buildings resistant to progressive collapse since a lot of neighboring buildings did not collapse although they suffered severe debris loadings. Also the attack on the Pentagon showed the progressive collapse resistance of this structure.

A recent case in The Netherlands showed again the potential hazard to progressive collapse. In 2003 four balconies of a newly completed housing project in Maastricht called Patio Sevilla collapsed. In this case the cause was a construction error at the base of the support of the lower balcony [VROM-Inspectie, 2003].

When investigating these historical cases two aspects are conspicuous. The first aspect is that the initiating events are various in nature and predictability. In the regarded cases the initiating events range from deliberate aggressive actions to accidental overloading to construction errors both in design and in execution.

The second aspect is that often progressive collapse is a matter of multiple causes leading to a total collapse. There is a chain of events leading to a collapse and it seems hard to determine exactly the nature and order of these events in hindsight. Often a dispute arises about the causes and if the expression progressive collapse is appropriate in the specific case. This is why the definition of progressive collapse should have some attention.

2.2 Definition of Progressive Collapse

Many different definitions of progressive collapse of building structures exist in different papers and standards. In Appendix A on page 79 some definitions from different authors are given. All definitions agree that progressive collapse of a building structure denotes a local failure or damage leading to a global collapse of the structure. In the U.K. the expression 'disproportionate collapse' is much used for the same phenomenon. This expression emphasizes the relation between the local initiating event and the global consequences and views the matter as the opposite of a proportionate collapse. The terms 'local', 'global' and '(dis)proportionate' are all relative. This is why discussion can arise on whether or not a case of collapse of a building structure or part of it should be categorized as a progressive collapse. The discussion above concerning the WTC Towers is an example, but also with respect to the collapse of the Oklahoma Federal building the presumed 'local' or 'global' cause is often discussed.

2.2.1 Chain of Events

Progressive collapse occurs when an initiating event leads to damage to part of the structure by which this part looses its load bearing capacity. As a consequence the loading pattern of the structure is changed leading to an overloading of other structural elements which are thereby also damaged. This process continues until the whole structure collapses or a greater part of it. Ellingwood [Ellingwood, 2002] has formulated a probabilistic approach to the chain of events leading to a progressive collapse (Equation 2.1). Because a progressive collapse consists of an initiating event, a local damage and structural collapse (Figure 2.4). The probability of progressive collapse is represented by a combination of the probability the initiating event or hazard occurs ($P[H_i]$), the probability of local damage given the initiating event ($P[D|H_i]$) and the probability of collapse given that initiating event and and local damage occur ($P[F|DH_i]$).

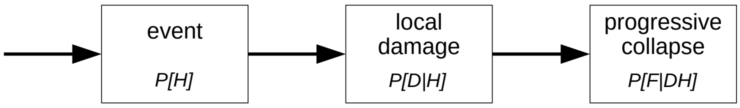

Figure 2.4: Elements of a progressive collapse and the probability of occurrence.

$$P(F) = \sum P[F|DH_i]\ P[D|H_i]\ P[H_i] \tag{2.1}$$

To gain insight in how a progressive collapse 'works' a flow chart of the process involved can be drawn. A flow chart provided by the U.S. public buildings service administration is displayed in Figure 2.5. This flow chart presents the sequence of events leading to a collapse and shows how it can be determined whether or not a collapse is labeled progressive. According to this flow chart the damage should be out of proportion to the initial failure *and* a chain reaction of failure should have occurred in order to speak of a progressive collapse.

The collapse starts with a hazard or event which damages part of the structure. This event can be categorized in the following six categories: misuse, fire, accidental impact, error in construction or design, foundation failure and blast loading. The common feature of these events is that they result in abnormal loading or deformation or both and have a small probability of occurrence. Due to these loadings or deformations one or more members lose their load bearing capacity. Since in this thesis focus is on the collapse itself rather than the initiating event no further elaboration of these subjects will be made in this document.

The main question within the scope of this project is what happens if one or more members fail. A redistribution of loads is inevitable and this might lead to failure of other members. If so, the first requirement for progressive collapse is met because a chain reaction of failures is present. This chain reaction continues until either a total collapse has occurred, or the structure finds a new equilibrium.

The next question is if the ultimate damage is disproportionate to the cause. If this question is answered with consent too one speaks of a progressive collapse. In Chapter 3 further elaboration is made on what happens if one ore more structural members fail. The subject of disproportionate damage is treated in the next section.

2.2.2 Disproportionate Damage

Different views exist on if damage is disproportionate to the cause. The preliminary Eurocode [CEN, 2005a] for example recommends an admissible local

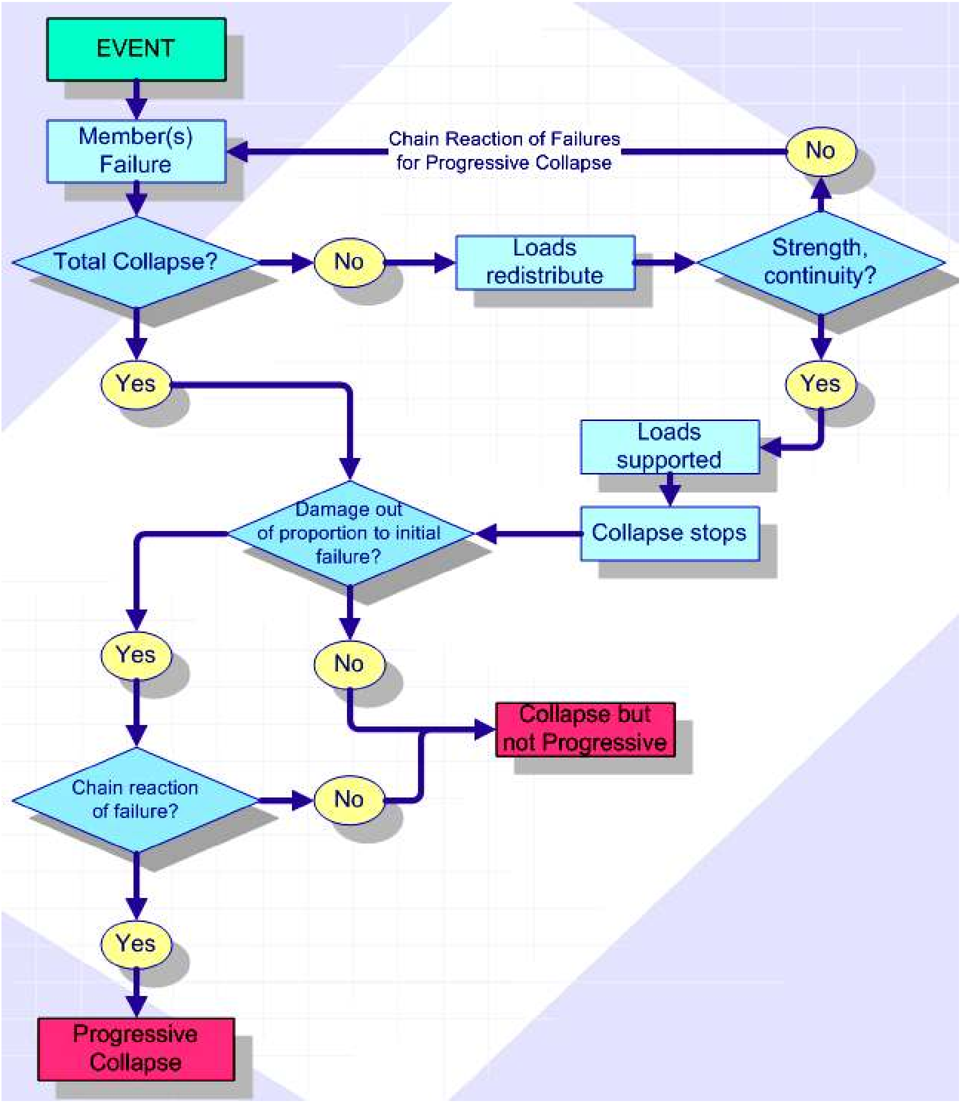

Figure 2.5: Events sequence of a progressive or non-progressive collapse. (source: http://www.oca.gsa.gov/PCA/images/eventsSequencecomp.jpg)

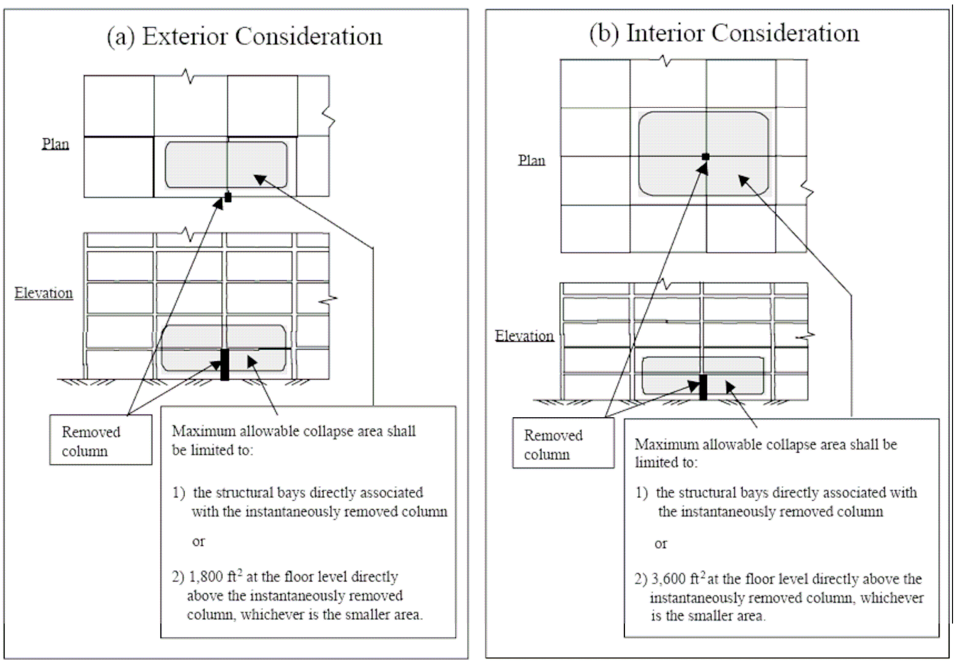

Figure 2.6: Maximum allowable collapse area provided by GSA guidelines. (source: [GSA, 2003])

failure upon removal of one load bearing element of 15% of the floor area with a maximum of 100 m^2 in each of two adjacent stories, but also states that this limit may be different for each type of building.

The UK building regulations [HMSO, 1991] have a similar approach only the maximum admissible damage is limited to 70 m^2.

In the American Unified Facilities Criteria issued by the Department of Defense [DoD, 2005] the British values are taken but a distinction is made between external and internal columns; in the latter case damage should be limited to twice the amount of damage of an external column; 30% of the floor area with a maximum of 140 m^2 whilst in the U.S. General Services Administration guidelines [GSA, 2003] the limit is set at the structural bays directly associated with

	floor area	**maximum**
Eurocode	15%	$100m^2$
UK Regulations	15%	$70m^2$
U.S. D.o.D.	$15-30\%$	$70-140m^2$
U.S. GSA	adjacent bays	$170-330m^2$
Canadian Regulations	adjacent elements	one bay

Table 2.1: Definition of disproportionate damage in various standards

the instantaneously removed vertical member in the floor directly above the removed vertical member with a maximum of 170 and 330 m^2 for a perimeter vertical member respectively an internal vertical member, see Figure 2.6.

The Canadian building regulations in a Commentary recommends limitation to the damaged element and one truss, beam or precast strip floor or roof panel on either side. As far as a cast in situ floor is concerned the damage should be limited to one bay of a full floor or roof slab. In Table 2.1 the definition of disproportionate damage in various standards is summarized.

2.3 Design Approaches to Progressive Collapse

The three elements of progressive collapse: (1) initiating event, (2) local damage and (3) structural collapse are the key to designing a structure resistant to progressive collapse. Three corresponding design approaches exist: (1) event control, (2) creating specific local resistance and (3) providing alternate load paths. Figure 2.7 depicts the chain of events leading to a progressive collapse and the corresponding design approaches.

It is important to distinguish collapse resistance from robustness. The collapse resistance of the structure is defined as a combination of the level of protection, the hardness and the robustness of the building. The collapse resistance can be enhanced by each of the three design approaches or a combination them. The level of protection of the building can be improved by event control and the hardness by creating specific local resistance. The robustness of the building is an indicator of the performance of a building in damaged state. By providing alternate load paths the robustness is of the building is enhanced.

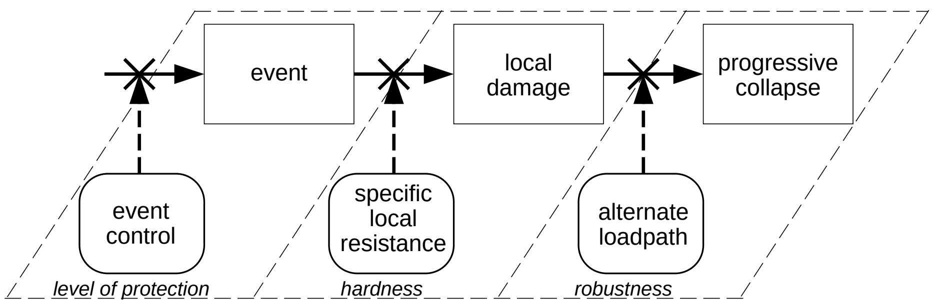

Figure 2.7: Design approaches to progressive collapse corresponding with the three aspects of collapse resistance.

2.3.1 Event Control

Event control is aimed at eliminating or reducing the probability of a hazard. In terms of Equation 2.1 the aim is to reduce the factor $P[H_i]$. Although event control can also be carried out by non design actions like intelligence gathering for example to prevent terrorist attacks or training and inspection to prevent design and construction errors there are some aspects of design of a building structure that can be considered. These aspects are usually related to building lay-out and accessibility. For example usage of deck parking instead of a parking garage under a building and positioning a building away from the main street are design measures sometimes taken to prevent car-bomb attacks. Also less rigorous measures like protecting exterior columns for vehicular collision by concrete ridges can be assigned to this category of design measures.

Event control can be the most rigorous and most effective solution for many hazards. In general event control is in addition very cost-efficient since small regulatory measures can have great diminishing effects on the probability of an event. However event control measures like restricted accessibility or collision prevention can have large social and aesthetical consequences.

2.3.2 Specific Local Resistance

Creating specific local resistance is aimed at reducing damage to key structural elements when an initiating event or abnormal loading occurs. In other words the factor $P[D|H_i]$ of Equation 2.1 is diminished. This approach addresses progressive collapse from the loading scenario point of view. Because this design approach explicitly provides strength to withstand a specific abnormal load, this approach is referred to as a direct design approach.

The advantage of this approach is that since it focuses on key parts of the structure one at a time, designing is less complicated than designing for an alternate load path and it is also relatively easily implemented in codes and standards, simply by prescribing the abnormal load for which an element has to be designed. The disadvantage of this approach is that it is hard to determine a threshold value for the abnormal load and prescribing a certain load at the same time provides information required to defeat the design. Furthermore it could be hard to design against specific abnormal loads in an economical manner, because requirements might be excessive. Although this can also apply for designing for an alternate load path in other cases.

2.3.3 Alternate Load Path

Designing a structure to develop alternate load paths when locally damaged addresses progressive collapse from the structural system point of view. The behaviour of the structure in a damaged state is considered. Related to this approach it is often noted that a structure should possess 'general structural integrity' or a certain level of 'robustness'. By creating alternate load paths the robustness of a structure is enhanced. In practice two ways to achieve development of alternate load paths are used.

Bridging

A direct design method which explicitly designs for alternate load paths consists of selecting an amount of damage and designing the structure to bridge over this damage. This method is also referred to as the notional element removal method. The idea behind this method is that since cases of damage are often not related to material failure or overloading, but to human errors or aggressive actions the safety of a construction is determined by factors outside the scope of conventional standards. With use of the notional element removal method consequences of local failure or damage can be investigated. This method is not necessarily meant to satisfy a specific threat scenario, but is often used to give an indication on a measurable level of robustness.

Tying

Another approach is providing general continuity and ductility throughout the structure by specifying minimum connection and tie forces. This is referred to as an indirect design method, since only minimum requirements with respect to strength and continuity are specified which implicitly creates boundary conditions for alternate load paths to develop when part of the structure is damaged. Note that both methods for developing alternate load paths can be interlinked because the minimum tie forces can be calculated using the notional element removal method. In Figure 2.8 required ties to ensure structural integrity of a precast concrete structure are depicted.

Often in literature the expression alternate path method is used with which only the bridging approach is indicated because this approach explicitly considers alternate load paths and the tying approach only provides minimum requirements which implicitly ensure presence of alternate load paths.

It must be noted that the system of mechanical ties does not only apply to concrete structures, but also to other structures. In steel structures for example the steel members and connections should be designed to be able to transfer the tensile forces, in this way these members act as mechanical ties. So in general, tie forces are the tensile capacities provided by the structural elements and connections and are intended to keep the columns vertical and to transfer loads from damaged portions of the structure to undamaged sections.

Designing a structure on tie forces especially puts a great demand on the design of connections. These connections should have a clearly defined beam-to-beam continuity across a column to be capable of transferring tensile loads as a column is damaged. Furthermore a connection should have a reliable inelastic rotational capacity.

There are some practical problems related to the design methods for developing alternate load paths. First of all it is hard to determine what amount of selected damage is appropriate and to what extent collapse should be tolerated if it should be tolerated at all. Also analysis of a structure in a damaged state

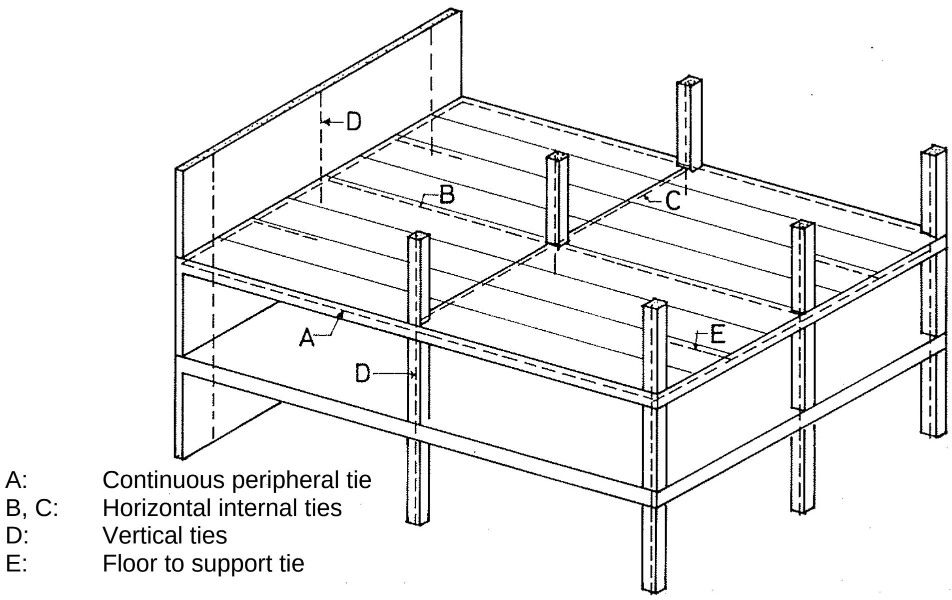

Figure 2.8: Ties (dashed lines) necessary to ensure structural integrity of a precast concrete structure. (source: [CUR, 1988])

is difficult due to dynamic aspects, plastic behaviour and debris loading. Furthermore it is difficult to implement requirements to general structural integrity or robustness in standards and codes.

Nevertheless the alternate load path approach is attractive, because in contrast to the specific local resistance approach it focuses on system behaviour instead of element behaviour and moreover the design method is threat independent. It can also in some cases prove to be more cost-efficient than the local resistance method.

2.4 Progressive Collapse Addressed in Standards and Codes

The statements concerning progressive collapse in many of the current standards evolved to the present state much influenced by the historical cases discussed in Section 2.1. Soon after the Ronan Point disaster many standards implemented some sort of statement to address the issue of progressive collapse. These statements are mostly of a general and qualitative nature and aimed at providing general structural integrity or robustness of buildings. According to Dusenberry [Dusenberry, 2002] this qualitative nature is partly due to the difficulty in defining progressive collapse and the numerous ways in which building robustness can be enhanced and partly due to the difficulty in defining for which conditions progressive collapse should be considered and how much damage a building may have under these conditions i.e. making a distinction between proportionate and disproportionate collapse. The qualitative nature leaves much room for interpretation and in practice leads to a lot of discussion.

Most building codes refer to the different design approaches as discussed above, but don't prescribe one of them exclusively. Since the need for provisions to prevent progressive collapse depends on the nature and dimensions of buildings, nowadays codes also tend to divide building structures into classes or categories or prescribe assessment of the level of threat of a building (eg. US Government Buildings). In the preliminary European code four consequence classes are distinguished with four corresponding recommended strategies to provide a building with an acceptable level of robustness [CEN, 2005b]. In the UK a building of five stories or more should be designed to prevent progressive collapse, but there are proposals to also apply a system of classes similar to the preliminary European code there.

Because codes generally fail to quantify the design goal for prevention of progressive collapse a lot of room is left for the interpretation of an individual engineer. In the Dutch practice for example application of the current codes repeatedly leads to discussion between designing and checking structural engineers [Stufib, 2005]. In this case the main point of the discussion is whether an alternate load path should always be present or specific local resistance could also be sufficient in some cases.

2.5 Conclusion: Reliability Based Approach

To avoid misunderstandings a distinction should be made between *robustness* and *collapse resistance*. In accordance with Starossek [Starossek, 2006] robustness is defined as insensitivity to local failure and collapse resistance as insensitivity to accidental circumstances. This means collapse resistance is a broader term which includes numerous conditions including the robustness of a structure. Robustness can also be seen as a measure of how a building structure performs in damaged state.

To again refer to Equation 2.1 the level of collapse resistance can be expressed by:

$$\sum P[F|DH_i]\ P[D|H_i]\ P[H_i]$$

whilst robustness is a property of the structure itself, regardless of the environment and possible causes of initial failures and its level can be expressed by:

$$P[F|DH_i]$$

disregarding the hazard or event initiating the collapse and its probability of occurrence $P[H_i]$ as well as the sensitivity of structural members to this event expressed by $P[D|H_i]$.

The notional element removal method can for example give a measure of robustness. The number and or size of elements that can be removed without a progressive collapse occurring could be an indicator on the level of robustness. When the notional element removal method is used, generally removal of one key element at a time is considered an indicator corresponding to an acceptable level of robustness.

Focusing merely on robustness could however limit the range of design possibilities to a great extent, possibly unnecessary because if a lower level of robustness is accepted still a high level of collapse resistance can be achieved by means of other measures such as providing a defended standoff distance or collision preventing obstacles or by providing local resistance.

Although it is obvious that the knowledge and skills of a structural engineer is capitalized on most if robustness is regarded, the other aspects of collapse resistance should not be ignored. Building codes should be aimed at creating an acceptable and uniform level of collapse resistance and therefore it should be possible for a designer to choose between the design approaches and combine them to achieve the required level of collapse resistance. The problem is that collapse resistance is hard to quantify and it seems harder to find consensus on the required level of collapse resistance than on the level of robustness.

Approaches to collapse resistance can be a more or less refined risk analysis using a fault tree, see for example [Siersma, 2006], but this leads to qualitative results and rapidly increasing complex analysis with the design progress. In a more performance based design approach focus can also be more on collapse resistance than merely robustness, for example by specifying for which scenario's a structure should be designed.

Building Codes are already designed to obtain a uniform level of safety in serviceability limit state and ultimate limit state. Generally the reliability is determined without explicit calculation of the probability of failure, by using partial safety factors. When collapse resistance is considered however, and a combination of different design approaches is required or preferred to obtain a sufficient level of safety, an explicit calculation of the global probability of failure is inevitable to be able to compare different design measures on basis of collapse resistance rather than just robustness.

On a more regional level there are already tools available which are able to perform a probabilistic analysis to determine the performance of an structural element taking uncertainties such as manufacturing tolerances, loads, material properties and boundary conditions into account. See for example in literature: [Cesare & Sues, 1999]. In reliability based analysis, uncertainties in numerical values are modeled as random variables with a certain probability distribution. A by-product of this reliability analysis are sensitivity factors which give an indication on which sources of uncertainty contribute most to the uncertainty in the predicted performance.

A quick building assessment tool for progressive collapse was proposed by Jeroen Coenders. For a more elaborate discussion of this tool [Coenders & Wagemans, 2005] is referred to. This analytical tool uses a probabilistic approach to the initial failure of elements of a structure and is able to give a crude indication of the sensitivity of a building to progressive collapse. The tool is basically an automated and probabilistic approach to the notional element removal design method.

The basic computational method of the tool is schematically depicted in Figure 2.9. The tool consists of two elements: a generator and a finite element analysis application. The generator uses the initial geometry of the structure and the chances of failure for each element of this structure to randomly create a 'damaged' structural geometry in which certain elements are missing based on their chances of failure. This randomly created geometry is analyzed by the finite element application.

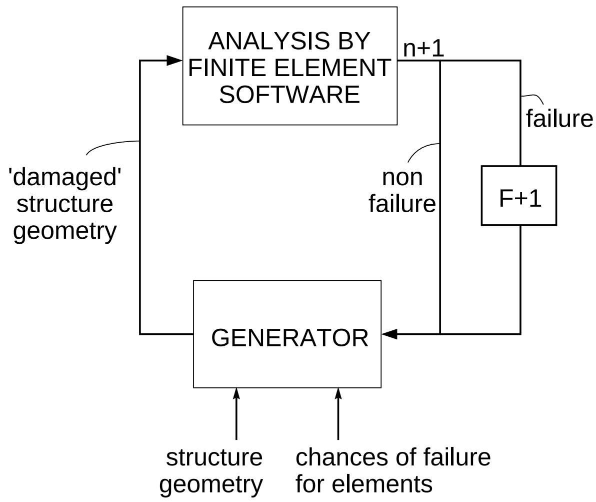

Figure 2.9: Schematical representation of the proposed tool for progressive collapse assessment.

The difficulty in applying this kind of reliability based analysis on a such a global level as in the collapse resistance of a building structure is that a large number of computational operations have to be performed, since not only are there a large number of uncertainties, but also the response of the structure itself is often highly complex and non-linear. This means the deterministic analysis which has to be performed many times to generate a probabilistic analysis is already very time consuming let alone the probabilistic analysis.

Furthermore there is no consensus on how the deterministic analysis should be performed and performing a thorough deterministic analysis is often complicated, because conventional methods for deterministic analysis will lead to extreme over dimensioning of structures if applied to structures in damaged state. Therefore the behaviour of structures in damaged state and the application of structural analysis on these structures is investigated in the next chapters. Focus will be on reinforced concrete structures although much information can be generalized to other structural configurations.

Chapter 3

Robustness and Ductility

Since in damaged state elements will be loaded differently than designed for and large deformations are allowed structural behaviour will be quite different than considered in original design. In this chapter structural behaviour of RC structures in damaged state is dealt with.

3.1 Failure Modes of Damaged Structures

For structural analysis concerning progressive collapse it is important to realize the analysis concerns the behaviour of a structure under abnormal loading conditions. In conventional structural analysis two limit states are distinguished: Ultimate Limit State and Serviceability Limit State. Focus is mainly on strength (ULS) and elastic deformation (SLS) of individual members. In an analysis under abnormal loading conditions and perhaps in damaged state larger plastic deformations can be accepted and focus is shifted toward stability, structural coherence and ductility. Furthermore if loads are redistributed structural elements will be loaded in different ways than they were designed for originally.

When adequate detailing is applied structural reserves can be mobilized. Main structural mechanisms to relie on for reserve capacity and finding alternate load paths are: walls acting as beams, vertical load bearing elements acting as suspension, Vierendeel action of moment-resisting frames and catenary or membrane action of floor systems.

3.1.1 Arch Action

Load bearing walls as well as non-structural slab elements can provide vertical resistance by acting as beams. For a corner wall a diagonal compression strut and a horizontal normal force at the top will develop as is depicted at the left side of Figure 3.1 and for a more central wall a compression arch and horizontal normal force at the base of this arch will develop as depicted at the right side of Figure 3.1. Special attention in these cases should be given to the development of tensile forces. These forces have to be absorbed by horizontal ties.

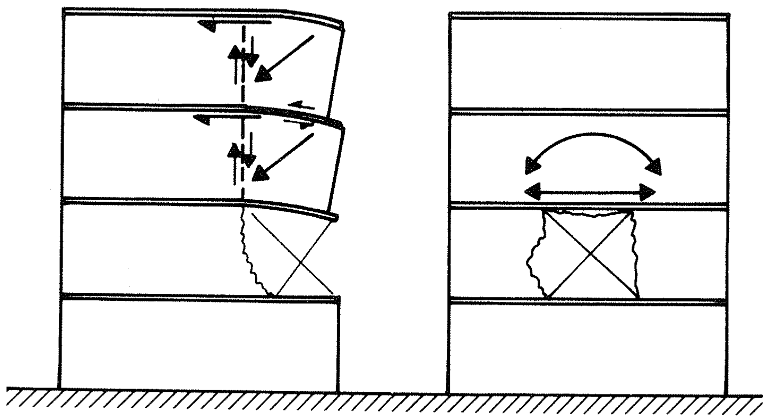

Figure 3.1: Walls acting as beams to bridge over failed elements.

When a wall acts as a beam it is important to know the span the wall has to bridge. The wall has to be able to transfer the resulting shear forces and normal forces as depicted in Figure 3.2. In guidelines see e.g. [ASCE, 2002] applying short returns on walls is recommended. This has two benefits. It gives the wall lateral support and because the wall is locally strengthened it is more likely that damage will be limited to the area between the returns if the wall is subjected to an extreme load. Tying the wall to the floor is also essential, because if this connection can transfer enough shear force, the resulting normal force can be absorbed by the ties in the floor edge.

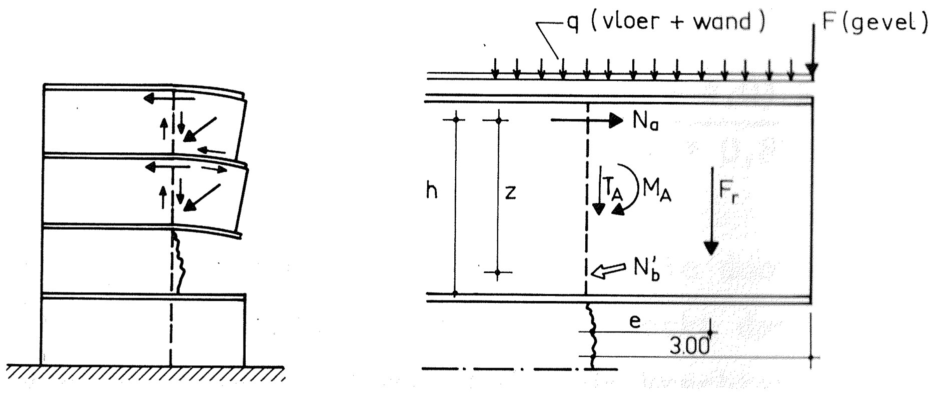

Figure 3.2: Internal forces occurring in a wall acting as cantilevering beam. (Source: [CUR, 1988])

3.1.2 Suspension Action

Suspension of vertical elements is primarily important if horizontal bracing is present at top floors or intermediate floors. This will often require an adaptation in the structural system with a possible effect on the usage programme. In Figure 3.3 for example diagonal bracings are added in the facade of the top floor. The needed reinforcement to withstand the tension forces will possibly already be present in form of the reinforcement in columns to prevent buckling. It is of utmost importance to provide adequate column-to-column and column-to-floor connections for an alternate load path to develop in this manner.

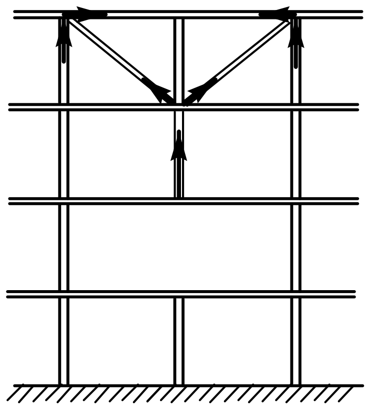

Figure 3.3: Loads of a missing column are redistributed by suspension action.

3.1.3 Vierendeel Action

In Figure 3.4 deformation of a frame in which vierendeel action has developed because of a missing column is illustrated. Vierendeel action can develop in moment resisting frames. It relies on 'conventional' behaviour (flexural resistance) of structures and does not have a major effect on the existing structural philosophy. Because in damaged state the bending moment at the failed vertical element is reversed it is essential to provide continuous bottom reinforcement in RC beams to be able to activate Vierendeel action. Also columns should have sufficient moment capacity, because columns normally only subjected to incidental moment forces will due to Vierendeel action be subjected to significant bending moments. It is important to make a non-linear structural assessment in case of Vierendeel action, because in such an assessment the redistribution of internal moment forces can be taken into account. Calculated internal forces using linear procedures will typically exceed the design capacity and will not give a reliable representation of actual occurring forces. The extend to which internal forces can be redistributed depends on the ductility of the structure. This is further elaborated on in Section 3.2.2.

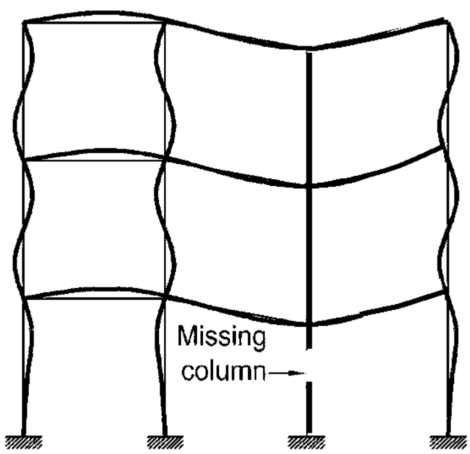

Figure 3.4: Vierendeel action in moment a resisting frame.

3.1.4 Catenary Action

When large deflections of the structure are made possible a transition from flexural resistance tot tensile catenary resistance can take place (Figure 3.5). Catenary action depends on geometrical non-linear behaviour of the structure. Catenary action can only be developed by proper detailing of connections. The connections should have a significant rotation capacity and also a relatively large elongation capacity is required. In case of catenary action of the floor slab or the supporting members the reserve axial capacity after large deformation is normative.

Also the distribution of stiffness is important in case of catenary action. The distribution of stiffness throughout the whole structure and especially between the damaged and the undamaged part of the structure should be assessed. If the structure as a whole is to ductile large deflections can be achieved without development of the required tensile forces to resist the load.

Apart from the distribution of the stiffness, the internal axial forces depend on the vertical deformation. In Figure 3.6 the relation between the deformation f and the tension force N_a is given for small deformation ($\cos\phi \cdot l \approx l$) and if moment capacity of the floor slab is neglected and rigid supports are assumed.

Especially in precast concrete structures catenary action can be an important if not the only way to bridge a damaged part in case of a double span condition. However as also illustrated in Section 3.2.1 it will require special detailing of tie connections.

To illustrate the deformations involved in catenary action and the demand it makes on detailing of the connections an example from Stufib study cell 2 [Stufib, 2005] is elaborated in Appendix B on page 81. Figure 3.7 illustrates the case. In a floor with span s in one direction and span L in the other direction, internal ties (marked with red) are present. When the interior column fails the

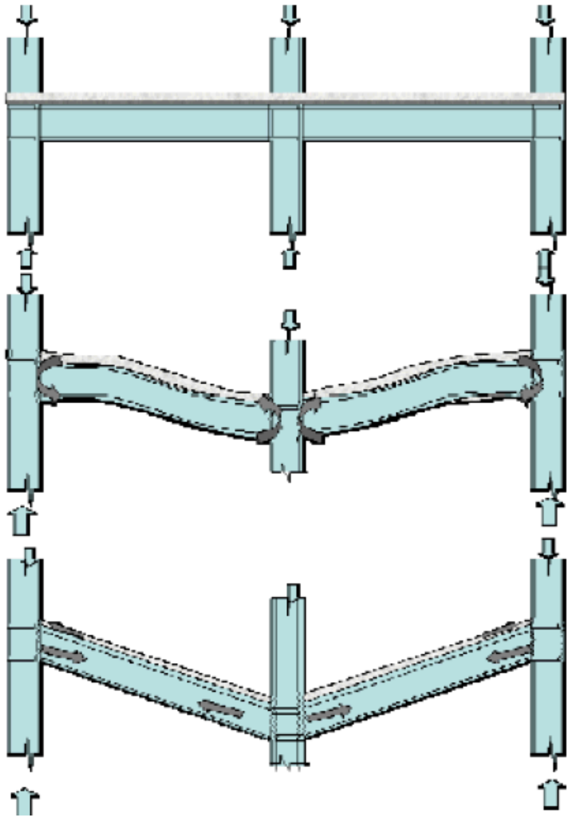

Figure 3.5: Transition from flexural response to catenary response for a steel frame. (source: [Hamburger & Whittaker, 2004])

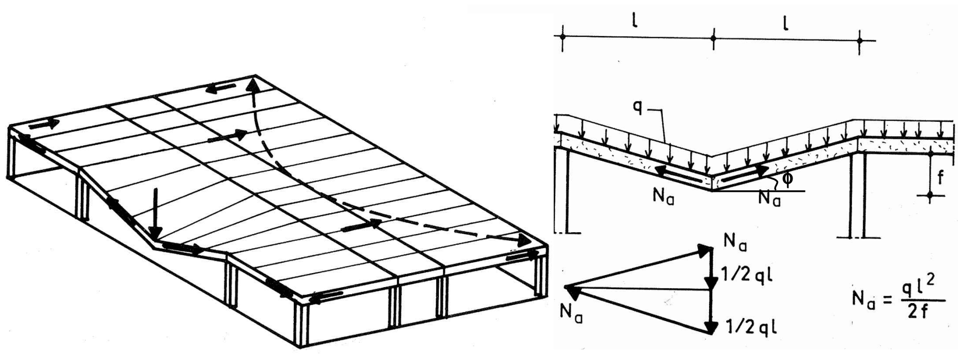

Figure 3.6: Catenary action of the floor slab. (Source: [CUR, 1988])

reaction force R from the floor load has to be absorbed by the internal ties. In the preliminary Eurocode prEN 1991-1-7 [CEN, 2005a] the minimum tensile force in internal ties is given as a fraction of the reaction force: $T_i = 0.8R$.

When the deflection δ is large enough equilibrium of forces can be found. According to the calculation in Appendix B equilibrium can be found if Equation 3.1 is satisfied:

$$\delta = \frac{sL}{1.6(s+L)} \tag{3.1}$$

This means if a column lay-out is present with a span s of 6.0 m in one direction and a span L of 7.2 m in the other direction equilibrium will be attained at a deflection δ of over 2.0 m. This means the internal tie has to lengthen with 340 mm (see Appendix B). Since this elongation will concentrate at the connections extremely ductile connections have to be applied.

As well as for connection details in precast structures as for continuous structures the behaviour is highly dependent on the ductility. Therefore it is appropriate to further study the ductility of RC structures.

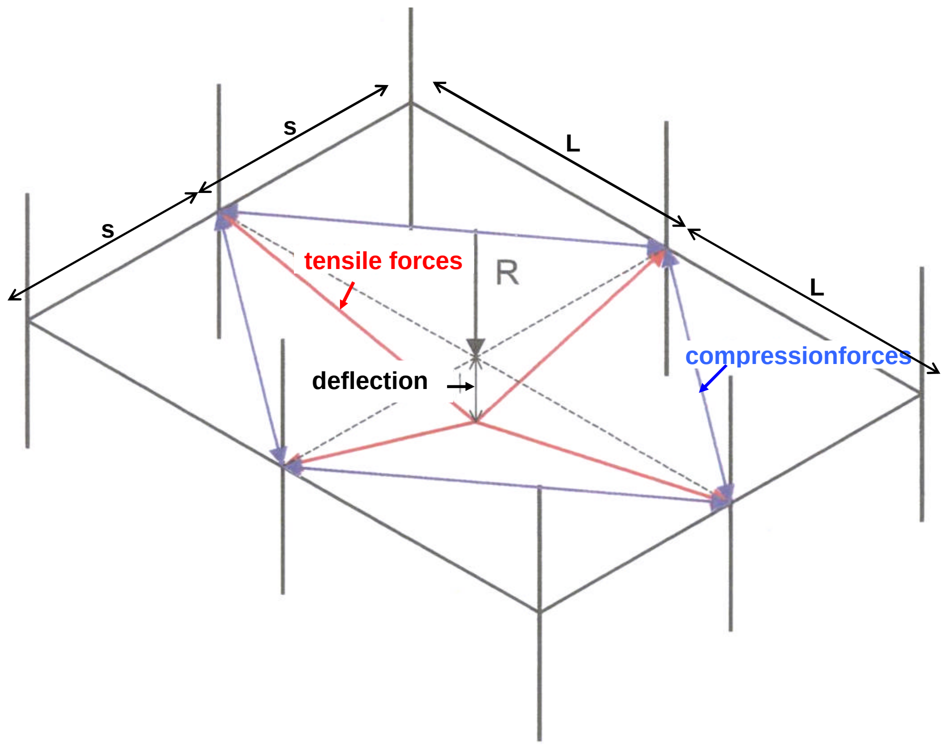

Figure 3.7: Schematical representation of forces if support of the central column is lost and the load is resisted in catenary mode. (source: [Stufib, 2005])

3.2 Ductility of RC Structures

When assessing non-linear behaviour of structures the ductility of a structure is very important. In order to attain a sufficient level of robustness it is important to make sure the structure has a sufficient level of ductility. A comparison can be made with earthquake resistant designing of structures. In literature concerning earthquake design eg. [Booth & Key, 2006] or [FEMA, 2000b] ductility is defined as the ability of a structure to withstand repeated cycles into the post-elastic range without significant loss of strength and without the development of instability and collapse. This can be quantified in terms of degree of plastic deformation.

Mathematically the ductility can be expressed as the ratio between the ultimate deformation and the deformation at yielding: $\mu = w_u/w_y$. As far as RC structures are concerned designing for ductility means brittle failure should be prevented. Hence proper detailing of joints has to be applied.

When investigating ductility of RC structures two essentially different joints have to be distinguished because the behaviour of these joints under large deformations is considerably different. On the one hand there are tie connections between precast elements which are designed to transfer tensile forces. In these connections the tensile force capacity of the tie is lower than the capacity of the members. These connections can be approached theoretically as a single crack case.

On the other hand connections designed for continuity are used in which the tensile capacity of the connection is in the same order as in the connected elements. As a consequence multiple cracks occur and a hinge region develops. In Figure 3.8 the behaviour of the different connections under a bending moment is depicted.

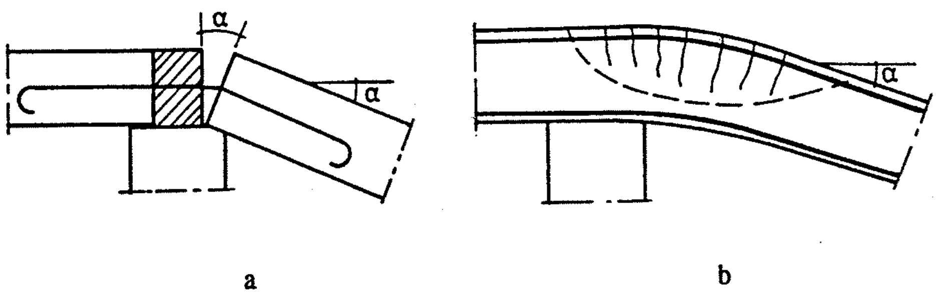

Figure 3.8: Tie connections (a) and continuous connections (b) in RC structures acting under a bending moment. (source: [Engström, 1992])

Extensive research on tie connections has been carried out by Björn Engström [Engström, 1992] who has conducted experiments with tie connections in hollow core floor elements and has presented a method for prediction of load-displacement characteristics of tie connections in the plastic stage. Agnieszka Bigaj [Bigaj, 1999] has conducted research on continuous connections. Her research focused on plastic hinging in RC members. Since ductile behaviour is important in progressive collapse situations to provide alternate load bearing systems, relevant information from both studies is presented in the next sections.

3.2.1 Ductility of Tie Connections – Engström

The experiments in the research of Engström focused mainly on tie connections in hollow core floor elements, but it was concluded that the results are also applicable for other tie connections. Two different configurations of connections were studied; ties anchored in the hollow core and ties anchored in the grout filled joint between floor elements. Also different types of tie bars where used; smooth and ribbed tie bars and ties consisting of prestressing strands.

Of special interest is how the non-linear load-displacement relationship of ductile tie connections can be predicted and which influence the detailing has on this relationship. Additionally dynamic effects during the transition stage are considered.

Load-Displacement Relations

From results from tests on idealized tie connections loaded in tension. consisting of ribbed or smooth tie bars with firm of slipping anchorage it was concluded that ductile behaviour with large plastic deformations can be achieved in two ways: by sufficient plastic elongation of the tie bar itself, or by controlled slip of the end anchors whilst the tie bar, in this case prestressing strand remains elastic.

Non ductile behaviour occurs if ribbed tie bars with high capacity are used. In this case critical stress concentrations are induced and ultimate failure is caused by splitting of the element.

Connections of both ribbed and smooth tie bars of mild steel have the same type of load-deformation characteristics as depicted in Figure 3.10. It can be divided in a stiff elastic stage, a plastic stage with load increase and an extensive failure stage with maximum and almost constant capacity. The elastic displacement is normally negligible in comparison with the ultimate displacement.

Bending tests on tie connections between hollow core elements showed a similar behaviour of tie connections as in the tensile tests where the tie bars were anchored until rupture (Figure 3.9) except for if the tie is positioned at the bottom of the element. In this case the bar tears out of the element. For smooth tie bars the ultimate displacement is considerably reduced in bending mode.

The ultimate displacement of the connection consists of the end slip of the tie bar and its elongation. By means of comparing the load-displacement relationships of the tie connections with the steel strain distribution of the

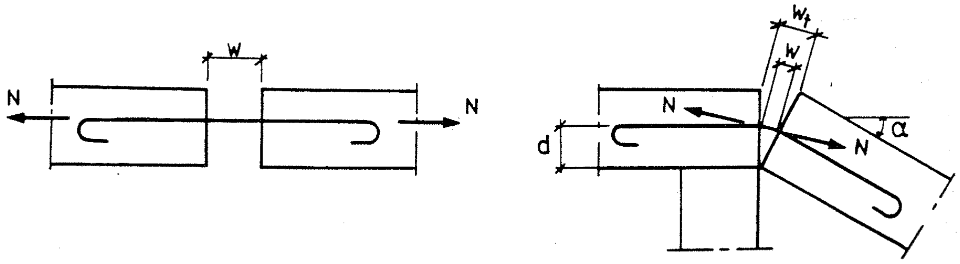

Figure 3.9: Definition of displacement w of tie connection in bending and in pure tension. (source: [Engström, 1992])

tie bar, the anchorage behaviour of the ties was studied. It proved that the yield penetration; extension of the plastic zone in the tie bar is an important parameter in the bond-slip relation. In the CEB-FIP Model Code 1990 the effect of yielding is not taken into account. Therefore the crack width is considerably underestimated if the bond-slip relation given in the CEB-FIP Model Code is used. A modified bond-slip relation is proposed.

Ribbed Bars

For ribbed bars the deformation capacity mainly depends on the dimension of the bar and the grout properties. In the case of ribbed bars the ultimate displacement was in the range of tens of millimeters.

Because for tie connections with ribbed tie bars of ductile types in Normal Strength Concrete (NSC) some parameters were almost the same for all the tests a schematic load-displacement relationship was established. Both a three linear as a more simplified bi-linear relationship was proposed. These are depicted in Figure 3.11. The bi-linear relationship can be used where large displacements are concerned. In this case the initial elastic deformations are neglected.

For ribbed bars the ultimate displacement mainly depends on the steel strain within the plastic zone. Formulas are proposed to estimate the ultimate displacement from the concrete compression strength and the steel characteristics of the tie bar. These formulas are presented in Appendix C.1.

Smooth Bars

For smooth bars the deformation capacity depends on strain capacity of the steel and the distance between the end hooks. This is because in the plastic stage bond is almost completely lost for smooth bars. In experiments an elongation capacity of over 200 mm was established by applying smooth bars.

Because smooth bars have the same type of load-displacement relationship the same schematic relationships as for ribbed bars (Fig. 3.11) are used. However the load transfer mechanism is very different. For smooth bars the maximum

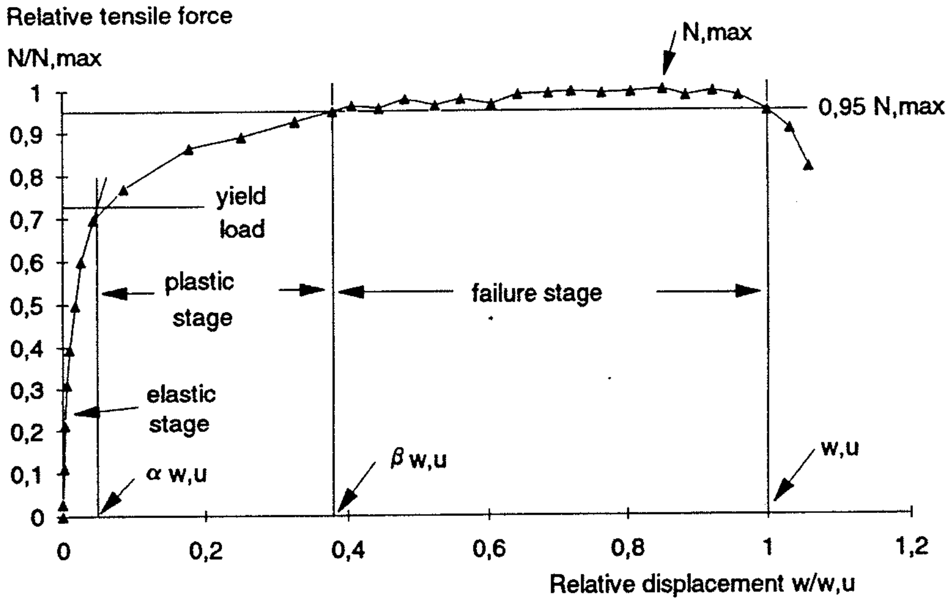

Figure 3.10: Typical load-displacement diagram for tie connections of mild steel (source: [Engström, 1992])

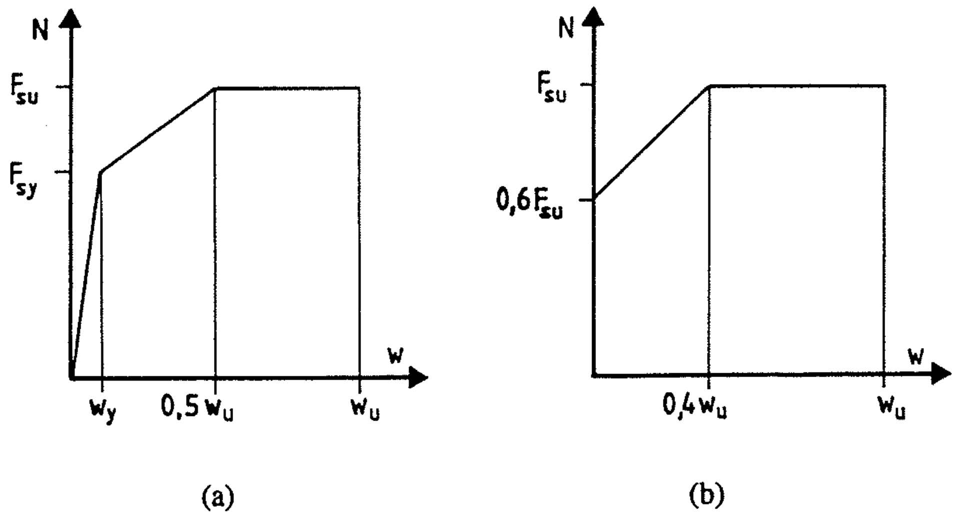

Figure 3.11: Schematic load-displacement relationship for tie connections with ribbed tie bars of ductile steel in NSC (a) tri-linear relationship (b) more simplified bi-linear relationship (source: [Engström, 1992])

bond stress is normally reached before yielding of the steel, whilst for ribbed tie bars the opposite is usually the case. Hence, in the plastic stage the tensile force is mainly resisted by the end hooks, although the frictional resistance can not be neglected. In Appendix C.2 a procedure for estimating the ultimate displacement of tie connections provided with smooth tie bars is given.

From tests it was proved that these equations give a good estimation for the ultimate displacement in tension, but for bending the deformability is considerably overestimated especially for large angles. Therefore a reduction of the ultimate displacement in bending with a factor 0.5 is is proposed, although it is admitted the effect of bending needs further concern.

Prestressing Strands

When the tie is made by a prestressing strand a different behaviour than for ribbed or smooth ties of mild steel is obtained. Because local bond strength is limited considerable displacements are achieved in the elastic stage. This behaviour is comparable to connections with intentionally slipping ties.

For ties from prestressing strands and wires only a qualitative description of the behaviour is presented because there were not enough tests and the results of the tests were not unambiguous. The main difference in behaviour from other ties is that in the elastic stage large slips up to 50 mm appear if the steel slips in a frictional mode. A bi-linear load-displacement relationship is proposed, in which the first break point should be determined by the bond strength level and the second break point by yielding of the steel. Further research is needed to specify these levels.

Detailing of Ties

Based on the research conducted, some recommendations on detailing of structural ties can be made. The aim of these recommendations is to secure that the full deformability of the ductile ties can be used.

Especially the anchorage should be subjected to certain concern to avoid brittle failure. The consistence and quality of the grout fill, the width of the joint, the placement of the tie bar in the fresh grout and the workmanship are important factors for the anchorage capacity. Sufficient transverse reinforcement or sufficient concrete cover should be applied to assure confinement. In addition the anchorage length has to be sufficient (Figure 3.12) to prevent pull-out failure due to the yield penetration in the plastic stage. For specific information on detailing FIP recommendations [FIP, 1988] are referred to. Smooth tie bars should always be provided with end anchorage and also for ribbed bars end hooks are recommended if anchoraged in (narrow) grout filled longitudinal joints to provide a reserve capacity in case of poor grout fill.

Also within a tie connections the elements providing the deformability should be designed in balance with the more brittle elements. This means for example that welds should have a certain overcapacity.

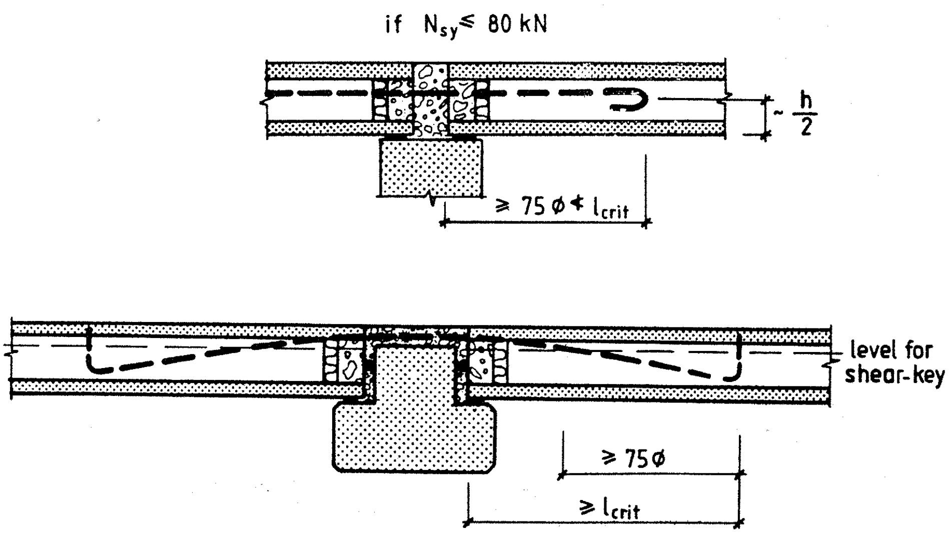

Figure 3.12: Example of additional requirements for anchorage of ribbed bars in narrow grouted joints

Alternate Load Path in Precast Structures

A separate chapter in Engströms thesis is dedicated to analysis of alternative bridging systems in precast structures. A simplified approach based on energy equilibrium is proposed. With this approach it is exemplified how behaviour and design of different tie connections influence the loading path and collapse mechanism of a structure.

The behaviour of the tie connections are expressed by two characteristics; the maximum tensile capacity N_{max} and the relative strain energy $\xi(w_{max})$. The relative strain energy represents the ductility capacity of a tie connection and can be used to predict the dynamic behaviour. It is found that the dynamic resistance for rotation systems with interacting tie connections and systems with catenary action depend directly on the elongation capacities of the tie connections.

Case Study on Catenary Action

To illustrate the results of the research of Engströms thesis the proposed procedure to calculate the ultimate displacement of tie connections for ribbed and smooth tie bars are applied to the catenary action example from Section 3.1.4 (Figure 3.6).

The elongation capacity of both ribbed and smooth tie bars with a diameter of 16 mm and an anchorage length of 1200 mm are calculated. Because in

Dutch practice precast elements often have a higher concrete quality the effect of a higher strength concrete (C 53/65) is also calculated. To assess the effect of more ductile steel, calculations have also been performed with characteristic values for steel quality FeB220. For both FeB500 and FeB220 a strain hardening of ca. 10% was assumed. Finally, because the characteristic steel values from the Dutch standard might be too conservative the elongation capacity of the tie connection is also calculated using steel characteristics derived from experimental research [Bigaj, 1999]. The material characteristics and results are given in Appendix C.3 and are summarized in Table 3.1.

Tie Configuration	**Ribbed Bars** w_u [mm]	**Smooth Bars** w_u [mm]
C 28/35; FeB500	5.2 - 7.4	14.7 - 26.1
C 53/65; FeB500	4.6 - 6.2	10.7 - 21.3
C 28/35; FeB220	3.0 - 4.7	11.3 - 20.3
C 28/35; FeB500 Bigaj*	10.6 - 18.7	55.1 - 81.5

**Experimentally obtained steel characteristics from [Bigaj, 1999]*

Table 3.1: Calculated elongation capacity w_u of ties ($\phi = 16$, $l_a = 1200$)

As can be seen from Table 3.1 the largest elongation is attained if using smooth tie bars, moderate strength concrete and very ductile steel. In common dutch situation where ribbed bars are used for tie connections and precast concrete elements of a higher concrete strength are used an elongation of approximately 5 mm can be attained according to these calculations. Additionally mostly in Dutch practice no end hooks are used and considerably smaller anchorage lengths. This means in practice the elongation capacity will be even lower and brittle behaviour can be expected.

It is also interesting to see what these results mean for the catenary action as in the example in Section 3.1.4. When in the situation of this example concrete quality C28/35 and ties consisting of ribbed bars ϕ 16 of steel quality FeB500 are used, the maximum deflection at the lost support is only 297 mm, which means a tensile force of 5,5 times the resultant force from the floor load will develop.

Even if the most ductile ties are used with an elongation capacity of 81,5 mm only a deflection of 993 mm will be possible, giving a tensile force of 1,7 times the resultant force from the floor load.

This means if the ties are designed according to the preliminary Eurocode, which prescribes a maximum tensile capacity of the ties of 0,8 times the resultant force from the floor load this structure will not reach a stable equilibrium due to catenary action.

Furthermore it should be noted that in catenary action the ties will be subject to combined horizontal and vertical loading. When only small concrete covering is present, as in hollow core slabs the ties till tend to tear out through the concrete cover because of the transverse forces. This is depicted in Figure 3.13. This could have a favorable effect on the tie elongation since elongation can take place at a greater length along the tie, but it also adds an extra demand on the anchorage length and strength of the ties.

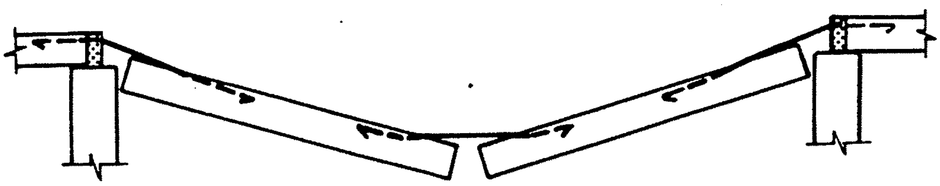

Figure 3.13: Catenary action in a precast floor with torn out ties due to transverse forces

Some experiments were conducted by Engström in which a floor element was pulled of the support (Figure 3.14) to assess ties under combined loading. From these experiments it was concluded that the ultimate elongation of the tie in combined horizontal and vertical loading is less than in pure tension, but due to local splitting as a consequence of the transverse forces overall ductile behaviour can be obtained.

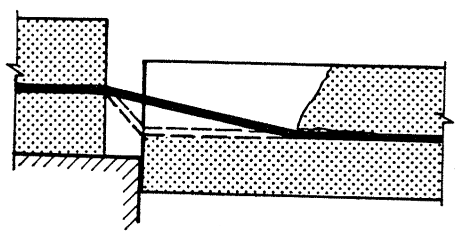

Figure 3.14: Tie subjected to combined vertical and horizontal loading. Splitting causes a new state of deformation

3.2.2 Plastic Hinges in RC Slabs and Beams – Bigaj

In a sense it could be stated that Bigaj picked up where Engström stopped. Bigaj took a more general approach to non linear behaviour of concrete. Where Engström focused on the single crack case of tie connections in precast structures Bigaj aims at a more general analysis of multiple crack case of plastic hinges in flexural RC beams and slabs.

Non-linear flexural behaviour of RC depends mainly on:

- The bond between the concrete and the reinforcement.
- The interaction of concrete between cracks.

- Shear transfer behaviour between cracks.
- Non-linear characteristics of concrete and the reinforcing steel itself.

The rotation capacity of RC elements is defined as the ratio of the rotation at ultimate load and the rotation at onset of reinforcement yielding. To be able to calculate the rotation capacity of RC elements research has been conducted with regard to cracking of concrete and the bond-slip relationship of reinforcing steel.

Cracking behaviour of Concrete

Two types of plastic hinges in RC are distinguished: flexural crack (FC) hinges and shear crack (SC) hinges. Which hinge develops depends on the magnitude of the shear force. Provided that the member has sufficient shear force capacity the SC-hinges exhibit significantly increased rotation capacity, because the hinge region is longer. This research focuses on FC-hinges which will give lower limit values for the ultimate rotation.

Another important distinction is that two essentially different crack patterns can occur in a three point bending test, being a symmetrical crack pattern with a large crack at mid-span providing a lower bound value of the rotation capacity and a crack pattern with dispersed cracking, without crack at the mid-span providing an upper bound value of the rotation capacity. The development of these different crack patterns depends on the micro-mechanic properties of the concrete. Since only a refined statistical analysis can model this behaviour both crack patterns are studied.

Failure localisation is included in the analysis using a fracture mechanics approach. The Fictitious Crack Model (FCM) is used to characterize the fracture of concrete in tension and the Compressive Damage Zone Model (CDZ) is adopted to describe the mechanical behaviour of concrete in compression. In Figure 3.15 the resulting stress-strain diagrams which are used in the calculation model are depicted. Strain localisation and concrete softening behaviour is thus included in the model.

For the cracking behaviour a model is developed to relate the crack spacing to the member geometry, the bond characteristics and the material strength. In this model the transfer length; the distance required to develop the cracking force in the concrete, is calculated using the bond-slip relationship from the bond model and the tensile strength and effective concrete area. Comparison with measured values show that this model is capable of accurately incorporating the member size influence on the crack development, the effect of bar diameter reduction and the effect of the concrete strength.

Bond-Slip of Reinforcement

Since in previous research on bond behaviour the mechanism of the steel-concrete interaction in the post yield regime remains not fully explained and the effect of the bar diameter is not sufficiently studied either an additional study has been performed to develop a general bond model for ribbed bars. This model takes into account the concrete quality, the bar contraction, the degree of confinement and the corresponding mode of bond failure.

From test results it is proved that the CEB-FIP Model Code 1990 formulation of bond stress-slip relation underestimates the bond stiffness for both Normal Strength Concrete (NSC) and High Strength Concrete (HSC) the modified relation proposed by Engström is much better (see Figure 3.16), but not applicable for HSC. The concrete confinement behaviour needs to be described better. A new bond model is proposed in which the confining capacity is analytically estimated taking into account the softening behaviour of concrete loaded in tension. In order to describe the resistance of the concrete cover against splitting a thick walled cylinder model is adopted. From comparison with experiments it is shown that the new bond model is capable of accurately predicting the stress-slip relationship for both NSC and HSC concrete and also to capture the bar diameter effects.

It is noted that is is important to use accurate steel characteristics if simulating phenomena where steel yielding may occur to conceive a reliable analysis.

Rotation Capacity of Plastic Hinges in RC

Based on the preceding components the rotation capacity of plastic hinges in RC can be calculated using a numerical procedure. First the crack spacing is determined, then the RC member is discretized in flexural crack elements. Using the stress-strain relationships for both concrete and reinforcing steel and the bond stress-slip relationship sectional forces at each crack are determined. Accordingly the distribution of strain within each flexural crack element is computed

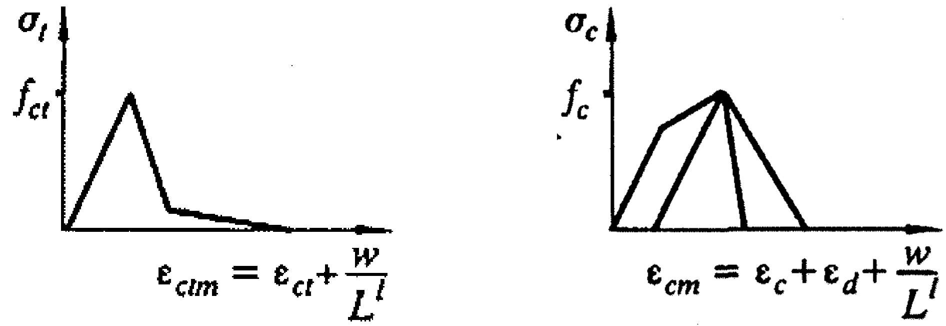

Figure 3.15: $\sigma - \epsilon$ diagrams used for concrete in tension (left) and concrete in compression (right) (source:[Bigaj, 1999])

and the rotations are obtained by an integration procedure.

After validation of the numerical procedure to calculate the rotation capacity, an extensive parameter study is performed to assess the influence of geometrical and material properties on the rotation capacity. This parameter study focuses only on NSC, because not enough information was available to validate the procedure for HSC.

Member size is proved to be influencing the deformation capacity. This is the case if the failure is initiated by concrete crushing as well as if the failure is initiated by steel rupture. Both the rotation at maximum load and the rotation capacity decrease with increasing member size, while the rotation at onset of reinforcement yielding is almost size independent. Especially for lower reinforcement ratios the size dependence is very much influenced by the detailing of the reinforcement and can even be superimposed in such a way that size dependence is nearly eliminated.

As far as the available ductility of plastic hinges is concerned it is concluded that steel properties are one of the key issues. The rotation capacity increases with increasing overall steel ductility. It is stressed that not only one characteristic steel property can be used, but a combination of steel properties should be considered. In this light a steel ductility parameter is introduced which is a slightly changed formulation of the equivalent steel concept introduced by other researchers. This steel parameter is proportional to the plastic rotation in cases where steel failure is prevailing. However it is considered premature to develop a standard formula that would directly provide the allowable rotation capacity from the steel parameter.

Since now the available rotation capacity of plastic hinges in RC beams can be calculated, the allowable degree of moment redistribution in a statically indeterminate RC beam can be calculated by means of evaluating the required and available rotation capacity. This is done for different steel types, reinforcement ratios and concrete strengths. It is concluded that existing codes overestimate the moment redistribution for some combinations of steel and concrete. A new proposal is presented for the allowable degree of moment redistribution for high ductile steel type S to low ductile steel B as a function of the design value of the relative depth of the compression zone. In Figure 3.17 the proposed redistribution is compared to the allowable redistribution according to VBC 1995.

3.3 Conclusion: Detailing for Ductility

From the behaviour examples in section 3.1 it is clear that in order to prevent progressive collapse, the structural system should have sufficient continuity and redundancy to provide alternate load paths.

To provide this a system of mechanical ties can be applied. The location of six different ties to ensure structural integrity of a precast concrete structure was given in Figure 2.8 (page 15), but it is noted that the tying approach can also

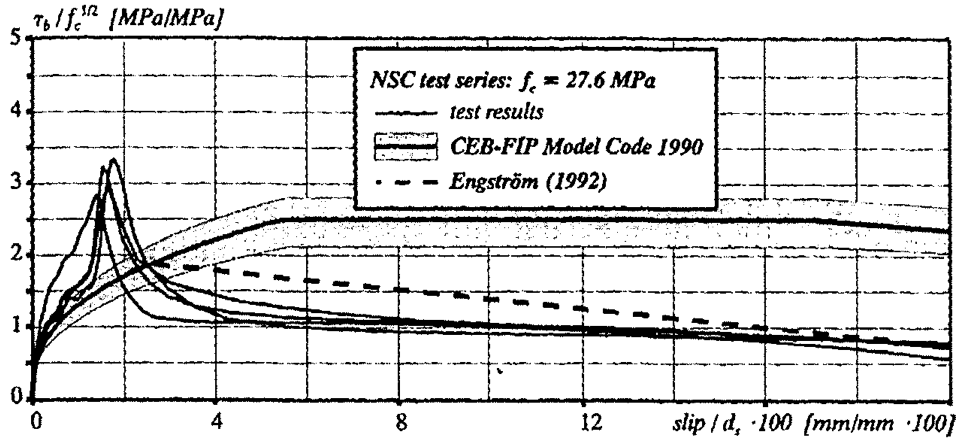

Figure 3.16: Bond stress-slip relationship for NSC (source:[Bigaj, 1999])

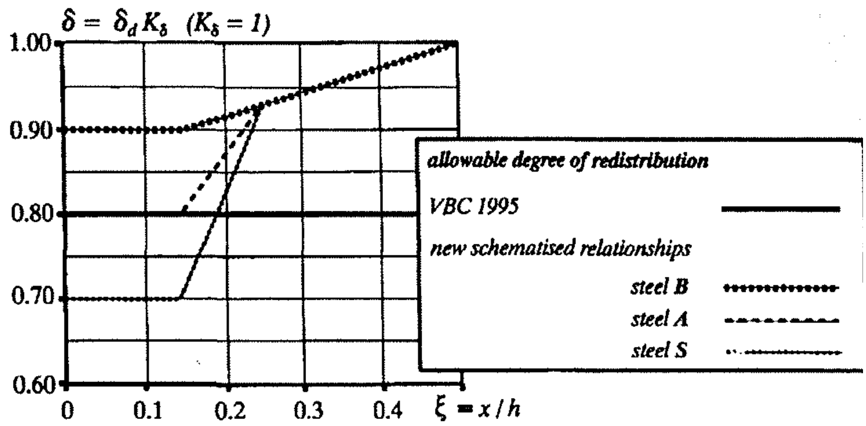

Figure 3.17: Proposed allowable degree of redistribution compared to VBC 1995 value. (source:[Bigaj, 1999])

be adopted in other structural configurations than a precast concrete structure.

When the structural behaviour is looked at, three out of the four failure modes depend highly on the presence of adequate ties. In RC structures not only the strength of the ties, but also the deformability of ties and the distribution of stiffness throughout the structure should be considered if designing a structure for robustness. A structure can be seen as a load transferring system with transferring elements. the elements providing the deformability should be designed in balance with the more brittle elements. If displacements are preferred at certain locations the corresponding links should be designed for ductility, while the other more brittle links are designed to balance the ultimate capacity of the ductile ones.

Because the mobilisation of reserve capacity depends highly on the tying system, tying systems must always be provided according to minimum requirements. However the possibility to concentrate ties to critical (alternate) load paths should be evaluated by means of analysis of appropriate collapse mechanisms in which the ductility of these ties is explicitly regarded. Therefore strength requirements for tying systems should always be accompanied by minimum deformation criteria. These deformation criteria can be met by adequate detailing.

Also if continuous connections in RC are considered ductility is a boundary condition for mobilisation of reserve capacity. Also in this case the ductility is in de detailing. In order to reach the full plastic deformation capacity high reinforcement ratio's should be avoided. Moreover, to superimpose negative member-size effects on the rotation capacity of RC elements the number of applied reinforcement bars can be increased and the bar diameter increased.

Another issue in detailing for ductility which comes to the fore in both the research of Engström as the research of Bigaj is the steel quality. The overall ductility of RC members and systems is highly dependent on not only the ultimate steel strength and elongation capacity, but also on the steel strain and elongation at yielding of the steel and even the elongation at onset of strain hardening. Therefore it would be advisable to use steel classes in which these characteristics are determined so more ductile steel can be prescribed.

Chapter 4

Numerical Analysis Concerning Progressive Collapse

From the previous chapter it became clear that ductile detailing is needed in order to mobilize reserve capacity of structures. In this chapter on the basis of a case study, the reserve capacity of a structure which is designed according to conventional linear elastic analysis is determined. In order to do this, first availability and capability of advanced analysis tools are discussed and procedures to deal with non-linear effects in a calculation are treated. Finally the ultimate load of a simple office building with damaged vertical members is calculated using analysis software capable of non-linear calculations. In this first instance dynamic behaviour is not taken into account.

4.1 Available Analysis Tools

Analysis tools can be divided into tools used for the alternate path direct design approach and tools used for the local resistance design approach. For a first approximation of sensitivity to progressive collapse linear elastic finite element analyses can be used. However, these analyses are not very accurate and far from realistic in case of an extreme loading, because redistribution of forces, second order effects (P-Delta instability), non-linear material properties and development of membrane modes of resistance are not taken into account. Also dynamic effects are not taken into account, but these can be accounted for by using a loading factor. Application of a linear elastic analysis usually leads to more conservative designs, but is faster and less expensive than application of more advanced analyses.

More advanced analyses use various inelastic finite element codes. These codes can take into account large non-linear, time dependent effects. Some tools using an inelastic finite element code also have libraries containing material failure models so structural elements can be analyzed through failure. Even if these advanced analyses are used there is large room for judgment on what level of analysis will give sufficient results. Very accurate predictions of structural behaviour can be obtained, but this will take much time and is computationally expensive. Also input for these models like strength properties of elements and joints requires considerable experience and expertise. To actually model a case of progressive collapse can take up to 100 hours using an advanced model.

Tools used for the local resistance design approach use the same type of computational approaches found in the alternate path direct design approach. However, the models are much smaller and efficient to run, since only key parts are considered one at a time.

4.2 Non-Linear Modeling

Since models are simplified representations of reality models always contain assumptions. For linear elastic models the assumptions are that Hooke's law ($\sigma = E\varepsilon$) is valid and there is a linear relation between stresses and strains of the material. Furthermore P-Δ (second order) effects are generally neglected. These assumptions are only valid for small deflections. Since in damaged state, large deflections are allowed linear elastic theory does not apply anymore to structural analysis of these structures. However it could be that although linear elastic modeling does not give an accurate representation of reality results from a linear elastic model can still be used to give a (conservative) approximation of the robustness of a building. In the following sections modeling of non-linear responses of the system and the elements will be discussed.

4.2.1 Geometric Nonlinearity

In conventional geometric linear calculation deflections are assumed to be so small that the relation between deformations and displacements can be linearized and equilibrium can be derived from the undeformed structure. As is clear from the example in Section 3.3 the deflection of structures in damaged state is so large that the resulting changes of the overall geometry must be taken into account to accurately analyze the structure. The most common numerical methods for the solution of geometrical non-linear response of structures as discussed in literature [Lewis, 2003] are the transient stiffness method (also referred to as the Newton Raphson method), the force density method and the dynamic relaxation method.

Transient Stiffness Method

Conventional small displacement theory assumes a linear dependence of deflections upon forces in the structure:

$$\{\mathbf{f}\} = [\mathbf{K}]\{\mathbf{u}\}$$

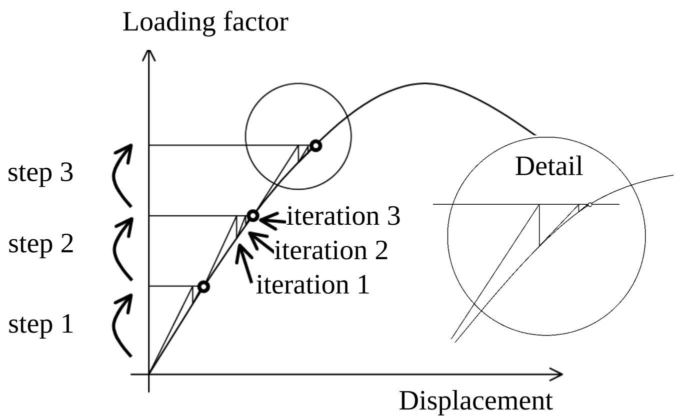

Figure 4.1: Schematical representation of the transient stiffness method with stepwise application of loads. (Source: [Hoogenboom, 2004])

in which $\{\mathbf{f}\}$ is the applied load vector, $[\mathbf{K}]$ is the global stiffness matrix and $\{\mathbf{u}\}$ is the nodal displacement vector. However if displacements are large the global stiffness matrix changes. In the transient stiffness method the final static equilibrium is determined in an iterative process as depicted in Figure 4.1. First the displacement vector is calculated using the original stiffness matrix:

$$\{\mathbf{u}\}_{k+1} = [\mathbf{K}]_k^{-1} \{\mathbf{f}\}$$

From this displacement vector follows a new geometry with which a new stiffness matrix $[\mathbf{K}]_{k+1}$ is calculated. When this new stiffness matrix is multiplied by the displacement vector an internal load vector is generated which does not balance the external load vector:

$$[\mathbf{K}]_{k+1} \{\mathbf{u}\}_{k+1} = \{\tilde{\mathbf{f}}\}_{k+1} \neq \{\mathbf{f}\}$$

The difference between these load vectors, the residual force vector $\{\mathbf{R}\}_{k+1}$:

$$\{\mathbf{R}\}_{k+1} = \left[\{\mathbf{f}\} - \{\tilde{\mathbf{f}}\}_{k+1}\right]$$

is used to find an increment $\{\boldsymbol{\Delta}\mathbf{u}\}$ for the displacement vector:

$$\{\boldsymbol{\Delta}\mathbf{u}\}_{k+1} = [\mathbf{K}]_{k+1}^{-1} \{\mathbf{R}\}_{k+1}$$

This increment of the displacement vector is used to update the geometry of the structure. Subsequently a new stiffness matrix is calculated and the steps described above are repeated. This iterative process continues until the residual force vector is zero which means the static equilibrium is reached.

This method uses a larger number of matrix manipulations which makes it only suitable for computers. For larger systems roundoff errors might be magnified due to the large number of arithmetic operations. This can be prevented by scaling of the matrices, but this is an extra operation which will add to the computational effort. The weak point of this method is that the stiffness matrix always lags one iteration behind. This means small iterative steps have to be used to ensure small displacements because if displacements between steps are to large, nodal forces and nodal displacements would be related to each other incorrectly. This can lead to a lack of convergence or a wrong solution. Of course using small iterative steps slows down the convergence of the solution.

A variant of the transient stiffness method is to calculate geometrical non-linear behaviour by stepwise applying the load. For each loading step the above mentioned iterative calculation is performed until residuals are very small, then a new loading step is taken. See Figure 4.1. In the iterative calculations the tangential stiffness can be used. The accuracy of this method is also highly dependent on the number of iterative steps.

Force Density Method

A quite different method to tackle geometrical non-linear problems is the force density method. This method is developed for pre-stressed cable nets. The method relies on the mathematical assumption that the ratio of tension force to length of each cable can be constant:

$$q_m = \frac{T_m}{L_m} = constant$$

in which q_m is the tension coefficient or force density, T_m is the pre-tension force and L_m is the length of a member. When q_m is assumed constant the system of non-linear equations changes in a system of linear equations. This method is commonly used to generate shapes of tension structures that are in static equilibrium. The method can be used effectively to find the initial shapes of membranes or cable nets under e certain pre-tension. However this method is still under development and seems less suitable for static analysis of structures.

Dynamic Relaxation

Dynamic relaxation is a much different method, which does not have to rely on matrix manipulations. It is used to analyze shell, skeletal and cable structures and plates. The basis of the method is that the structure is represented as a system of concentrated masses at given points. This system oscillates about the equilibrium position under the influence of out-of-balance forces. It comes to rest under influence of 'damping'. The objective is not to follow the actual motion of a real structure, but to determine the position of its static equilibrium by simulating a pseudo-dynamic process in time. In an iterative process the displacements are determined until the residual forces approach zero.

In literature [Lewis, 2003] a comparison is made between the transient stiffness method and the dynamic relaxation method analyzing the non-linear static response of pre-stressed cable nets. The dynamic relaxation method uses more iterative steps, but less arithmetic operations per step. Only for very simple structures the transient stiffness method is computationally more efficient. For more complex structures the dynamic relaxation method converges faster and is more stable.

4.2.2 Material Nonlinearity

Material or physical non-linear behaviour is about non-linear relations between stress and strain components. When structural members or components are stressed beyond the elastic range material non-linear properties will become important.

In Figure 4.2 a generalized force versus deformation curve can be seen. From point A till B the linear response is given, point B represents the effective yield point. The line from B to C represents the plastic response, this response is only present in ductile material, brittle material will lose strength after point B. Due to strain hardening the strength increases until point C, from this point the material loses it's strength. The values of the points A till E for different structural members or connections can be obtained from tests. When these curves are implemented in analysis software non-linear behaviour of structures can be modeled.

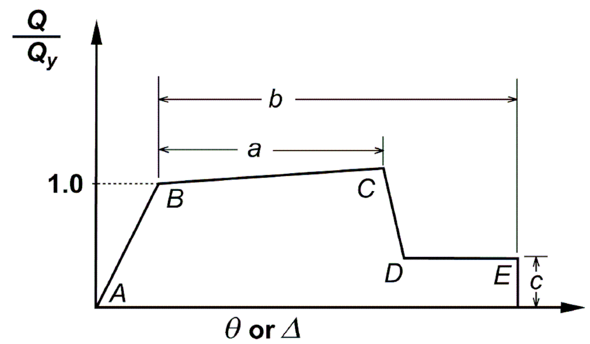

Figure 4.2: A generalized force-deformation curve. (source: [FEMA, 2000a])

In advanced numerical models cross sections of members will be discretized in strips and for each strip the stresses are calculated based upon the strains, using the stress-strain curves. With these stresses the internal forces can be determined by integrating over the strips. In this way higher order effects can be approximated like the spread of plasticity. Also axial, flexural and shear modes of failure can be characterized. This discretization can be done with various levels of refinement. To really capture bond failure or failure of rebar splices in reinforced concrete for example a very high level of discretization is needed. Of course the higher the level of discretization the higher the computational effort is.

4.3 Numerical Determination of Limit Loads

A series of both material and geometrical non-linear calculations were performed with the analysis software *SCIA.ESA PT* [SCIA Groep nv, 2006] to assess the ultimate load of a structure in case of damage to a vertical load bearing member (double span condition). As a case a five story office building was taken.

4.3.1 Review of Used Software Package

A choice was made to use the software package *SCIA.ESA PT* (which is the successor of *ESA Prima Win*) because it was readily available at the office where the graduating project took place and some experience with this package was already gained. Moreover *ESA* is a widely used software package in engineering praxis in The Netherlands which will make it easier for other structural engineers to assess the findings of this case study or apply the procedure on other structures.

Non-Linear Calculation Method

ESA makes use of the Newton Raphson method as discussed in Section 4.2.1 for non-linear calculations. The load acting on the structure can be divided in several steps denoted as increments. Furthermore a convergence criterium and a maximum number of iterations can be entered. If the maximum number of iterations is reached without meeting the convergence criterium a warning is issued. The accuracy of the method can be increased through refinement of the finite element mesh, increase of the total number of increments or by adjusting the convergence criterium.

Physical non-linear behaviour is modeled by using M-N-kappa diagrams. The member is discretized in a number of sections and during the calculation process the stiffness is modified for the sections where cracking takes place. Thus the stiffness is adjusted along the beam and hinge regions are modeled. Through the Newton Raphson method the equilibrium for internal forces and adjusted stiffness is found.

After the calculation of the internal forces the strains and stresses in the cross sections are calculated from the internal forces. The strains in the cross sections have to be checked. If the deformations in equilibrium state are too large the strains exceed the ultimate strain of the concrete or reinforcement dependent on whether concrete crushing failure or reinforcement yielding failure prevails.

Comparison With Bigaj Experiments

To assess the feasibility and accuracy of the results of the used software package a comparison has been made with experimental results of non-linear behaviour of concrete beams in a three point bending test. For a discussion on the results of this experimental research literature [Bigaj, 1999] and Section 3.2.2 is referred to.

Results of bending tests on three different beams have been re-calculated using *ESA*. The member geometry of the treated beams as well as the steel and concrete characteristics are presented in Appendix G. Specimen B.0.2.4 and B.0.3.4 both have a low reinforcement ratio of 0.28 %, specimen B.1.3.4 has a higher reinforcement ratio. The yield load F_y as well as the ultimate load F_u were determined.

In *ESA* the beams were modeled. The ultimate and yield load calculated using *ESA* was compared to the experimentally obtained values. The yield load according to *ESA* calculations was defined as the load at which yield stress of the reinforcement was reached.

Furthermore, for the yield load and the ultimate load obtained by experiments the calculated deformation and strains were compared to the experimental results (Appendix G Figure G.2).

For specimen B.0.2.4 a load-deflection curve was presented in the report of the experimental research. This curve is compared to the load-deflection curve generated by *ESA* calculations (Figure 4.3). In the calculations the size of the finite element mesh was varied from 0.01 to 0.4 m corresponding with curve 1 to 4 in Figure 4.3. Note that the ultimate load according to the calculation is 9.8 kN. When the ultimate load is exceeded the software still calculates a deflected equilibrium state for the internal forces and stiffness, but the limit strains in the cross

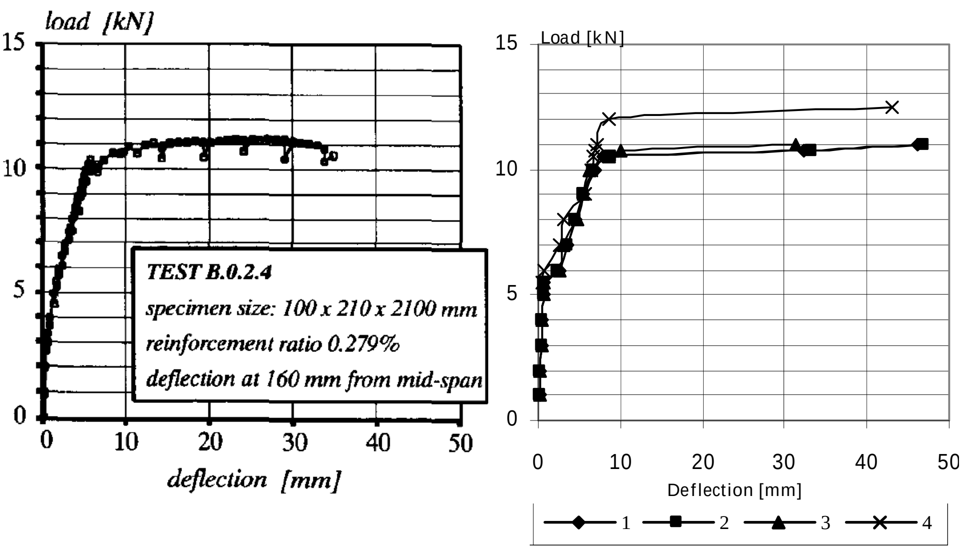

Figure 4.3: Comparison of experimental values (left) and calculated values (right) of deflections in a three point bending test.

Specimen	**B.0.2.4**			**B.0.3.4**			**B.1.3.4**		
	F_y [kN]	F_u [kN]		F_y [kN]	F_u [kN]		F_y [kN]	F_u [kN]	
Experiment	10.3	11.2	SR*	50.2	64.9	SR	210.2	214.8	CC
Calculation	8.6	9.8	CC*	50.0	56.2	CC	198.5	209.0	CC
Ratio	0.83	0.88		1.00	0.87		0.94	0.97	

*SR = Steel Rupture Failure; CC = Concrete Crushing Failure

Table 4.1: Yield and ultimate load of specimens obtained by experiments compared to calculated values.

When Figure 4.3 is considered, the conclusion can be drawn that the software is able to model the actual non-linear beam behaviour fairly good. It should be noted that whereas the experimentally obtained deflections are taken 160 mm from midspan, the displayed calculated deflections are deflections at midspan which are larger than the deflections at an offset of midspan.

For meshes up to approximately beam height (2100 mm) the behaviour is accurately modeled. When the finite element mesh is too large (curve 4) the deflections are underestimated.

When the ultimate and yield loads are compared it is noted that the calculated values of the ultimate load are somewhat below the actual limit load. This means the calculated ultimate loads are somewhat conservative. For specimen B.0.2.4 and B.1.3.4 the calculated ultimate load is even below the experimentally obtained yield load.

Failure is not well modeled, since in the calculations concrete crushing always prevails, whilst in the experiments steel rupture failure takes place if low reinforcement ratio's are used.

Comparison of the strains and rotations give a somewhat confusing image. Note should be taken that measuring concrete and steel strains is difficult and considerable scatter in results were found. Also if the experimental limit load is applied on the calculation model the strains in the calculation model are already well beyond limit strain, so the calculation results will be less accurate. When the strains are below or around the limit strain, which is so for the model of specimen B.0.3.4 and B.1.3.4 with a load of respectively 50.2 and 210.2 kN, the deformations are overestimated by approximately 80%.

It is acknowledged that for more profound assessment of the used software package more parameters should be varied and more experimental data should be compared. However this is beyond the scope of this research. Although some concern rises around the determination of limit load in the calculation model, because the model seems unable to model the failure mode correctly for now the conclusion is drawn that the calculation results are in the same order of magnitude of the experimental results and moreover the values from the calculation are conservative because the deformations are overestimated resulting in an underestimation of the limit loads.

It is remarked however, that in the experiments and corresponding calculation models no redistribution of internal moments is present. More experimental and numerical data should be present in order to assess the capability of the software to model this effect accurately. However, because redistribution is directly dependent on the deformation capacity and the deformations are modeled fairly good, it is assumed that redistribution of internal moments will also be adequately modeled.

4.3.2 Case: Five Story Office Building

As a case a five story office building is assessed for behaviour in damaged state. The studied structure is taken from the report of Stufib study cell 2 on structural integrity of building structures [Stufib, 2005].

The office building has a structural lay-out of columns and beams with a stability core and a stability wall. In Appendix D a technical drawing of the bearing structure is given (see also Figure 4.4 for a 3D impression). The properties are summarized in Table 4.2.

First via a conventional linear elastic calculation the internal forces are calculated and the required amount of reinforcement for the beams and columns is calculated according to NEN 6720 [NNI, 1995]. The calculated design values of the forces in ultimate limit state as well as the chosen reinforcement are presented Appendix E. Also a graphical representation of the design moments in the primary beams is given (Figures E.1 and E.2 on pages 90 and 91).

Three cases of column removal were investigated: a facade column at the long side of the building, an interior column and a corner column. Since a full scale non-linear calculation of the complete building model would be too time consuming for each case only the primary load bearing beam(s) which should bridge over the column were modeled. In Figure 4.5 the removed columns and corresponding primary beams are indicated in the lay-out drawing. Also in Appendix H the parts of the building structure which are modeled for non-linear calculation are indicated. For each case the limit bearing capacity was determined with and without a load bearing contribution by the floor elements.

4.3.3 Calculation Procedure

For each of the three situations of column removal, the load bearing beam, or in the case of the corner column two beams are isolated. The corresponding models that were subject to the geometrically and physically non-linear calculation are depicted in Figure 4.6.

Input of Reinforcement

The required reinforcement as calculated from the original linear building model and loadings where introduced in the model. The reinforcement lay-outs of

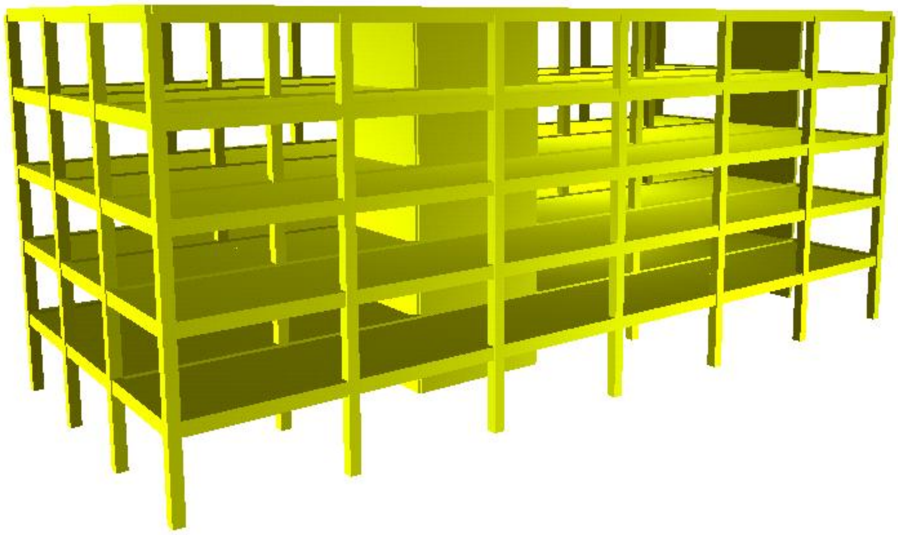

Figure 4.4: 3D view of studied office building.

Materials	Concrete	B35		
	Reinforcing steel	FeB 500		
Dimensions	Columns	400 x 400	mm2	
	Beams	400 x 600	mm2	
	Stabilizing walls	d = 250	mm	
	Floor slabs	d = 200	mm	(hollow core slab)
	Roof slab	d = 150	mm	(hollow core slab)
Loads	Dead Load	floors: 2.0	kN/m2	
		facade: 0.5	kN/m2	
	Live Load	floors: 4.0	kN/m2	($\psi = 0.5$)
		roof: 1.0	kN/m2	($\psi = 0.0$)

Table 4.2: Input parameters of the building model.

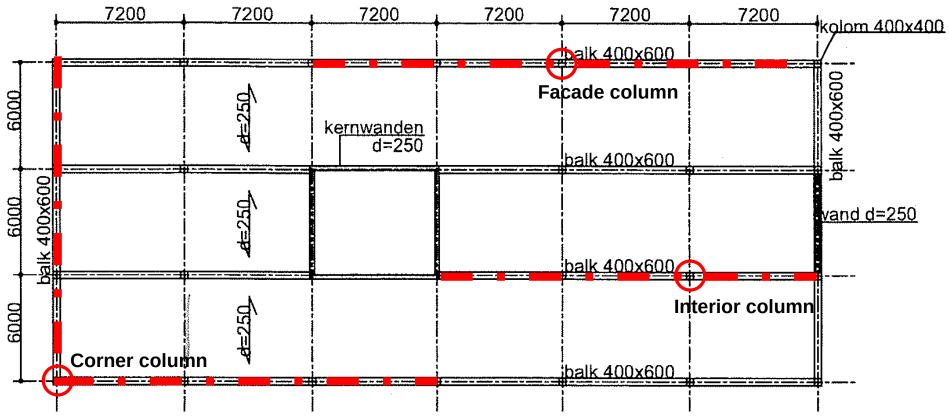

Figure 4.5: Three investigated cases of column removal. The modeled primary beams are indicated.

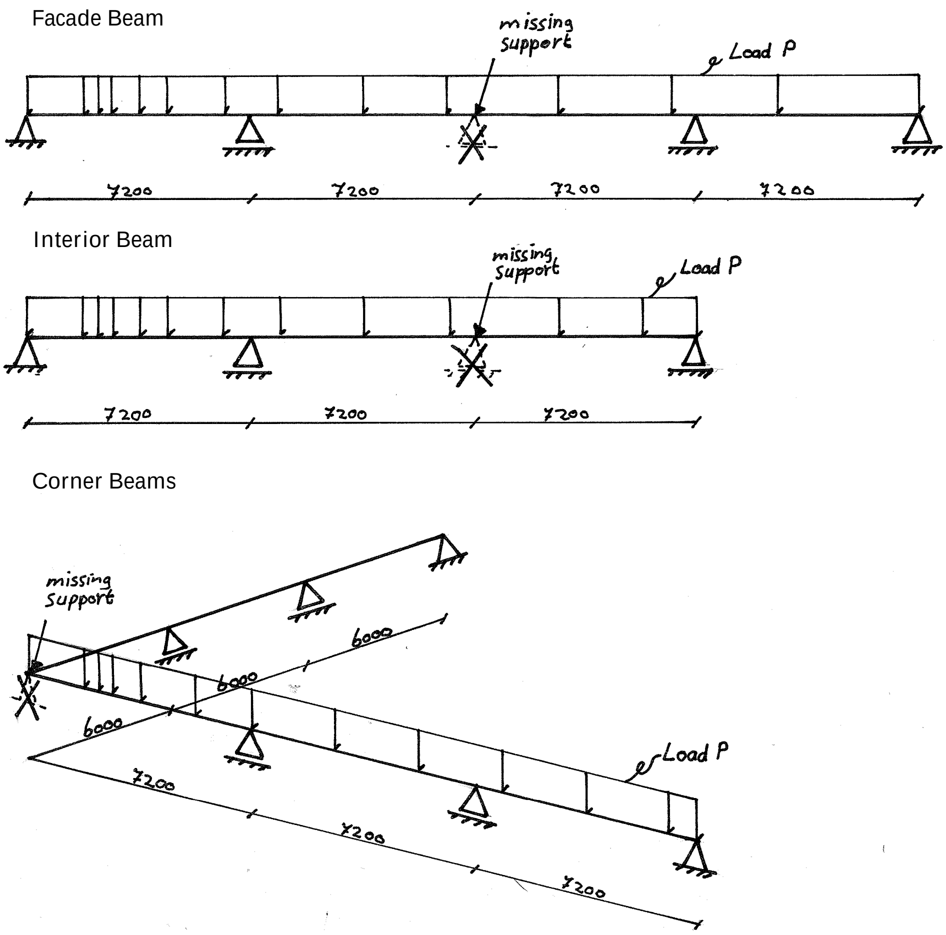

Figure 4.6: Calculation models used for non-linear calculation.

the beams are depicted in Appendix E.3. For the models the floor beam reinforcement was taken. *ESA* has two options on how reinforcement is taken into account in the calculation (Figure 4.7). A theoretical reinforcement area (strip) can be introduced from which internal stresses and strains are calculated, but also practical reinforcement can be inserted. In this case the stresses and strains of steel are concentrated at the actual position of the reinforcement bars.

The latter option is chosen because more accurate results can be obtained this way. Also in case of the corner beams it is the only option, because unsymmetrical bending occurs in this case and this cannot be adequately modeled if a theoretical strip of reinforcement is used in the model. The only difference between the designed reinforcement lay-out as depicted in Figures E.4 to E.6 in Appendix E and the reinforcement in the model is that in the model the lap splices are not taken into account.

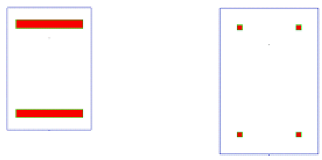

Figure 4.7: Two ways of taking reinforcement into account in the calculation. The option on the right side was chosen.

Floor Contribution

In the original design of the office building hollow core slabs spanning 6.0 m are applied. Since hollow core slabs span only in one direction and also only have reinforcement in this direction membrane action is assumed to be negligible. However when the supporting beam starts to deflect the hollow core slabs will undergo a rotation in the longitudinal direction. This means a torsional moment will develop which is directed opposite to the rotation of the supporting beam.

To determine the rotation capacity of a hollow core slab, the slab was modeled as a hollow box girder with a wall thickness of 40 mm. In Appendix I the torsional capacity is calculated.

Although no torsion experiments with hollow core slabs were known, torsion tests on beams show a failure pattern in which a long helix-like crack develops. Since this crack is very long a long yield traject is provided. It is assumed that hollow core slabs will fail in a similar manner so relatively large plastic deformation can be achieved and a long yield traject will occur.

In the model the floor contribution was taken into account by adding bilinear rotational supports tot the calculated beam every 1.2 m. In Figure 4.8 the non-linear characteristics of this support are depicted. For an interior beam twice the ultimate moment capacity was used since these beams support two hollow core slabs.

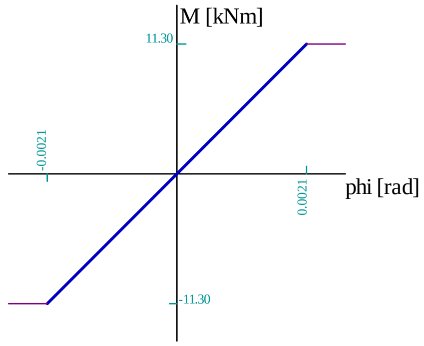

Figure 4.8: Assumed torsion rotational characteristics of hollow core slab.

Material Properties

For concrete the characteristic bi-linear stress-strain diagram for C28/35 with a tension-branch was used. This means the concrete has an elastic strain of 1.75 $^0/_{00}$ and a limit strain of 3.5 $^0/_{00}$.

For the reinforcement steel, FeB500 the standard diagram was fitted with a linear 10% strain-hardening branch. For both materials the material factor γ_m was set to 1.0 per NEN6720 art. 6.1. Both diagrams are depicted in Figure 4.9.

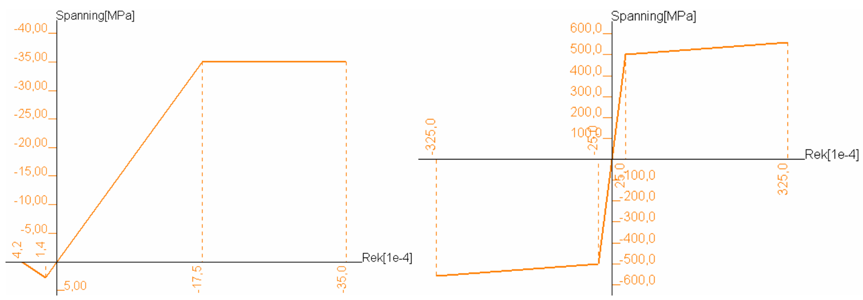

Figure 4.9: Applied σ-ϵ diagrams for concrete and reinforcing steel.

Calculation Parameters

Each of the models were calculated a number of times with different loading. The finite element mesh for the stiffness calculation was set to 0.2 m which is one third of the beam height. The number of load increments was increased from 5 up to 200 as the applied load approached the ultimate load. The convergence criterium was set to 5% and the maximum number of iterations to 500, but because the number of load increments were increased as the limit load was approached the number of iterations required to find equilibrium within one load increment was generally below 5. The parameters are summarized in Table 4.3.

Finite Element Mesh	0.2 m
Load Increments	5 - 200
Convergence Criterium	5%
Maximum Number of Iterations	500

Table 4.3: Most important calculation parameters used for determination of limit loads of structural beams.

Cross-sectional Check

Each calculation was followed by a detailed cross-sectional check to determine if the strains in the critical regions were not exceeded (Figure 4.11. Where the critical region was at a support, where the bending moment peaks, the normative cross-section was chosen at an offset of 200 mm from the support node because in the model the supports are represented by nodes, whereas in reality the supports (the columns) have a width of 400 mm. Therefore the region above the support is in reality a discontinuous region and the peak of the bending moment will be leveled off.

4.3.4 Discussion of Results

In Appendix J the calculation results are given. In Table 4.4 the results for the models in which the floor action is taken into account is summarized. As an example a graphical representation of the results of the limit load case for the facade beam (P = 23.5 kN/m) is given in Figure 4.10. In Figure 4.11 a representation of stresses and strains in the critical cross section of the facade beam with floor is given, which is at an offset of 200 mm from the support node.

	Limit Load	**Maximum Deformation**		**Moments in critical cross-sections**	
	P	uz	fy	Mdsup	Mdspan
	[kN/m]	[mm]	[mrad]	[kNm]	[kNm]
Facade Beam	23.5	259.9	43.9	-329.8	195.9
Interior Beam	29.0	108.7	26.6	-606.5	323.4
Corner Beams	21.5	132.8	25.7	-298.8	-134.7

Table 4.4: Limit loads for three models taking the floor action into account. Note that the presented design moments are the calculated values in the non-linear calculation after moment-redistribution.

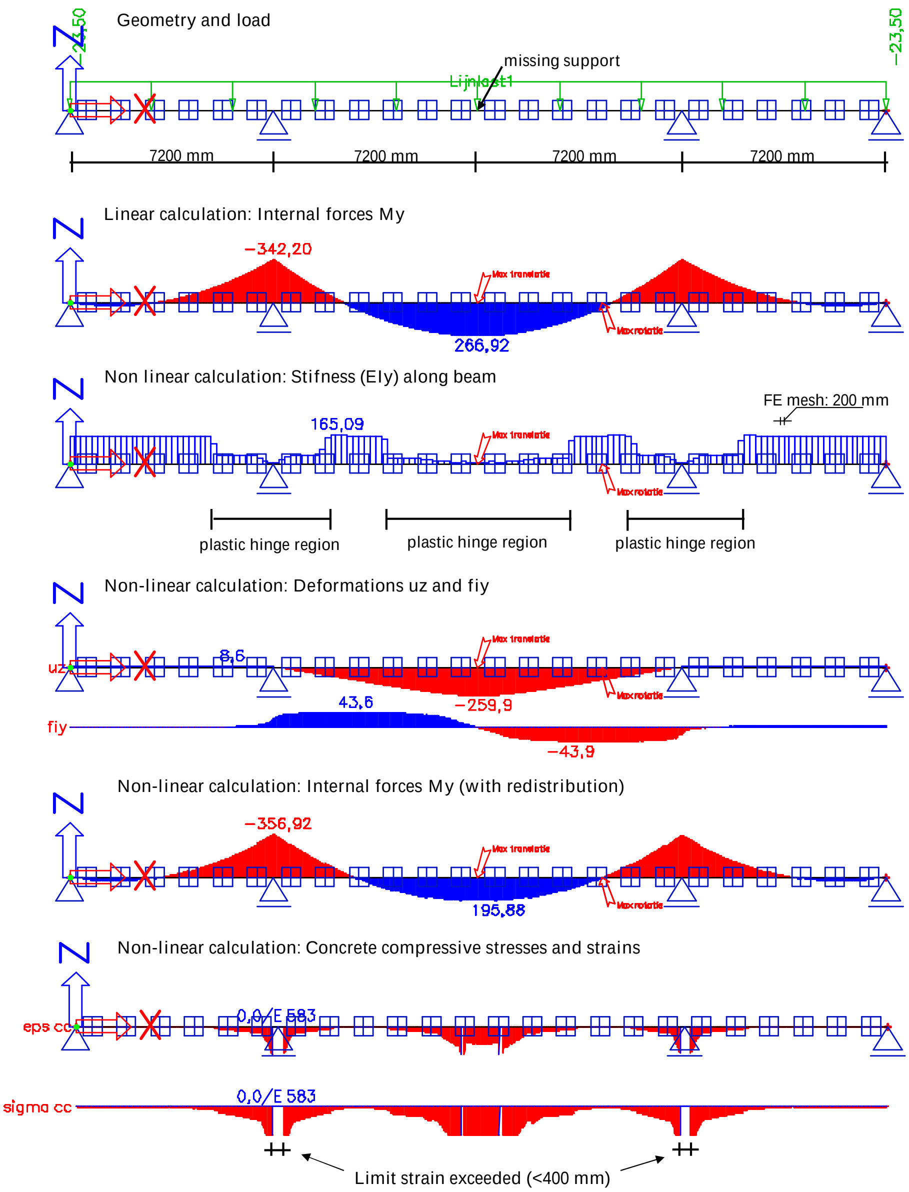

Figure 4.10: Results for limit load case of the facade beam with floor.

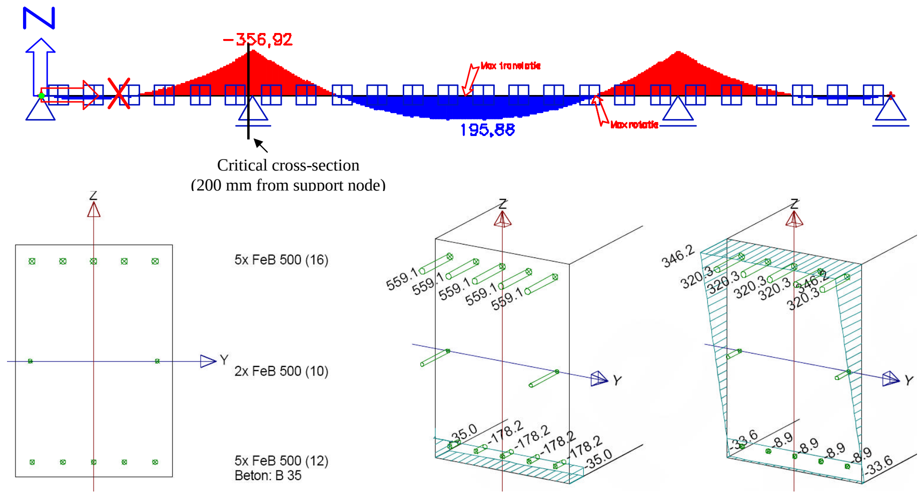

Figure 4.11: Detailed representation of stresses and strains in the critical cross section of the facade beam.

As can be seen from Table 4.4 the ultimate deformations are relatively small. This is because conservative $\sigma - \epsilon$ diagrams are used. The assumed ultimate strains of the materials are therefore small. The maximum deformation found was 43.9 mrad, which is less than half of the maximum deformation in non-linear conditions allowed by U.S. guidelines on progressive collapse (see Appendix M).

In reality the deformation capacity will be probably larger than calculated, because in the calculations the positive effect of confining shear reinforcement on the deformation capacity and also the bond-slip behaviour is not taken into account.

When the limit loading point in the load-displacement diagrams is considered it is noted that for the facade beam and the corner beams the limit load is at or just beyond the yield point in the diagrams whereas the limit loading point of the interior beam is reached before the yield point.

Results Facade Beam

For the facade beam the deformation capacity is large enough to enable an optimal redistribution of moment forces so the maximum capacity at the supports and at midspan is reached at the same time. The order of magnitude of redistribution is 15%. According to the model steel rupture failure occurs, but the concrete strain at failure is also very close to the limit strain.

It appears that the ultimate deformation for the model with floor action is larger than the ultimate deformation for the model without floor action, but this probably has to do with the accuracy of limit load determination. The chosen limit load of the model with floor is somewhat too large and the chosen limit load of the model without floor somewhat too small and since the load-displacement curve is very flat a small deviation in load gives a considerable deviation in displacement.

Due to moment redistribution and strain hardening a load capacity increase of almost 60% is obtained. An extra load capacity increase of 12% is generated if the floor action is taken into account.

Results Interior Beam

The behaviour of the interior beam is different than the behaviour of the facade beam. Because of a different geometry the reinforcement at the support will not have reached full capacity by far when the beam starts to collapse in the span. This is why the limit loading point in the load-displacement diagram is considerably below the yielding point. The positive effect of moment redistribution for the moment in the span stops at 8%.

The critical section of the interior beam is located at the place of the original support. In the original situation the field moment in the middle span will be relatively small, and so in original design not much bottom reinforcement will be used. In the damaged situation the maximum moment in the span will occur near the location of the removed support. See Figure 4.12. It is of utmost important in this case that the bottom reinforcement is continuous over the supports with sufficient lap splices.

For the interior beam the redistribution and strain hardening effects enable a load capacity increase of about 40%. The effect of the floor action is larger than in case of the facede beam because the interior beam supports a hollow core slab at each side. This creates an extra load capacity increase of another 30%.

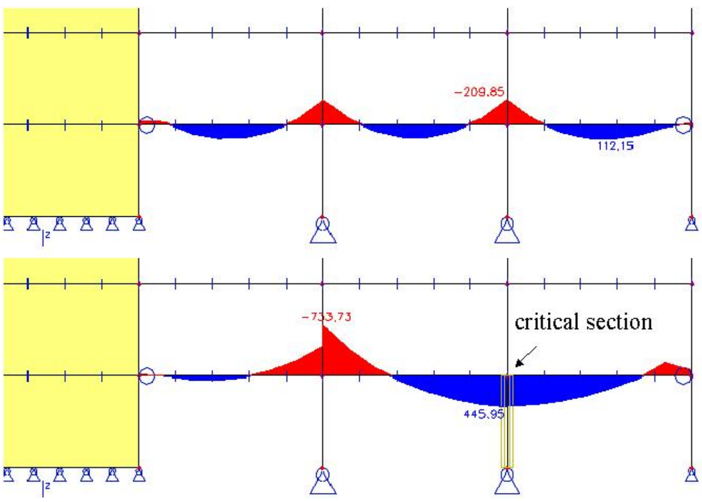

Figure 4.12: Moment distribution of interior beam in normal situation (top) and in damaged situation (bottom).

Results Corner Beams

For the results for the corner beams the different load-displacement behaviour stands out (Figure J.10 on page 121). The load-displacement curve is much flatter and a distinct yield point is hard to conceive. Also from this figure it can be seen that for the model with floor action it was difficult to find the right equilibrium state if the beams were loaded beyond the limit load case. The difference in behaviour can be explained by the 3-dimensional bending effects. Torsional and bi-axial bending occurs which results in a stiffer behaviour.

Also in this case steel rupture failure occurs, first in the weaker beam at the short side of the building although due to the moment redistribution the maximum capacity of the stronger beam at the long side of the building is also almost reached. Moment redistribution is considerable with 30% redistribution of internal forces.

Although the deformation pattern is different, in a relative sense the performance is comparable to the performance of the facade beam since the load capacity increase for non-linear behaviour is in the same order of magnitude. In an absolute sense the performance is less good, because the limit load of the corner beams is about 10% smaller than the limit load of the facade beam.

Extended Models

To investigate the effects of Vierendeel action and assess the extent of normal forces in the structural members, a non-linear calculation was performed for extended models. In these models all floor beams and the roof beam were calculated. In Appendix K the models are depicted.

Only the limit load case as calculated from the previous models were considered. All floor beams were equally loaded and the load of the roof beam which has a lower reinforcement ratio is reduced to take into account that in reality the roof beam does not have to carry live load.

The behaviour of the facade model is stiffer than the behaviour of the model of one facade beam. The maximum deflection is 108 mm which is half of the maximum deflection in the small model. But as stated earlier the ultimate deflection in the small model was overestimated. The load redistribution seems somewhat smaller but in the same order of magnitude. The development of tensile forces in the vertical member above the missing column is very limited. A tensile force of only 8 kN is present if all floor beams are equally loaded. Due to buckling of columns some normal forces develop in the horizontal beams, but this is also limited.

The behaviour of the extended model for the interior beams is comparable to the small model where one beam was modeled. The order of magnitude of moment redistribution is the same and the ultimate deflection which is 100 mm is also almost the same as for the one-beam model.

The vertical member above the missing column loaded in compression and

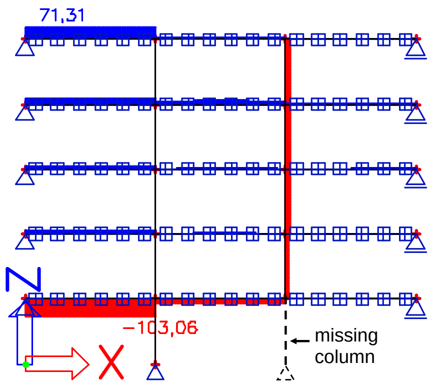

Figure 4.13: Development of normal forces in interior beams.

the normal force is 29 kN. An interesting effect is that since the interior beams are at one side attached to the stability core, the structure as a whole tends to hang from this core. This is depicted in Figure 4.13. In the upper beams a tensile force develops, whereas in the beam of the first floor a considerable compression force occurs. According to the calculation the tensile force in the roof beam does not initiate premature failure of this beam.

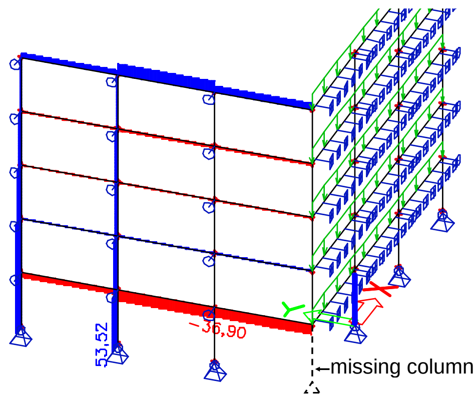

Figure 4.14: Development of normal forces in head facade on corner column removal.

For the extended corner model a much stiffer behaviour is apparent. Also the load capacity is increased, since in the extended model at ultimate load the strains in the critical cross-sections are smaller. The ultimate deflection is only 14 mm. The capacity increase can be explained be the action of the entire head facade frame. It acts as a Vierendeel beam over the full height of the building with the roof beam acting as a tensile member and the beam of the first floor as a compression member (see Figure 4.14).

All extended models demonstrate furthermore that the columns have sufficient combined bending and normal force capacity.

4.4 Conclusion: Demand Capacity Ratio

Based on the comparison with experiments (Section 4.3.1) and on the relatively small calculated deformations compared to limit values brought forward in U.S. guidelines (Appendix M) the calculated limit loads are assumed to be safe estimates of the actual limit loads of the investigated structural members of the office building.

Moreover, from the extended models it can be concluded that some extra safety is present in the Vierendeel action of the beam-column systems which is not taken into account in the models from which the limit loads are determined.

Now that these limit loads are known it is interesting to compare the linearly calculated internal forces associated with these limit loads to the member capacity. The member capacity is typically exceeded if linear analysis is performed. When the member capacity in special loading conditions as calculated in Appendix F is used, the available Demand Capacity Ratio (DCR) of the beams can be calculated as follows:

$$DCR = \frac{M_{d;lin}}{M_{u;special}}$$

This is thus an expression of the available extra capacity of the structural member if the non-linear effects of strain hardening, moment redistribution and the floor action are taken into account. In Table 4.5 the DCR's obtained in this way are given for the six calculated models.

	Load [kN/m]	$M_{d;lin}$ [kNm]	$M_{u;special}$ [kNm]	DCR [-]
Facade Beam	21.0	238.5	153.1	1.56
Facade Beam w/f*	23.5	266.9	"	1.74
Interior Beam	22.5	384.3	266.5	1.44
Interior Beam w/f	29.0	496.7	"	1.86
Corner Beams	18.5	-198.9	-123.1	1.56
Corner Beams w/f	21.5	-231.2	"	1.82

**w/f means with floor contribution*

Table 4.5: Available DCR for three simplified models with and without taking the floor action into account. Note that the presented design moment is the maximum moment at the critical cross-section according to the linear calculation.

When the three non-linear effects are considered separately the DCR value can be divided in three parts. The calculation model with floor gives the total DCR for combination of all three effects. The calculation model without floor gives the DCR for the strain-hardening effect combined with the moment redistribution effect. To assess the contribution of the strain hardening in this combined effect the ultimate moment capacity according to the calculation of Appendix F was compared to the ultimate moment capacity in the non-linear calculation where the actual stresses and strains are considered:

$$\text{Strain hardening effect} = \frac{M_{u;FNL}}{M_{u;lin}}$$

Because the strain hardening effect thus determined is different for the different critical cross-sections within one member, the total strain hardening effect for the member was determined as the mean of the effect for the two cross-sections of the member where the maximum moment forces occur.

In Figure 4.15 the thus obtained subdivision of the DCR value is depicted. It must be noted that this subdivision of the DCR value is not entirely correct, because the three effects act together. The floor effect as well as the strain hardening effect influence the moment redistribution and vice versa. However this approach does give some insight in the relative order of magnitude of the three effects.

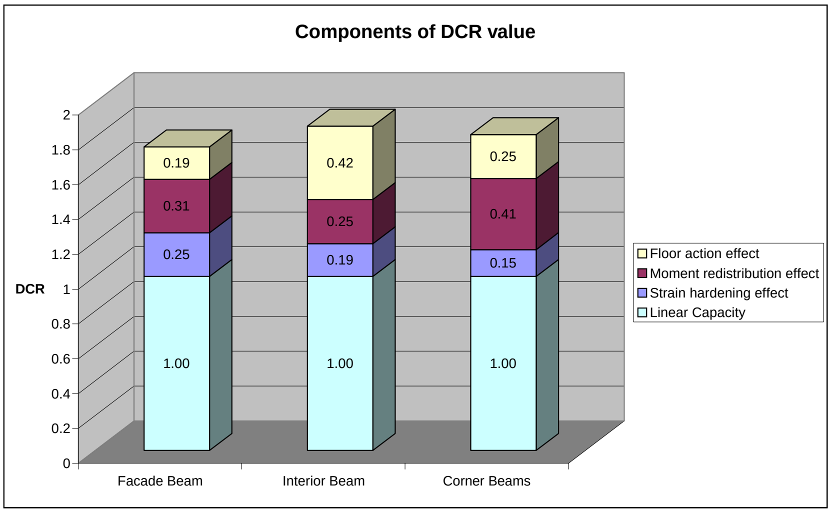

Figure 4.15: Contribution of three different non-linear effects to the DCR value.

It appears the strain hardening effect is smaller for the interior beam and the corner beams than for the facade beam. For the interior beam this can be explained by the limited moment redistribution as a result of which the strain hardening effect of the not fully strained reinforcement at the support is less pronounced. For the corner beams the limited strain hardening effect is because of the bi-axial bending, as a result of which the maximum capacity of the reinforcement bars is not reached at the same time.

The larger moment redistribution effect of the corner beams compared to the facade beam has to do with the difference in reinforcement ratio between the two corner beams. For the facade beam the difference in reinforcement ratio for the supports and the span is smaller, so full redistribution is reached at a lower redistribution ratio. As already mentioned in the interior beam full redistribution is not reached as a result of which the redistribution effect is lowest for this beam.

As for the floor action, it is clear that the effect is largest for the interior beam, because this beam supports a slab on each side. It is more difficult to explain why the floor action effect for the corner beams is larger than for the facade beam. At first thought it is expected that the floor effect for the corner beams would be the same or smaller than for the facade beam. It probably has to do with interaction between the floor contribution and the moment redistribution.

From the calculation results the conclusion can be drawn that if the floor action is taken into account the Demand Capacity Ratio for this building is around 1.8. However it varies with the investigated cases of column removal.

Two cases of column removal which will give a significant different behaviour are not investigated. These cases are the column removal of an interior column at opposite side of the stability core of the investigated interior column, and the column removal of a corner column at the opposite end of the building from the investigated corner column. In both cases moment-redistribution is not possible so the obtained DCR values can not be used in these two cases and the expected DCR for these cases is much smaller.

Chapter 5

Alternate Path Analysis

This chapter aims at translating the findings of the research presented in the previous chapter to practical measures. Therefore an alternate path analysis for the office building studied in last chapter is performed. First on the basis of two U.S. guidelines dealing with progressive collapse the performed notional element removal alternate path analysis is elaborated.

5.1 Notional Element Removal

To date two guidelines explicitly dealing with progressive collapse in the U.S. exist. The U.S. General Services Administration (GSA) developed the *Progressive Collapse Analysis and Design Guidelines* [GSA, 2003] which provides criteria for Federal buildings. The UFC 4-023-03: *Design of Buildings to Resist Progressive Collapse* [DoD, 2005] which is issued by the Department of Defense is the second guideline which contains a lot of information directly taken from the former guideline. This guideline provides technical criteria for military construction.

Besides minimum strength requirements and detailing guidance for the tying approach to structures of different materials, a procedure for the notional element removal method is given in the guidelines.

5.1.1 Loading in Damaged State

The first issue which has to be cleared is what kind of loading should be assumed to be present if the notional element removal method is used.

Load Combination

A progressive collapse is initiated by an extreme load or load situation with a small probability of occurrence. The probability of occurrence of this extreme load simultaneously with the occurrence of the maximum value for other live loads is negligible. Therefore, for an progressive collapse analysis the design live load may be reduced.

In the two American guidelines on progressive collapse analysis, different loading combinations are prescribed:

$$\begin{aligned}\text{GSA} &: \quad D + 0.25L \\ \text{UFC} &: \quad (0.9\ or\ 1.2D) + (0.5L\ or\ 0.2S) + 0.2W\end{aligned}$$

in which:

$$\begin{aligned}D &= \text{Dead load} \\ L &= \text{Live load} \\ S &= \text{Snow load} \\ W &= \text{Wind load}\end{aligned}$$

The difference between these guidelines is striking. The UFC requirement is derived from the commentary on the ASCE Standard 7 [ASCE, 2002] in which this combination is recommended for checking the ability of a damaged structure to maintain its overall stability for a short time following an abnormal load event.

Ellingwood [Ellingwood, 2002] gives some background information on this load combination. In contrast to the Dutch guidelines the dead load is factored 1.2 (or 0.9 if the dead load is stabilizing). This is maintained because engineers tend to underestimate the dead load. The other factors are introduced to obtain the sustained live load, daily snow load and hourly maximum wind load from the nominal prescribed ASCE load. In this light the prescribed load combination by the GSA seems on the lower bound.

The same principle of load combination is accounted for in many standards though not specifically for progressive collapse, but for other incidental or special load combinations. In the Dutch code NEN 6702 [NNI, 2001] for example, for special loading combinations the loading factor γ is set to 1.0 and for live loads an instantaneous value is used which is obtained by multiplying with a momentary factor ψ which varies from 0.25 for passageways to 1.0 for storage areas. For wind load this factor is 0.2 for some special combinations and else 0.0. For snow load a value of 0.0 is used.

Dynamic Action

Because of the energy released in a system as members fail dynamic effects will play an important part in a progressive collapse. To account for these effects in a static analysis both the GSA as the UFC guidelines require an increase in loading by a factor two in a static analysis to obtain a static equivalent load.

In the UFC guidelines this amplified load only has to be applied to the area directly influenced by the damaged element, see Figure 5.1. In the commentary UFC states: *'The factor 2.0 is used in GSA 2003 and has been validated as conservative through a number of numerical simulations of progressive collapse.'* In these numerical simulations the assumed damaged vertical element was removed instantaneously and a time history analysis was performed.

Dynamic action of a structure depends on the plastic behaviour. Engström for example [Engström, 1992] proposed a method to assess the dynamic behaviour of precast structures from the load-displacement characteristics of the structural ties. According to literature [Marchand & Alfawakhiri, 2005] the factor of 2.0 is very conservative and a factor of 1.3 to 1.5 would be more realistic if members can achieve significant plastic deformations.

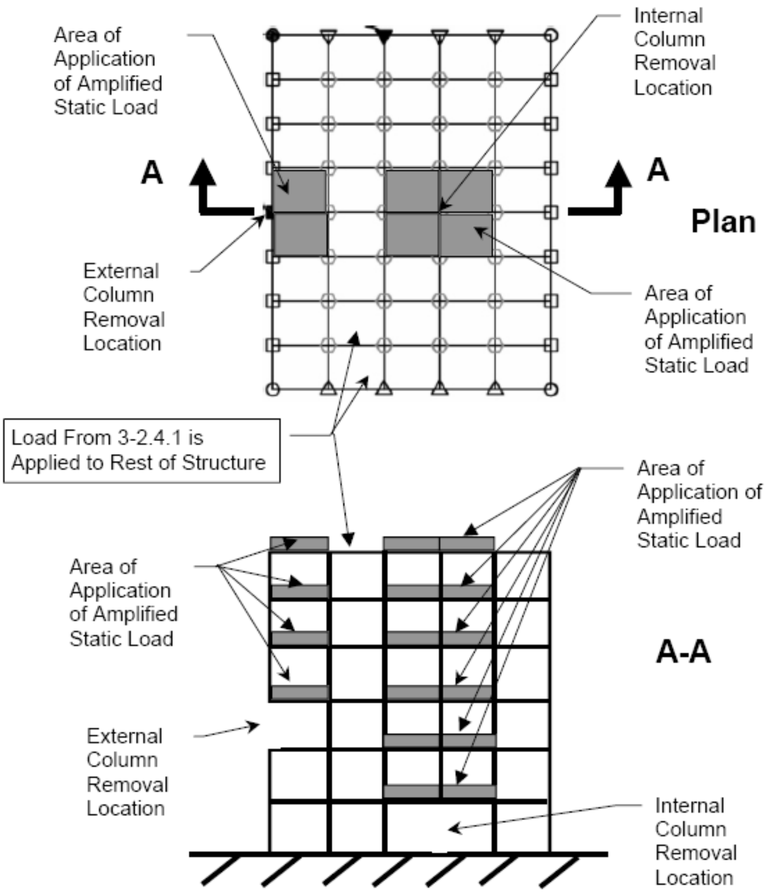

Figure 5.1: Areas of load amplification in static analysis prescribed by UFC 4-023-03. (Source: [DoD, 2005])

Debris Loading

A special loading case of particular importance in a progressive collapse analysis is debris loading. Although debris loading is widely recognized in literature as an important aspect of progressive collapse and well known historical cases of progressive collapse are directly related to debris loading, no literature or research specifically dealing with debris loading could be found.

In the U.S. guidelines this phenomenon is approached by instantaneously applying the load of upper elements on the element below upon failure of the upper element. The debris loads are amplified by a factor of 2.0 to account for dynamic impact. If these loads were already amplified by a factor 2.0 to take dynamic action into account, no further amplification is required to account for the the dynamic impact of debris.

This approach of factoring and instantaneous applying dead and live loads associated with failed members to members below, can also be found in many other proposals for progressive collapse analysis, but the amplification varies. For example in literature [Gilmour & Virdi, 1998] the debris loads are factored up by 1.25 in order to take into account the effects of impact from the falling debris.

In the commentary on the UFC the choice of a factor of 2.0 for debris loading is motivated. In section B-4.2.3 it is stated that this factor is based on engineering judgment. Although peak loads in a perfect impact will be much higher it is unlikely that elements will fail completely and fall intact upon the lower level due to still embedded reinforcement or non-structural elements like non-load-bearing walls according to this commentary.

In a rational approach however at least the floor to floor height should be taken into account. This is for regular buildings very similar, but for buildings containing an atrium or a conference room for example the distance from the floor to the ceiling could significantly differ.

In most cases it is probably best to design a structure in such a way that upon notional element removal non of the members fail, so debris loading does not have to be taken into account.

5.1.2 Removal of Elements

When consensus is reached on the applied load, it has to be determined which amount of damage the structure must be able to bridge. In the U.S. guidelines and many other standards dealing with notional element removal one vertical element at the same time has to be removed. This can be a column or load bearing wall. Removal over one floor height is deemed appropriate. In case of a load bearing wall the width to be removed varies. In the preliminary Eurocode a width of 2.25 times the floor height is recommended. Other guidelines provide similar requirements.

As a minimum the U.S. guidelines prescribe removal of a perimeter column near the middle of the short side of a building, near the middle of the long side of a building and a corner column. Removal of interior columns only has to be checked if the building contains uncontrolled public areas for example a parking garage.

As far as load bearing walls are concerned a similar approach is aimed at. The length of the wall which has to be removed is twice the wall height, but not less than the distance between expansion or control joints.

5.1.3 Material Properties

Expected rather than the lower bound design strengths such as yield stress and failure stress of materials can be used in the analysis of instanteneouss loss of a vertical member. Factors are presented to obtain expected values from by standards prescribed lower bound values of design strengths. In the UFC for example an over strength factor of 1.25 is given for the ultimate and yield strength of reinforcing steel and the compressive strength of concrete.

In NEN 6720 art. 6.1.1, 6.1.2 and 6.2.1 material factors γ_m are presented from which the lower bound strength of concrete and reinforcing steel can be calculated from the expected strength. It is allowed to reduce these factors in abnormal loading conditions such as blast or impact loading.

5.1.4 Analysis Procedures

Both the UFC and the GSA allow three different analysis methods and corresponding acceptance criteria:

- Linear Static Analysis
- Non-Linear Static Analysis
- Non-Linear Dynamic Analysis

In case of linear analysis the acceptance criteria are directed at the occurring forces and in case of non-linear analysis the acceptance criteria are directed at the occurring deformations. The proposed methods are derived from an earthquake design guideline.

FEMA 356: Modification Factor

FEMA 356: Prestandard and Commentary for the Seismic Rehabilitation of Buildings [FEMA & ASCE, 2000] is a specific reference document for making buildings more resistant to earthquakes. It is now being balloted by the American Society of Civil Engineers (ASCE) and if approved will become a nationally recognized standard in the U.S.

Since the analysis procedures in the UFC and GSA guidelines and moreover also the corresponding acceptance criteria are derived from this standard the basics of the prescribed analysis procedures in FEMA 356 are briefly discussed.

The FEMA prestandard presents four procedures for seismic analysis of structures (the three mentioned above and a Linear Dynamic procedure) and corresponding acceptance criteria.

The actual forces and behaviour can be estimated by non-linear analysis. When this analysis is performed structural assessment is done by checking if deformation capacities are not exceeded. To this purpose tables of non linear deformation capacities of various structural members and connections are presented.

Within the framework of the Federal Emergency Management Agency in the U.S. numerous experiments were conducted to determine inelastic capacities of structural assemblies. This resulted in a prestandard [FEMA & ASCE, 2000] which supplies detailing guidelines and deformation capacities for different structural members and connections.

However non-linear analyses take much effort and experience and with the current computational means can be very time consuming. Therefore in earthquake engineering a simplified linear approach was developed.

Simplified Linear Analysis

The basis of the linear procedures in the earthquake guideline is that loads are selected in such a way that if applied to the linearly elastic structure model the deformations will approximate maximum expected displacements in case of an earthquake (pushover method). It is recognized that since the expected behaviour is inelastic rather than elastic the actual internal forces that would develop in the building will be less than the calculated forces in the model. Calculated forces will typically exceed the design limits. Therefore the calculated forces are evaluated through acceptance criteria which include modification (m) factors to account for anticipated inelastic demands and capacities.

When a linear analysis is performed, a distinction is made between force-controlled and deformation-controlled actions. For deformation-controlled actions the design actions may exceed the actual strength of the component or element to resist the action. This is taken into account by the factor m which is an indirect measure of the non-linear deformation capacity. For force-controlled actions expected strength of the component may not be exceeded, because non-linear deformations associated with force-controlled actions are not permitted.

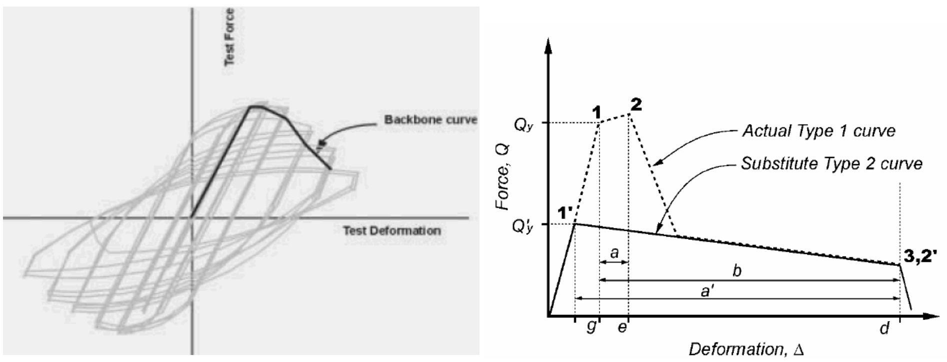

Figure 5.2: Experimental data (left) and an averaged multi linear representation of the force-deformation curve (right) of a structural member or joint.

In short the deformation criteria and m-factors are determined as follows:

- From experimental data an idealized force-deformation curve is developed which gives an average multi-linear representation through a prescribed procedure. This is depicted in Figure 5.2.
- The tested assembly is classified force or deformation controlled. When force controlled a substitute curve (type 2 curve) is drawn and corresponding value Q'_y is used as a strength limit. When deformation controlled, the actual curve (type 1 curve) is used to determine deformation limits for Immediate Ocuppancy, Life Safety and Collapse Prevention (point 3 on the curve) performance levels.
- m-factors for the performance levels are calculated by determining the ratio of the deformation limits corresponding to the performance level and the deformation at yield and multiplying this by a safety factor of 0.75.

$$m = \frac{\Delta_u}{\Delta_y} \cdot 0.75$$

In Appendix L an example of resulting m-factors and deformation capacities from FEMA 356 are given. These are values for earthquake loadings involving three fully reversed deformation cycles to the design deformation levels, in addition to similar cycles to lesser deformation levels. As can be seen from the definition, the m-factor is an indirect measure of the non-linear deformation capacity of a component or element of a structure.

It should be emphasized that these m-factors cannot be derived directly from a calculated $M - \kappa$ diagram and also should not be applied to a static load case unmodified. This is because the factors determined from experiments are greatly dependent on the dynamic behaviour of the structural member or connection. In a dynamic earthquake situation the overloading is temporary, whilst this is not the case in an extreme loading due to local damage.

In the FEMA Standard m-factors are used to determine to what extent the *flexural* design actions calculated by a *linear* method may exceed the actual strength of the component or element to resist these actions. The following equation should be satisfied:

$$DCR = \frac{Q_{UD}}{m \cdot Q_{CE}} \leq 1$$

where Q_{CE} is the expected strength at the deformation level under consideration for deformation-controlled actions

Q_{UD} is the deformation-controlled design action due to gravity loads and earthquake loads

GSA & UFC: Demand Capacity Ratio

In the UFC and PCADG guidelines the FEMA approach is adopted and adapted to perform alternate path analyses. A redistribution of moments is allowed by inserting plastic hinges at locations where moment capacity is exceeded. A summary of the Linear Static Analysis procedure is presented below.

1. A vertical load bearing element is removed from the structure and loads are applied, the structure is analyzed.

2. If the acceptance criteria on force-controlled (shear) actions is exceeded the element concerning is removed from the model and loads are redistributed. If the acceptance criteria on deformation-controlled actions are exceeded the moments are redistributed by applying an hinge with maximum plastic moment capacity of the member concerned applied on both sides.

3. The model is re-analyzed until either no acceptability criteria are violated anymore or damage criteria (see Section 2.2.2) are violated.

If non-linear static analysis is applied the loads should be applied in a number of discrete steps. If at a load step an acceptance criteria is violated the member concerning is removed and the loads are redistributed. If the damage criteria are not violated the analysis is re-started at this load step. This continues until either the damage criteria value is exceeded or the total load is applied without damage criteria exceeded.

In a dynamic analysis first the undamaged model is brought to a static equilibrium under the applied loads. Then the load bearing member is instantaneously removed. If during the analysis an acceptability criterium is violated the analysis is halted and the concerning member is removed. The analysis then proceeds until either the damage criteria value is exceeded or the total load is applied without damage criteria exceeded.

Because the acceptance criteria from both guidelines are derived from FEMA 356 caution should be taken. These criteria are based on earthquake tests. Therefore although the values are conservative to a certain extend because of the cyclic nature of these loading tests this conservatism might be not present in the analysis because axial loading is not included in the tests. Alternate paths however depend on the axial strength of members during deformation. Moreover the dynamic behaviour in the tests is different than in analyzed cases of local damage.

The acceptance criteria (deformation limits) from these guidelines for reinforced concrete are presented in Appendix M. As can be seen the values from both guidelines are very similar. The acceptance criteria values are derived from FEMA 356 and although these values are derived from earthquake tests as stated in the previous paragraph these values were considered conservative enough.

The main difference between the guidelines is that in the GSA Guideline inserting hinges for redistribution of moments in a a linear analysis is only necessary if the calculated forces exceed the design value by a factor more than 1.5 for irregular structures and a factor over 2.0 for regular structures:

$$DCR = \frac{Q_{UD}}{Q_{CE}} \leq 1.5 \ or \ 2.0$$

This is because the actual internal forces that would develop in the building in an extreme loading situation will be less than the calculated forces in the linear model of this situation. Forces calculated by means of a linear elastic method will typically exceed the design limits in such a case.

Only if this factor is exceeded the element is assumed to be collapsed or severely damaged. As an explanation of these factors the m-factors of FEMA 356 are directly referred to. When the FEMA values are compared to the GSA values it can be seen that the GSA provides a lower bound value from the FEMA table for beams controlled by flexure.

The UFC does not contain these factors and simply states that equivalent plastic hinges should be inserted at locations where the expected design moment capacity is exceeded:

$$DCR = \frac{Q_{UD}}{Q_{CE}} \leq 1.0$$

Also it is states explicitly in the commentary that acceptance criteria utilized in FEMA 356 for linear procedures are not applicable.

5.2 Analysis Using Simplified Method

In this section a hybrid approach to assess the robustness of a building via the notional element removal method is presented and illustrated by means of the case of the five story office building of Section 4.3. The method is denoted as hybrid because a linear calculation method is used, for the notional element removal method as described in the previous sections, but for acceptance criteria the DCR's of Table 4.5 are used which were determined using non-linear calculations.

5.2.1 Procedure

The most important starting points are listed below:

- One column is removed at a time and each column is removed once.
- Removal of a stability wall is for this research not considered.
- Loading factors are set to 1.0 and for live load a momentary factor of 0.5 is applied.

- Debris loading and dynamic effects are not taken into account.
- The building model used in linear calculation is presented in Appendix H.
- The material factors for special loading are used per NEN 6720 articles 6.1 and 6.2.
- For shear failure the DCR is set to 1.0.
- For flexural failure the DCR's of Table 4.5 which include the floor action effect are applied.

A first prototype of a tool was developed to perform this assessment in combination met Finite Element software of *SCIA.ESA PT*. The model was build in this software package and the geometry was adjusted by making use of XML files. The tool uses these steps:

- For each case of column removal an XML file is generated which defines the adjusted geometry of the structure.
- These XML files are processed one by one by *ESA* end for each geometry the output is stored in separate text files.
- The output files are processed automatically by an Excel based Visual Basic procedure to collect the output of all cases of column removal in one Excel sheet.
- In Excel the output is processed and a list of failed members is generated (In Figure 5.4. A screendump of the Excel sheet with the processed output is given.)

In Figure 5.3 the checked values in Excel are depicted.

Check values

	Reinforcement						
Name	Stirrups	Top	Bottom	Vu	Mu-	Mu+	DCR
Head facades	8-300	4r12	4r12	262.5	-123.1	123.1	1.82
Floor beams long facad	8-300	5r16	5r12	262.5	-266.5	153.1	1.74
Roof beams long facade	8-300	5r12	4r12	262.5	-153.1	123.1	1.74
Interior Floor beams	10-100	5r25	5r16	464.5	-604.8	266.5	1.86
Interior Roofbeams	8-150	5r16	4r12	318.2	-266.5	123.1	1.86

	Reinf.	Nu- (com)	Nu+ (ten)	Muy/Mux	DCR	Nu- without bending
Columns	8r12	-1580	450	240.1	1.5	-4500

Figure 5.3: Used ultimate capacities and DCR to determine failure of elements.

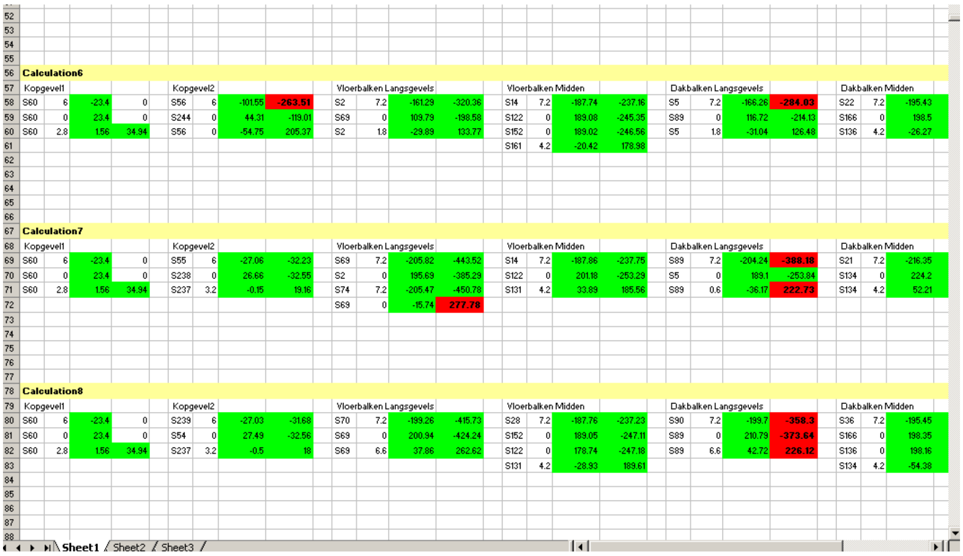

52																								
53																								
54																								
55																								
56	**Calculation6**																							
57	Kopgevel1				Kopgevel2				Vloerbalken Langsgevels				Vloerbalken Midden				Dakbalken Langsgevels				Dakbalken Midden			
58	S60	6	-23.4	0	S56	6	-101.55	**-263.51**	S2	7.2	-161.29	-320.36	S14	7.2	-187.74	-237.16	S5	7.2	-166.26	**-284.03**	S22	7.2	-195.43	
59	S60	0	23.4	0	S244	0	44.31	-119.01	S69	0	109.79	-198.58	S122	0	189.08	-245.35	S89	0	116.72	-214.13	S166	0	198.5	
60	S60	2.8	1.56	34.94	S56	0	-54.75	205.37	S2	1.8	-29.89	133.77	S152	0	189.02	-246.56	S5	1.8	-31.04	126.48	S136	4.2	-26.27	
61													S161	4.2	-20.42	178.98								
62																								
63																								
64																								
65																								
66																								
67	**Calculation7**																							
68	Kopgevel1				Kopgevel2				Vloerbalken Langsgevels				Vloerbalken Midden				Dakbalken Langsgevels				Dakbalken Midden			
69	S60	6	-23.4	0	S55	6	-27.06	-32.23	S69	7.2	-205.82	-443.52	S14	7.2	-187.86	-237.75	S89	7.2	-204.24	**-388.18**	S21	7.2	-216.35	
70	S60	0	23.4	0	S238	0	26.66	-32.55	S2	0	195.69	-385.29	S122	0	201.18	-253.29	S5	0	189.1	-253.84	S134	0	224.2	
71	S60	2.8	1.56	34.94	S237	3.2	-0.15	19.16	S74	7.2	-205.47	-450.78	S131	4.2	33.89	185.56	S89	0.6	-36.17	**222.73**	S134	4.2	52.21	
72									S69	0	-15.74	**277.78**												
73																								
74																								
75																								
76																								
77																								
78	**Calculation8**																							
79	Kopgevel1				Kopgevel2				Vloerbalken Langsgevels				Vloerbalken Midden				Dakbalken Langsgevels				Dakbalken Midden			
80	S60	6	-23.4	0	S239	6	-27.03	-31.68	S70	7.2	-199.26	-415.73	S28	7.2	-187.76	-237.23	S90	7.2	-199.7	**-358.3**	S36	7.2	-195.45	
81	S60	0	23.4	0	S54	0	27.49	-32.56	S69	0	200.94	-424.24	S152	0	189.05	-247.11	S89	0	210.79	**-373.64**	S166	0	198.35	
82	S60	2.8	1.56	34.94	S237	3.2	-0.5	18	S69	6.6	37.86	262.62	S122	0	178.74	-247.18	S89	6.6	42.72	**226.12**	S136	0	198.16	
83													S131	4.2	-28.93	189.61					S134	4.2	-54.38	
84																								
85																								
86																								
87																								
88																								

Sheet1 / Sheet2 / Sheet3

Figure 5.4: Screendump of developed tool.

5.2.2 Results

According to the output of this tool shear failure only occurs at the interior roof beams, so these beams should be fitted with extra shear reinforcement.

Flexural failure occurs in a large number of the roof beams of the facade as well as the interior roof beams. For the floor beams of the facade the capacity is only significantly exceeded if corner columns are removed. The capacity of the interior floor beams of the office building are only significantly exceeded upon removal of the column on ground floor level at the left side of stability core.

As far as the columns are concerned the columns of the head facade are too weak to carry the redistributed loads if the adjacent interior column is removed.

The collapse of head facade beams of the head facade with the stability wall is not correctly assessed by this tool because it is only aimed at forces and because the beams in this facade are provided with hinges at both sides it can freely rotate and no internal forces will develop upon corner column removal.

5.3 Conclusion: Enhancing Robustness

An DCR value of 2.0 as suggested in GSA would probably be an unsafe estimate for the current building and can probably only be applied on buildings with smaller column to column distances. Instead the hybrid approach should be used.

From the results of this approach the following set of design measures is proposed to enhance the robustness of the studied office building:

- Provide continuous bottom reinforcement. This is indispensable if double span conditions are considered.

- The roof beams should be designed with the same amount of reinforcement as the floor beams. If the roof beams are designed according to normal loading these beams will first collapse upon column removal. Since the floor beams are also already loaded to the limit collapse of the roof beams will surely cause a progressive collapse.

- Extra bottom reinforcement at the shorter interior beam at the left side of the building must be provided (see Figure 5.5). Here only limited redistribution of moments is possible so only the strain hardening and floor effects can be taken into account in determining the required extra reinforcement.

- Provide extra reinforcement in the columns of the head facade without stability wall. This is also depicted in Figure 5.5.

- For the head facade with stability wall a different approach is needed, to prevent progressive collapse in case of a corner column removal. Two options are proposed which are depicted in Figure 5.6. The first option is preferred if the usage programme and facade lay-out allows for it. In this case the head facade beams can be suspended from the stability wall. If this is not feasible the second option can be used: an infilled frame with beams which are designed for cantilever action.

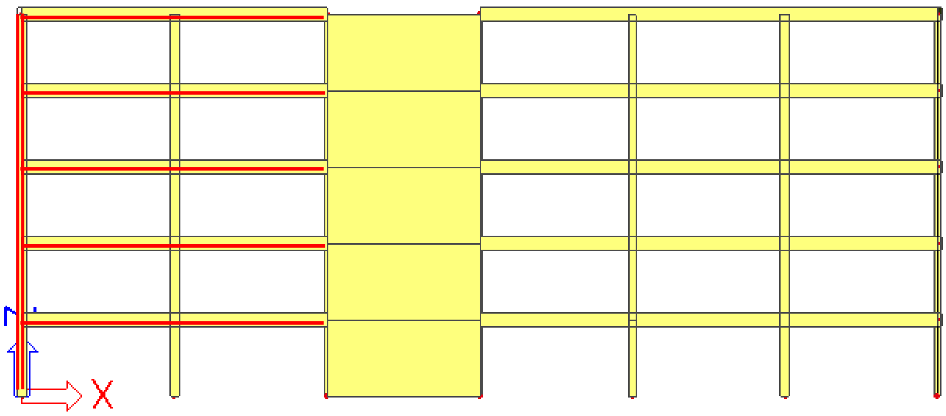

Figure 5.5: Extra reinforcement (red) is required in the shorter beams at the left side of the stability core and in the columns of the head facade at this side of the building.

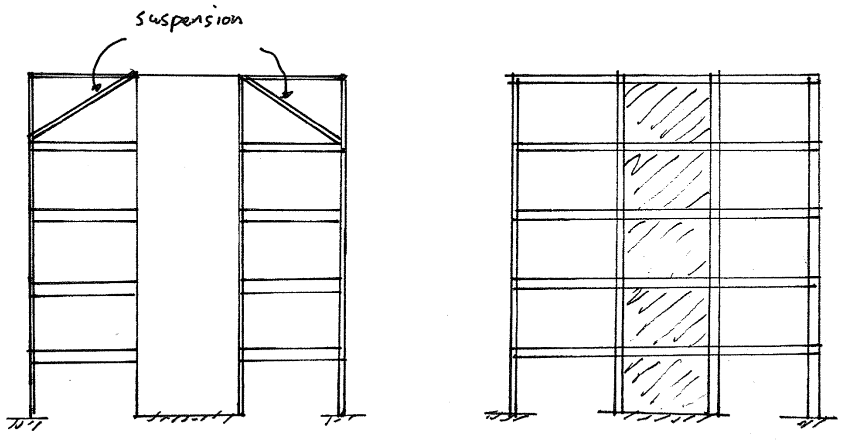

Figure 5.6: Proposed solutions for head facade with stability wall. Suspension of corner columns (left) or an infilled frame (right).

Chapter 6

Concluding Remarks

The most important findings of the research conducted are summarized in this chapter and recommendations for further research are made.

6.1 Findings

Collapse Resistance

Collapse resistance should be distinguished from robustness. Robustness can be defined as the performance of a structure in damaged state, whereas collapse resistance is a broader expression. Collapse resistance of a building can be achieved not only by providing sufficient robustness, but also by other measures. Building Codes should be aimed at providing a sufficient level of collapse resistance, because unilateral focus on robustness reduces the freedom of the designer which is possibly unnecessary because a sufficient level of collapse resistance can still be be attained with a lower level of robustness.

Secret is in Details

Building structures can be economically designed for robustness if boundary conditions are created that enable the structure to mobilize reserve capacity. This reserve capacity is typically present in non-linear effects like strain hardening and redistribution of forces. Non-linear behaviour is highly dependent on ductile detailing. With the right detailing significant reserve capacity can be mobilized.

Overcapacity due to Non-Linear Effects

In regular RC building structures physical non-linear effects can create an overcapacity of almost twice the capacity calculated via conventional linear analysis methods. Caution should be applied if using a factor to calculate the available overcapacity. Overcapacity factors derived from earthquake tests such as FEMA 356 should not be directly applied on alternate path analyses, because this would be an unsafe estimate of the actual overcapacity. The available overcapacity depends on the used structural lay out and the amount of reinforcement and its lay-out. This overcapacity should be calculated using an advanced non-linear analysis.

Designing Against Progressive Collapse

Progressive Collapse can be economically designed for. In regular RC structures applying just marginal more reinforcement provides sufficient robustness. When double span conditions are considered continuous bottom reinforcement should be applied. Furthermore for low-rise buildings robustness is enhanced by providing the roof beams with the same amount of reinforcement as the floor beams. Los of corner columns is more difficult to design for and should be considered separately.

6.2 Recommendations

Probability of Failure

This research focused entirely on robustness of building structures. When collapse resistance is considered progressive collapse should also be treated directed from the initiating event or abnormal load point of view. Chances of occurrence of initiating events and abnormal loads and chances of occurrence of failure should be investigated because the combination of these chances and the robustness defines the collapse resistance.

Dynamic Action

Investigation of dynamic effects is also recommended. In this thesis focus was on the static loading case, but it is acknowledged that dynamic behaviour can have a significant effect on progression of local failure.

Non-Linear Calculations

In non-linear calculations of deformations and redistribution of forces two aspects are of primary importance. The first aspect is the calculation method and (micro mechanical) model. From previous research [Bigaj, 1999] a more refined calculation model is proposed than the one used in this research which could be applied to refine the results and since the results from this research are presumed conservative, a refinement of results will enable a more economical redesign.

Second, the non-linear characteristics of the used material especially the characteristics of the reinforcing steel, is very important. To obtain more accurate results than obtained in this research more accurate $\sigma - \epsilon$ diagrams should be established and implemented in the calculations.

Catenary Action

Especially for precast concrete structures catenary action seems a promising concept for providing alternate load paths or at least preventing debris loading. However extreme ductile detailing of joints is needed in order to create a reliable catenary effect. The relation between strength and ductility in catenary action and also the influence of the distribution of stiffness throughout the structure seems to be neglected in codes prescribing only minimum tensile strength for structural ties. More research should be performed in order to make the catenary approach reliable.

Appendix A

Definitions of Progressive Collapse

In this appendix several definitions of progressive collapse found in literature are given. Many building codes give implicit descriptions of progressive collapse when they state to which event a building should be resistant. Some of these implicit descriptions are also given.

> *'A progressive collapse of a building is a catastrophic partial or total failure that ensues from an initiating event that causes local damage that cannot be absorbed by the inherent continuity and ductility of the building structural system. Following this local damage or failure, a chain reaction of failures propagates vertically or horizontally and develops into an extensive partial or total collapse, where the resulting damage is disproportionate to the local damage caused by the initiating event.'*

Prof. B. R. Ellingwood [Ellingwood, 2002]

> *'Progressive collapse denotes an extensive structural failure initiated by local structural damage, or a chain reaction of failures following damage to a relatively small portion of a structure. This can be also characterized by the loss of load-carrying capacity of a relatively small portion of a structure due to an abnormal load which, in turn, triggers a cascade of failures affecting a major portion of the structure.'*

Prof. T. Krauthammer et al [Krauthammer *et al.*, 2002]

> *'Progressive collapse is the result of a localized failure of one or two structural elements that lead to a steady progression of load transfer that exceeds the capacity of other surrounding elements, thus initiating the progression that leads to a total or partial collapse of the structure.'*

NIBS Multihazard Mitigation Council [MMC, 2002]

> *'...failure of part of the structure [...] lead to disproportionate damage.'*

Dutch Building Code NEN6700:1991 article 5.3.3 [NNI, 1991]

> *'...an initial local failure of a structural element, caused by an abnormal event or severe overload, [...] spread to other structural members and precipitate the collapse of a disproportionately large portion of the structure.'*

National Building Code of Canada, 1977 [NRCC, 1998]

> *'...in the event of an accident [...] suffer collapse to an extent disproportionate to the cause...'*

UK Building Regulations 1991 [HMSO, 1991]

> *'...being damaged to an extent disproportionate to the original local damage...'*

US Department of Defense, Interim Antiterrorism/Force Protection Construction Standards [DoD, 2001]

Appendix B

Catenary Action

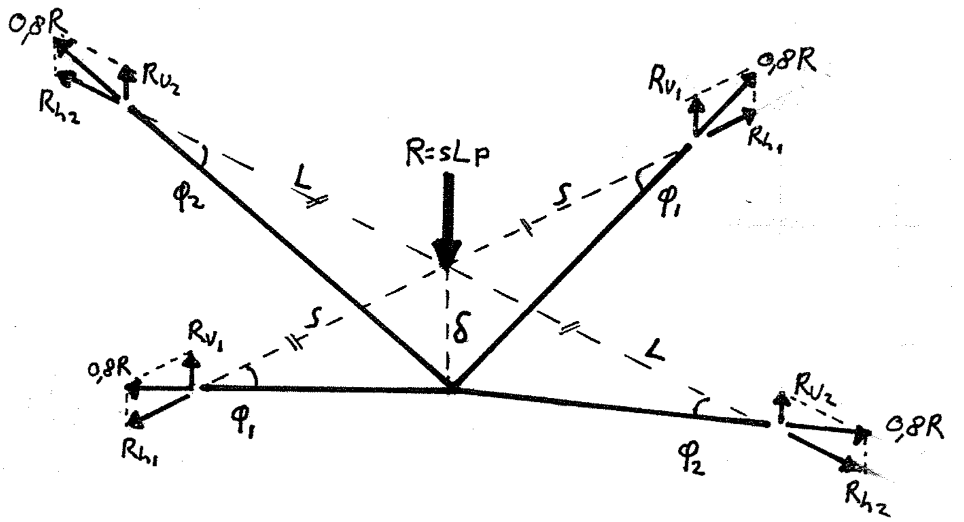

Figure B.1: Force diagram of the catenary effect of two perpendicular ties.

Figure B.1 depicts a schematical representation of two perpendicular ties. In double span condition these ties have a total length of length of respectively $2s$ and $2L$. A load R is applied at the intersection of the ties. The load R is the resultant of the surface load p so it is represented by:

$$R = sLp$$

Starting point of the calculation of the displacement δ is that the supports are rigid so the deflection has to be fully enabled by elongation of the ties. Furthermore the tensile force in both ties should not exceed 80% of the applied load R.

The tensile force has a vertical component Rv and a horizontal component

Rh. From vertical equilibrium of forces it follows that:

$$R = 2Rv_1 + 2Rv_2 \tag{B.1}$$

Furthermore Rv_1 and Rv_2 can be defined as:

$$Rv_1 = \sin\phi_1 \cdot 0.8R \tag{B.2}$$
$$Rv_2 = \sin\phi_2 \cdot 0.8R \tag{B.3}$$

When Equations B.2 and B.3 are combined with Equation B.1 it follows that:

$$1.6\sin\phi_1 + 1.6\sin\phi_2 = 1 \tag{B.4}$$

From basic algebra it follows that:

$$\delta = s\tan\phi_1 = L\tan\phi_2 \tag{B.5}$$

This can be rewritten as:

$$\sin\phi_1 = \frac{\delta}{s}\cos\phi_1 \tag{B.6}$$
$$\sin\phi_2 = \frac{\delta}{L}\cos\phi_2 \tag{B.7}$$

When we combine these two equations with Equation B.4 we obtain:

$$1.6\frac{\delta}{s}\cos\phi_1 + 1.6\frac{\delta}{L}\cos\phi_2 = 1 \tag{B.8}$$

Now we assume ϕ to be small so $\cos\phi \approx 1$ so Equation B.8 reduces to:

$$1.6\frac{\delta}{s} + 1.6\frac{\delta}{L} = 1 \tag{B.9}$$

This can also be written as:

$$\delta = \frac{sL}{1.6(s+L)} \tag{B.10}$$

As an example a building with a normal span s of 6.0 m in one direction and a span L of 7.2 m in the other direction is considered. The tensile capacity of the ties is indeed 80% of the resultant of the surface load. If one column is removed and a double span condition is created we obtain a displacement δ of:

$$\delta = \frac{6 \cdot 7.2}{1.6(6+7.2)} = 2.05m$$

This means the elongation of the shorter tie of 6.0 m will be:

$$\Delta s = \sqrt{6^2 + 2.05^2} - 6 = 0.34m$$

Note that the assumption that ϕ is small is not valid with this kind of deflection, so the solution is not exact. However, the case illustrates the order of magnitude of the deformations in catenary action if the ties are designed according to Eurocode recommendations.

Appendix C

Elongation Capacity of Tie Connections

In this appendix the proposed formulas for estimation of tie displacements derived from [Engström, 1992] are given. These formulas are then applied to calculate tie elongations in four different cases.

C.1 Ribbed Bars

For ribbed bars the ultimate displacement mainly depends on the steel strain within the plastic zone. It can be calculated from the mean bond stress in the plastic zone $\tau_{m,pl}$:

$$\begin{array}{rrcll} & \tau_{m,pl} & \approx & 0.27\tau_{max} & \\ \text{with} & \tau_{max} & = & 2.5\sqrt{f_{cc}} & \text{for 'good' bond conditions} \\ \text{and} & \tau_{max} & = & 1.25\sqrt{f_{cc}} & \text{for 'poor' bond conditions} \end{array}$$

where τ_{max} is the bond strength
f_{cc} is the compressive strength of concrete or grout (cylinder strength according to Standard test)

The ultimate extension of the plastic zone $l_{t,pl}$ can be determined as:

$$l_{t,pl} = \frac{f_{su} - f_{sy}}{\tau_{m,pl}} \cdot \frac{\phi}{4}$$

where f_{su} is the tensile strength of the reinforcing steel
f_{sy} is the yield strength of the reinforcing steel
ϕ is the diameter of the reinforcing bar

Under assumption that the steel strain distribution in the plastic zone is approximately linear, the mean value of the steel strain $\epsilon_{m,pl}$ is:

$$\epsilon_{m,pl} \approx 0.5\epsilon_{su}$$

where ϵ_{su} is the total elongation of reinforcing steel at maximum load (limit strain)

The ultimate displacement (elongation capacity) w_u can be calculated as:

$$w_u = \epsilon_{su} \cdot l_{t,pl} + w_y$$

where w_y is the maximum elastic displacement of the tie connection

C.2 Smooth Bars

For smooth bars the tensile force in the plastic stage is mainly resisted by the end hooks, although the frictional resistance can not be neglected.The frictional bond stress in the plastic zone $\tau_{f,pl}$ can be estimated as:

$$\begin{aligned} \tau_{f,pl} &= 0.05\sqrt{f_{cc}} \quad \text{for 'good' bond conditions} \\ \tau_{f,pl} &= 0.025\sqrt{f_{cc}} \quad \text{for 'poor' bond conditions} \end{aligned}$$

The length of the plastic zone $l_{t,pl}$ is again calculated as:

$$l_{t,pl} = \frac{f_{su} - f_{sy}}{\tau_{f,pl}} \cdot \frac{\phi}{4} \text{ for } l_{t,pl} \leq l_a$$

where l_a is the anchorage length between the joint face and the end hook

The ultimate displacement w_u is estimated as:

$$w_u \approx l_{t,pl} \cdot \epsilon_{su}$$

When $l_{t,pl} \geq l_a$ the yield penetration has reached the end hooks and the steel stress at the end anchor σ_{sa} is determined as:

$$\sigma_{sa} = f_{su} - \frac{4 \cdot l_a \cdot \tau_{f,pl}}{\phi}$$

The ultimate displacement w_u is estimated using the mean steel stress over the anchorage length σ_{sm}:

$$\sigma_{sm} = \frac{\sigma_{sa} + f_{su}}{2}$$

$$w_u \approx \frac{\sigma_{sm} - f_{sy}}{f_{su} - f_{sy}} \epsilon_{su} \cdot 2 \cdot l_a$$

In pure tension the calculated elongation with the proposed formulas showed good agreement with experiments, but in bending mode the elongation was considerably overestimated. Therefore a reduction factor 0.5 is recommended for elongation in bending mode.

C.3 Calculation Examples

For a tie connection with bar diameter ϕ of 16 mm and an anchorage length l_a of $75\phi = 1200$ mm the estimated elongation has been calculated from the formulas above. This is done for four cases with varying concrete and steel characteristics as given in Figure C.1.

The calculated tie elongations were applied to the example treated in Appendix B. Considering the ties in this example the obtained deflection δ can be calculated from the elongation of the ties. The required tensile capacity of the internal tie T_i as related to the vertical reaction force R is then calculated. The results are given in Figure C.2 for ribbed tie bars and in Figure C.3 for smooth tie bars.

No.	Concrete quality	fcc [N/mm2]	Steel quality	fy [N/mm2]	fu [N/mm2]	εy [%]	εu [%]	ϕ [mm]	la [mm]
1	C28/35	28	FeB500 HWL, HK	500	560	2,50	3,25	16	1200
2	C53/65	53	FeB500 HWL, HK	500	560	2,50	3,25	16	1200
3	C28/35	28	FeB220 HWL	220	250	1,10	5,00	16	1200
4	C28/35	28	FeB500 Bigaj*	580	661	2,00	9,00	16	1200

* Experimentally obtained values taken from [Bigaj, 1999]

Figure C.1: Applied numerical values for the calculation of the elongation of structural ties.

Ribbed bars:

No.	bond	τmax [N/mm2]	τmpl [N/mm2]	ltpl [mm]	wy [mm]	wu [mm]	δ [m]	Ti/R [-]
1	good	13,23	3,57	67,19	3,00	5,18	0,25	6,56
	poor	6,61	1,79	134,39	3,00	7,37	0,30	5,50
2	good	18,20	4,91	48,84	3,00	4,59	0,23	6,97
	poor	9,10	2,46	97,68	3,00	6,17	0,27	6,01
3	good	13,23	3,57	33,60	1,32	3,00	0,19	8,62
	poor	6,61	1,79	67,19	1,32	4,68	0,24	6,90
4	good	13,23	3,57	90,71	2,40	10,56	0,36	4,59
	poor	6,61	1,79	181,42	2,40	18,73	0,47	3,45

Figure C.2: Calculated elongation and required tensile capacity of ties consisting of ribbed tie bars.

Smooth bars:

No.	bond	τfpl	ltpl	σsa	σsm	wu	0,5wu	δ	Ti/R
		[N/mm2]	[mm]	[N/mm2]	[N/mm2]	[mm]	[mm]	[m]	[-]
1	good	0,26	907,11			29,48	14,74	0,42	3,89
	poor	0,13	1814,23	520,31	540,16	52,20	26,10	0,56	2,92
2	good	0,36	659,33			21,43	10,71	0,36	4,56
	poor	0,18	1318,66	505,40	532,70	42,51	21,25	0,51	3,24
3	good	0,26	453,56			22,68	11,34	0,37	4,43
	poor	0,13	907,11	210,31	230,16	40,63	20,31	0,49	3,31
4	good	0,26	1224,60	581,63	621,31	110,17	55,08	0,81	2,01
	poor	0,13	2449,21	621,31	641,16	163,08	81,54	0,99	1,65

Figure C.3: Calculated elongation and required tensile capacity of ties consisting of smooth tie bars.

Appendix D

Technical Drawing of Studied Office Building

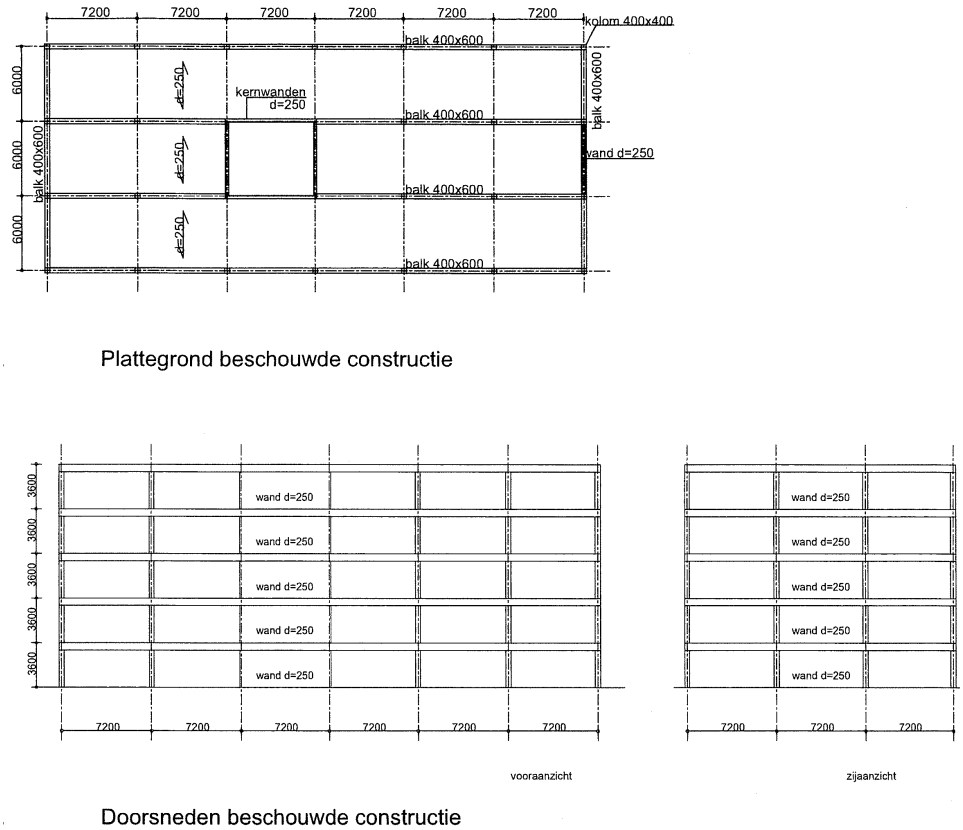

Figure D.1: Technical drawing of the bearing structure of the studied office building. (source:[Stufib, 2005])

Appendix E

Design of Office Building

The required amount of reinforcement for the studied office building is calculated using a linear calculation model.

E.1 Design of Beams

In Figure E.1 and Figure E.2 the calculated internal moments and shear forces are depicted. Because these models were also used for calculation of the required reinforcement for the columns, the live load of the first three floors was reduced by the momentary factor. Therefore the beam of the fourth floor gives the normative values for the internal forces. For the interior beams the bottom reinforcement of the middle bay of the right beam is less because of the lower internal moment force.

In Figure E.1 and Figure E.2 the design values in Ultimate Limit State are indicated. In Table E.1 and E.2 the design values, the applied reinforcement and the limit load of the applied reinforcement is given. For calculation of limit load of the members Appendix F is referred to. For the beams in the head facades minimum reinforcement was sufficient. The models and design values for the internal forces are not depicted.

E.2 Design of Columns

For the columns a universal four-sided reinforcement lay-out was chosen. The columns have a chosen minimum reinforcement of $\phi 12$ bars. Because the normal force in the columns at the top floor is small these columns give the normative design reinforcement. The required reinforcement was calculated by means of interaction diagrams. In Figure E.3 the interaction diagram for the critical cross-section of the corner columns is depicted. In Table E.3 the design values and chosen reinforcement is presented.

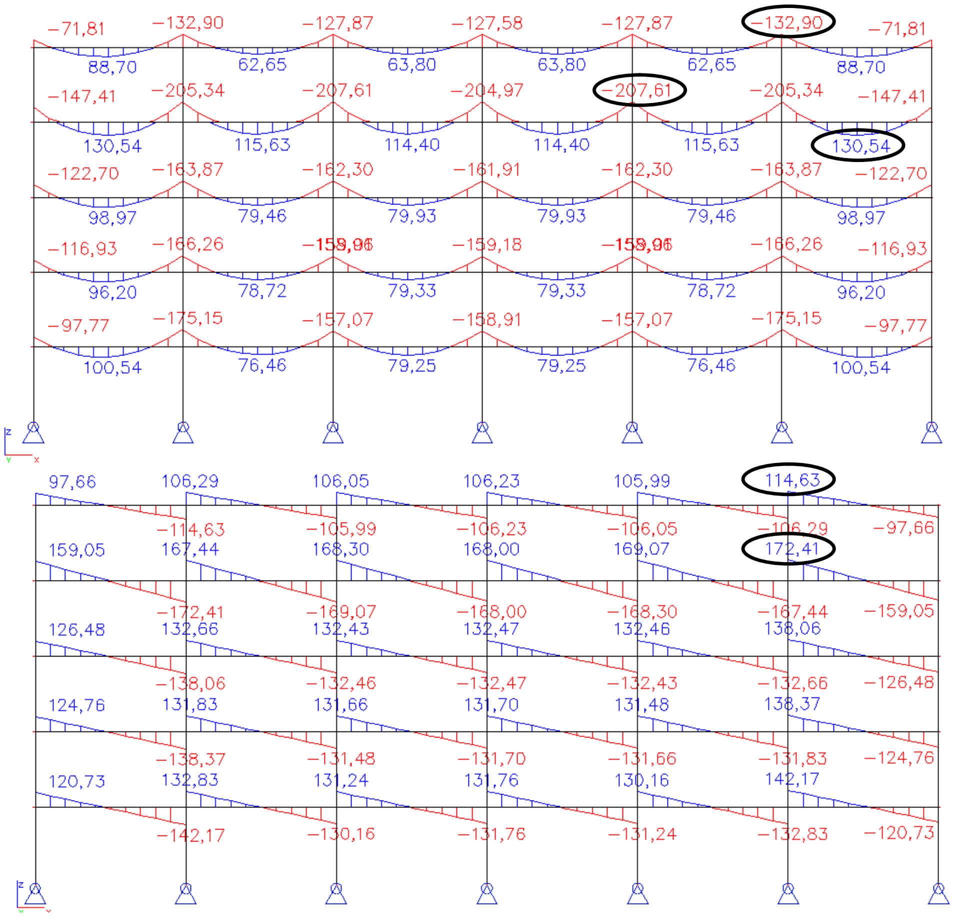

Figure E.1: Internal moment forces (top) and shear forces (bottom) of the facade beams in Ultimate Limit State.

Facade Beams

Floor Beams	**Span**	**Support**	**Shear**
Md/Vd	+130.5 kNm	-207.6 kNm	172.4 kN
reinforcement	$5\phi12$	$5\phi16$	$\phi8-300$*
Mu/Vu	133.0 kNm	231.2 kNm	172.5 kN
Roof Beams			
Md/Vd	+88.7 kNm	-132.9 kNm	114.6 kN
reinforcement	$4\phi12$*	$5\phi12$	$\phi8-300$*
Mu/Vu	107.0 kNm	133.0 kNm	172.5 kN

* prescribed minimum reinforcement

Table E.1: Design and ultimate forces of the facade beams.

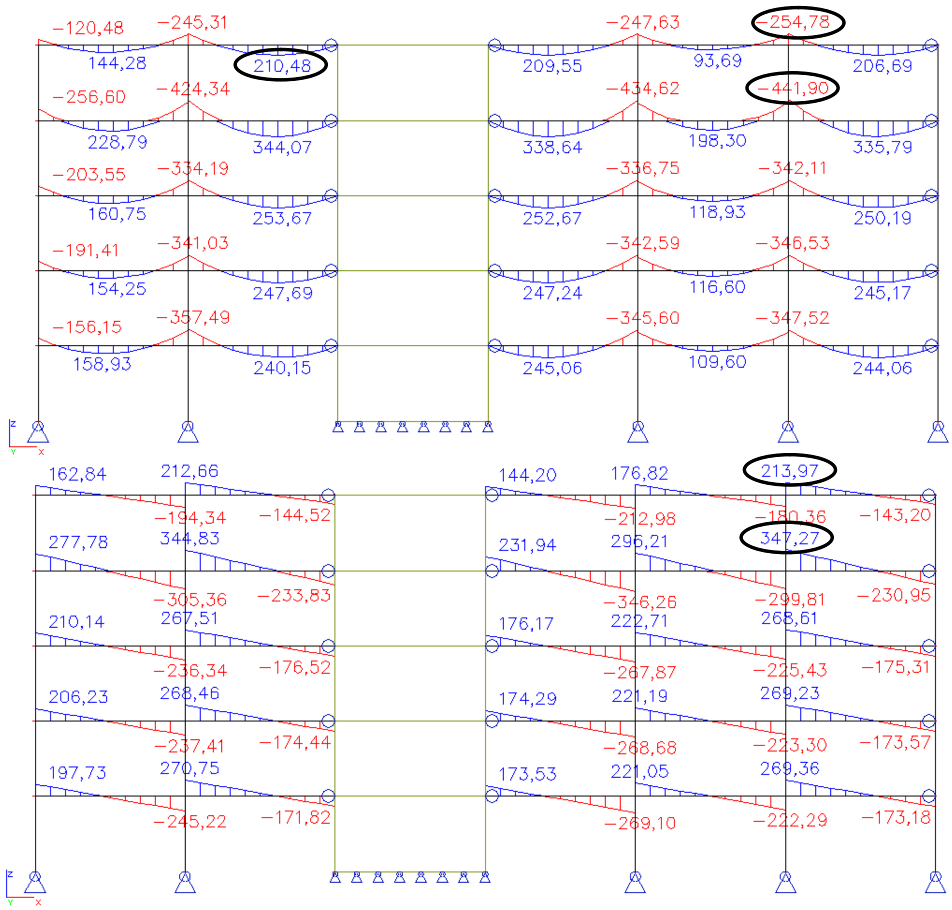

Figure E.2: Internal moment forces (top) and shear forces (bottom) of the interior beams in Ultimate Limit State.

Interior Beams

Floor Beams	**Span**	**Midbay**	**Support**	**Shear**
Md/Vd	+344.1 kNm	+198.3 kNm	-441.9 kNm	347.3 kN
reinforcement	$5\phi20$	$5\phi16$	$5\phi25$	$\phi10-100$
Mu/Vu	350.9 kNm	231.2 kNm	523.0 kNm	348.6 kN
Roof Beams				
Md/Vd	+210.5 kNm	+93.7	-254.8 kNm	214.0 kN
reinforcement	$5\phi16$	$4\phi12$*	$5\phi20$	$\phi8-150$
Mu/Vu	231.2 kNm	107.0 kNm	359.9 kNm	318.2 kN

* prescribed minimum reinforcement

Table E.2: Design and ultimate internal forces of the interior beams.

Columns

Corner Columns	Nd	Mx	My	Reinf.	Mu
Nmax	-840.1 kN				176.3 kNm
Critical Section	-140 kN	80 kNm	50 kNm	$8\phi12$	91.0 kNm
Facade Columns					
Nmax	-1374.6 kN				203.9 kNm
Critical Section	-220 kN	20 kNm	15 kNm	$8\phi12$	103.4 kNm
Interior Columns					
Nmax	-2278.2 kN				174.4 kNm
Critical Section	-350 kN	40 kNm	0 kNm	$8\phi12$	122.7 kNm

Table E.3: Design values for internal forces of columns and the corresponding chosen reinforcement.

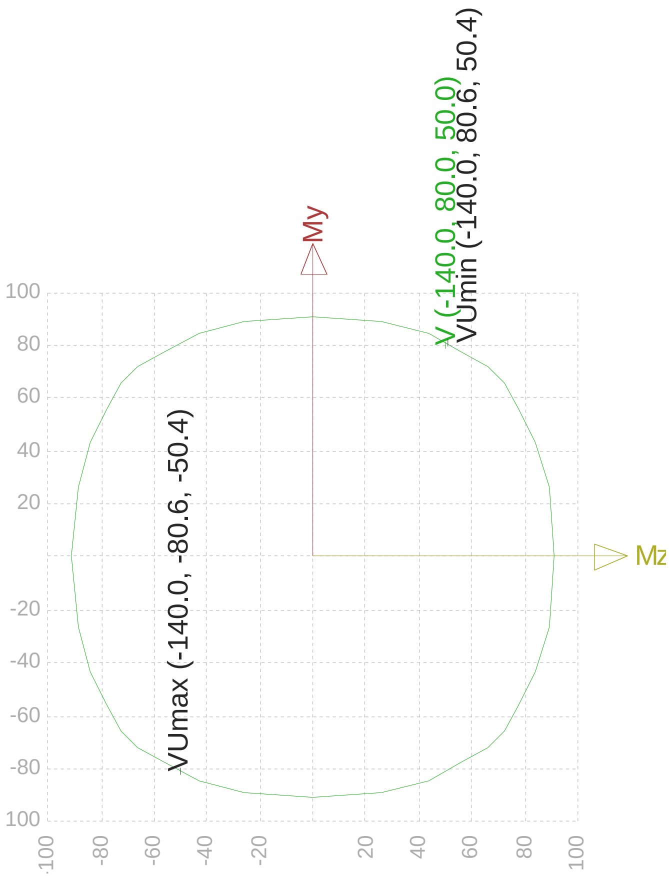

Figure E.3: Check of critical cross section of the corner columns.

E.3 Reinforcement Lay-out

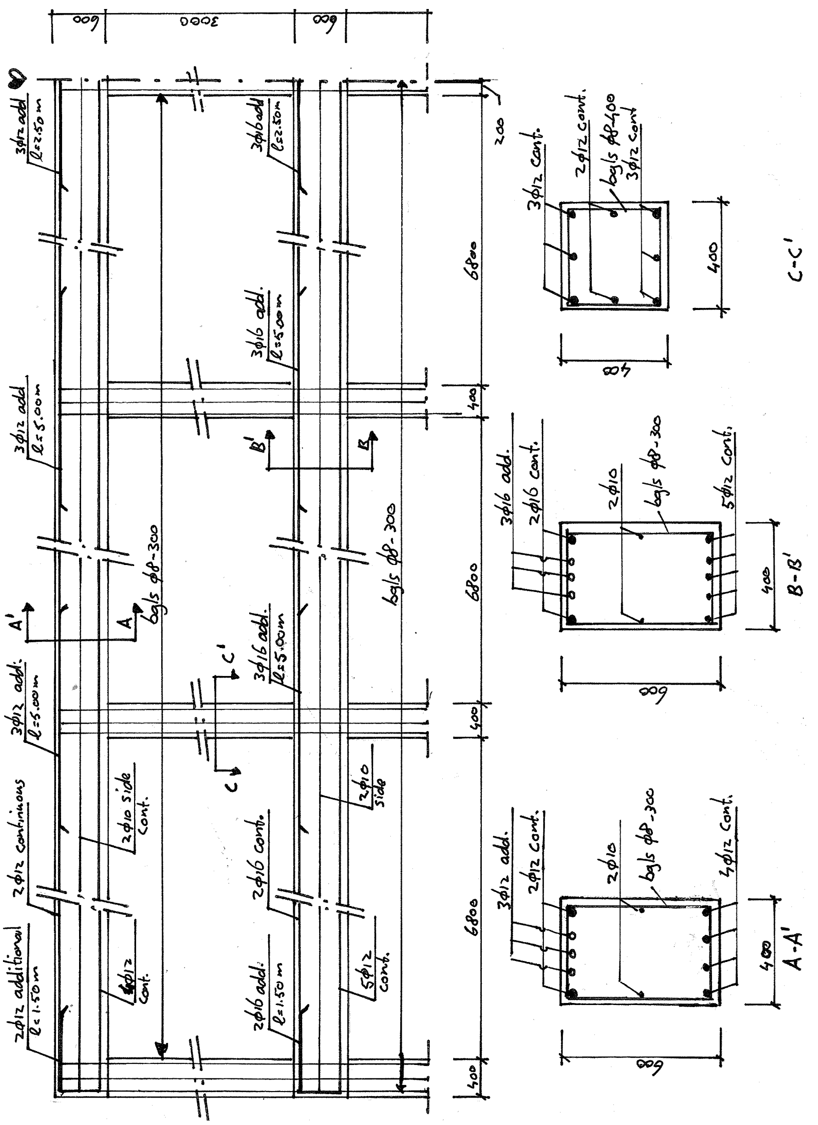

Figure E.4: Reinforcement lay-out of facade beams long side. Roof- and floor beam depicted.

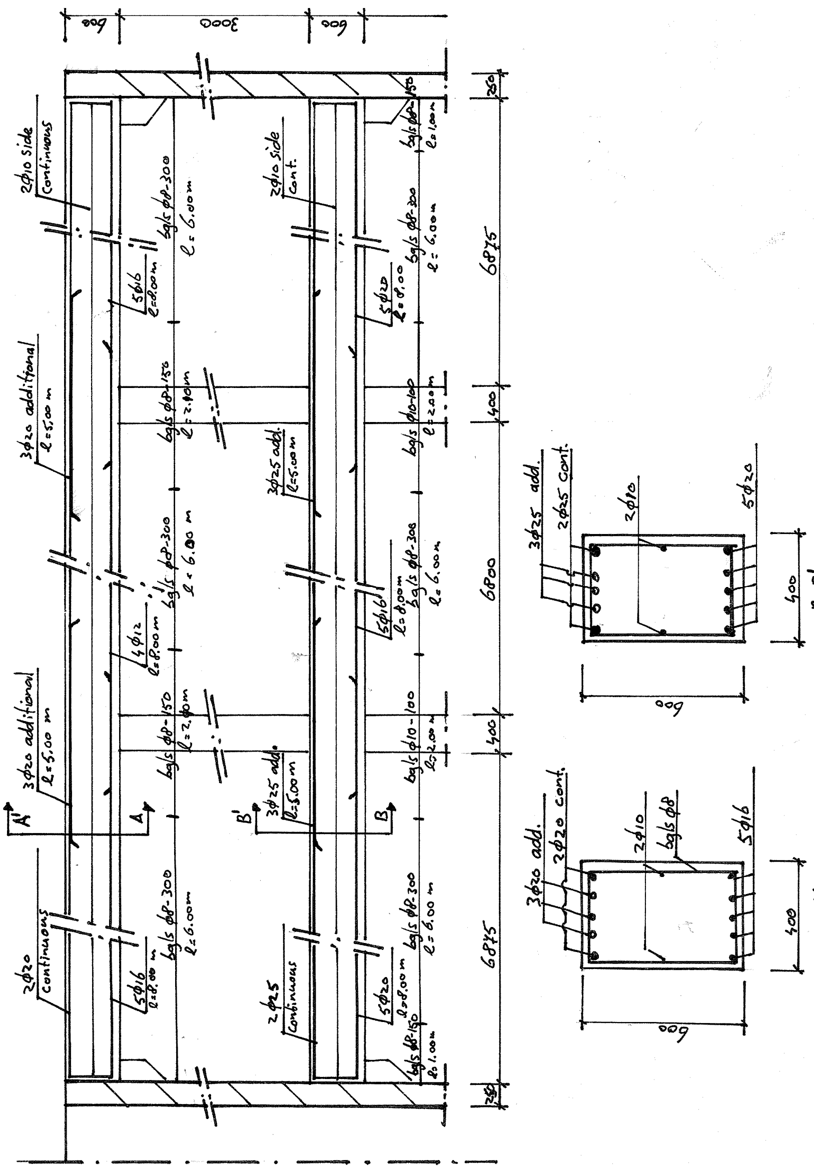

Figure E.5: Reinforcement lay-out of interior beams. Roof- and floor beam depicted.

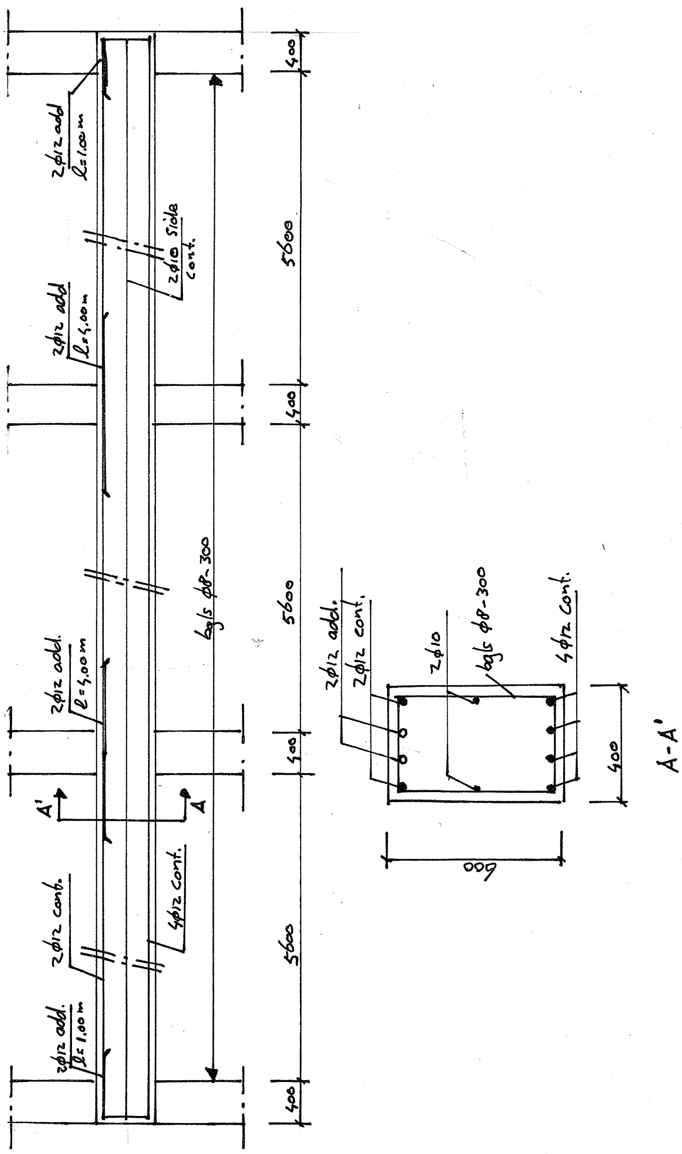

Figure E.6: Reinforcement lay-out of beams head facade.

Appendix F

Member Capacity

Flexural capacity beams

Dim:	b: 400 mm		h: 600 mm		A: 240000 mm2		
Concrete: C28/35	γm	f'b	γm	fb	Steel: FeB500	γm	fs
Normal loading:	1,2	21	1,4	1,40		1,15	435
Special loading:	1,0	25,2	1,2	2,33		1,0	500
ωmin	0,18 %	Asmin	432 mm2				
Details:	c: 30 mm		φstirrup: 8 mm				

Applied reinforcement:					Normal load:		Special load:	
n	φ	d	As	ω0	M/bd2	Mu	M/bd2	Mu
[-]	[mm]	[mm]	[mm2]	[%]	[-]	[kNm]	[-]	[kNm]
4	12	556	452	0,203	865	107,0	996	123,1
5	12	556	565	0,254	1075	133,0	1238	153,1
5	16	554	1005	0,452	1870	231,2	2155	266,5
5	20	552	1571	0,706	2838	350,9	3275	405,0
5	25	550	2454	1,104	4230	523,0	4891	604,8

Shear capacity beams

	2 bars		
τ1;norm	0,56 N/mm2	V1	124,1 kN
τ1;spec	0,93 N/mm2		

Applied stirrups:				Normal load:			Special load:		
φ	s	d	Asv	τs	τ	Vu	τs	τ	Vu
[mm]	[mm]	[mm]	[mm2]	[N/mm2]	[N/mm2]	[kN]	[N/mm2]	[N/mm2]	[kN]
8	300	554	335	0,22	0,78	172,5	0,25	1,18	262,5
8	150	554	670	0,44	1,00	221,0	0,50	1,44	318,2
10	100	550	1571	1,02	1,58	348,6	1,18	2,11	464,5

Figure F.1: Calculation of the ultimate capacity of beams under normal and special loading conditions.

Ultimate Capacity of Columns

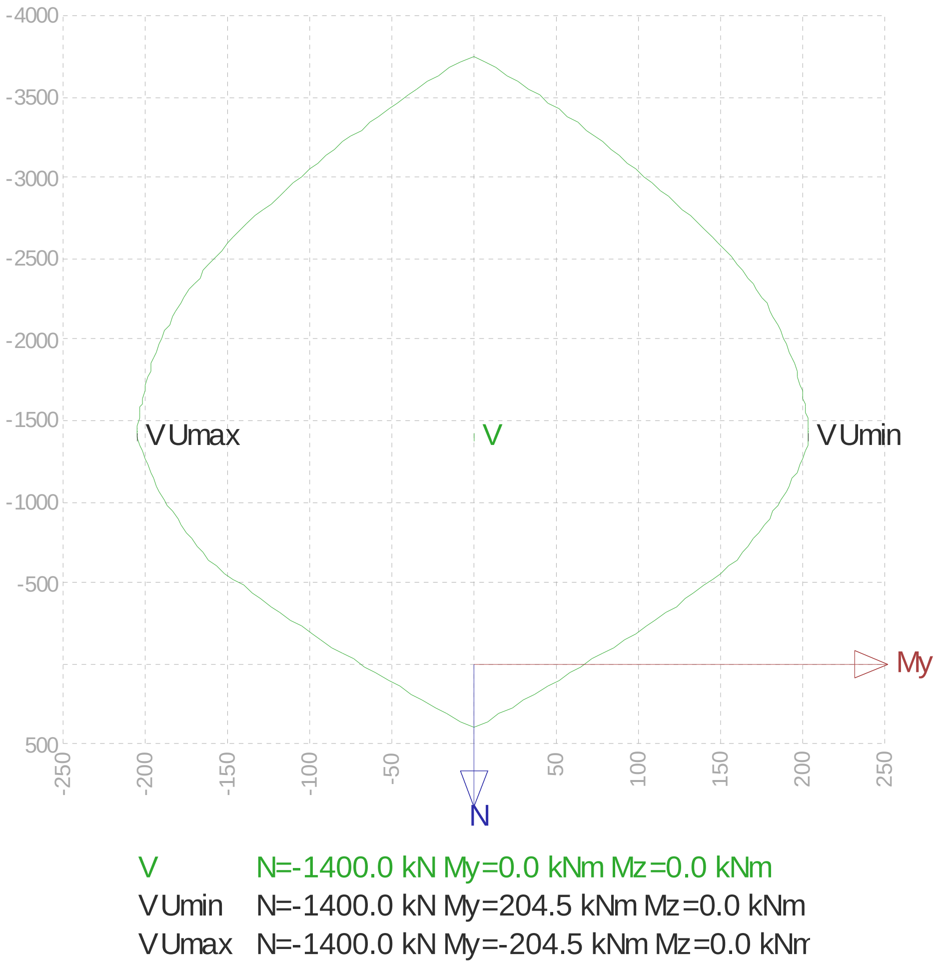

Figure F.2: Interaction diagram of columns under normal loading conditions generated according to NEN6720 [NNI, 1995]

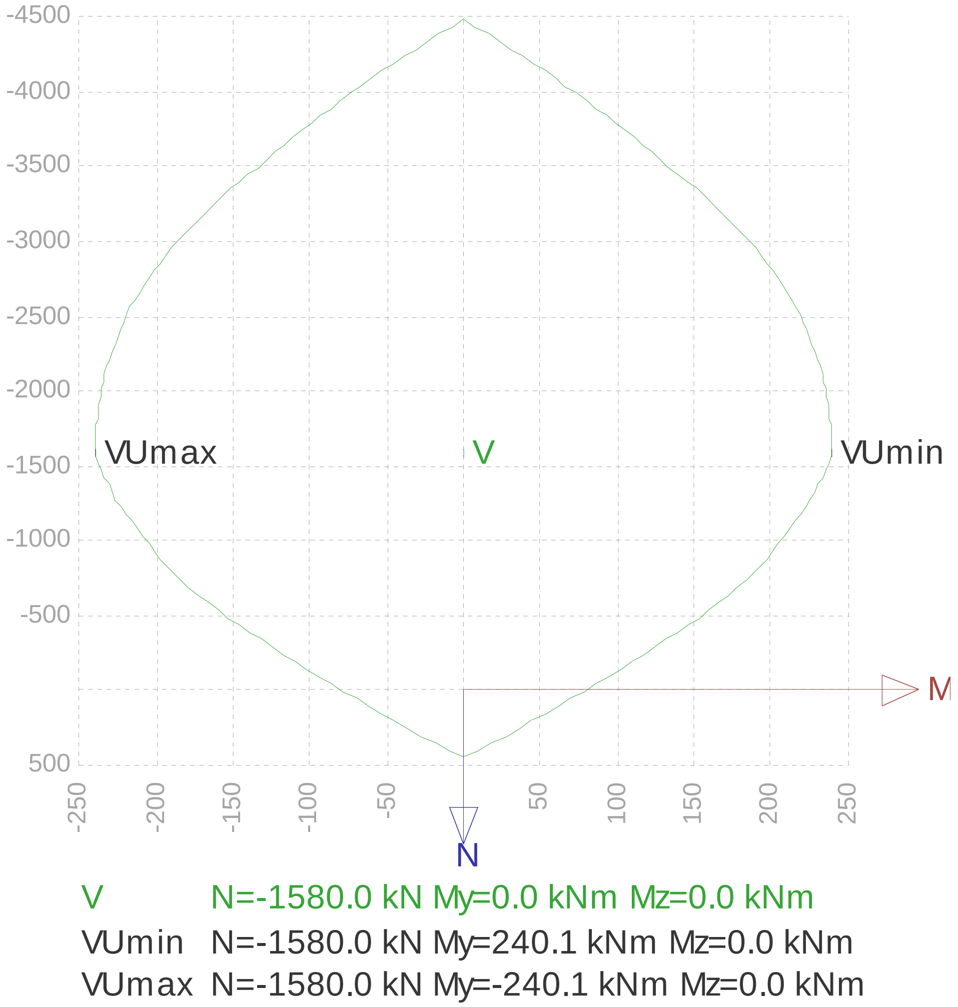

Figure F.3: Interaction diagram of columns under special loading conditions ($\gamma_m = 0$) generated according to NEN6720 [NNI, 1995].

Appendix G

Test Specimens Bigaj

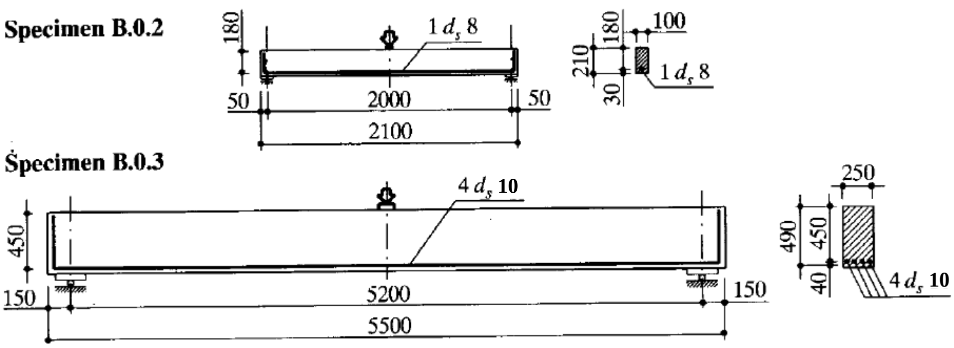

Figure G.1: Geometry of test specimens. (source:[Bigaj, 1999])

Specimen	Size	Reinforcement	ω_o
B.0.2.4	100x210x2000	$1\phi8$	0.28 %
B.0.3.4	250x490x5200	$4\phi10$	0.28 %
B.1.3.4	250x490x5200	$4\phi20$	1.12 %

Table G.1: Characteristics of test specimens.

Steel	d_s [mm]	f_y [MPa]	f_t [MPa]	f_t/f_y [-]	ϵ_u [%]
FeB 500 HWL	8	562	641	1.14	9.17
	10	568	641	1.13	9.36
	20	550	650	1.18	9.27

Concrete	Specimen	f_{cc} [MPa]	f_{cts} [MPa]	E_c [MPa]
C28/35	B.0.2.4	34.40	2.37	31823
	B.0.3.4	33.52	2.31	31407
	B.1.3.4	32.26	2.26	32440

Table G.2: Mechanical characteristics of reinforcing steel and concrete used in the experiments.

B.0.2.4						
Load	**10,3 kN**			**11,2 kN**		
	εc [·1e-4]	**εs** [·1e-4]	**fu** [mrad]	**εc** [·1e-4]	**εs** [·1e-4]	**fu** [mrad]
Experiment	7.0	45.5	13.0	16.3	991.8	76.0
ESA	35.0	478.5	9.7	35.0	483.0	67.8
Ratio	5.00	10.52	0.75	2.15	0.49	0.89

B.0.3.4						
Load	**50,2 kN**			**64,9 kN**		
	εc [·1e-4]	**εs** [·1e-4]	**fu** [mrad]	**εc** [·1e-4]	**εs** [·1e-4]	**fu** [mrad]
Experiment	4.9	24.2	4.2	7.1	578.4	32.9
ESA	7.6	24.9	7.6	35.0	488.7	55.0
Ratio	1.55	1.03	1.81	4.93	0.84	1.67

B.1.3.4						
Load	**210,2 kN**			**214,8 kN**		
	εc [·1e-4]	**εs** [·1e-4]	**fu** [mrad]	**εc** [·1e-4]	**εs** [·1e-4]	**fu** [mrad]
Experiment	23.2	39.8	7.0	32.4	199.8	16.1
ESA	35.0	99.2	12.7	35.0	99.2	13.0
Ratio	1.51	2.49	1.81	1.08	0.50	0.81

Figure G.2: Comparison of calculated and experimentally obtained values of concrete strain ϵ_c, steel strain ϵ_s and ultimate rotation f_u of three test specimens.

Appendix H

Original Model of Building

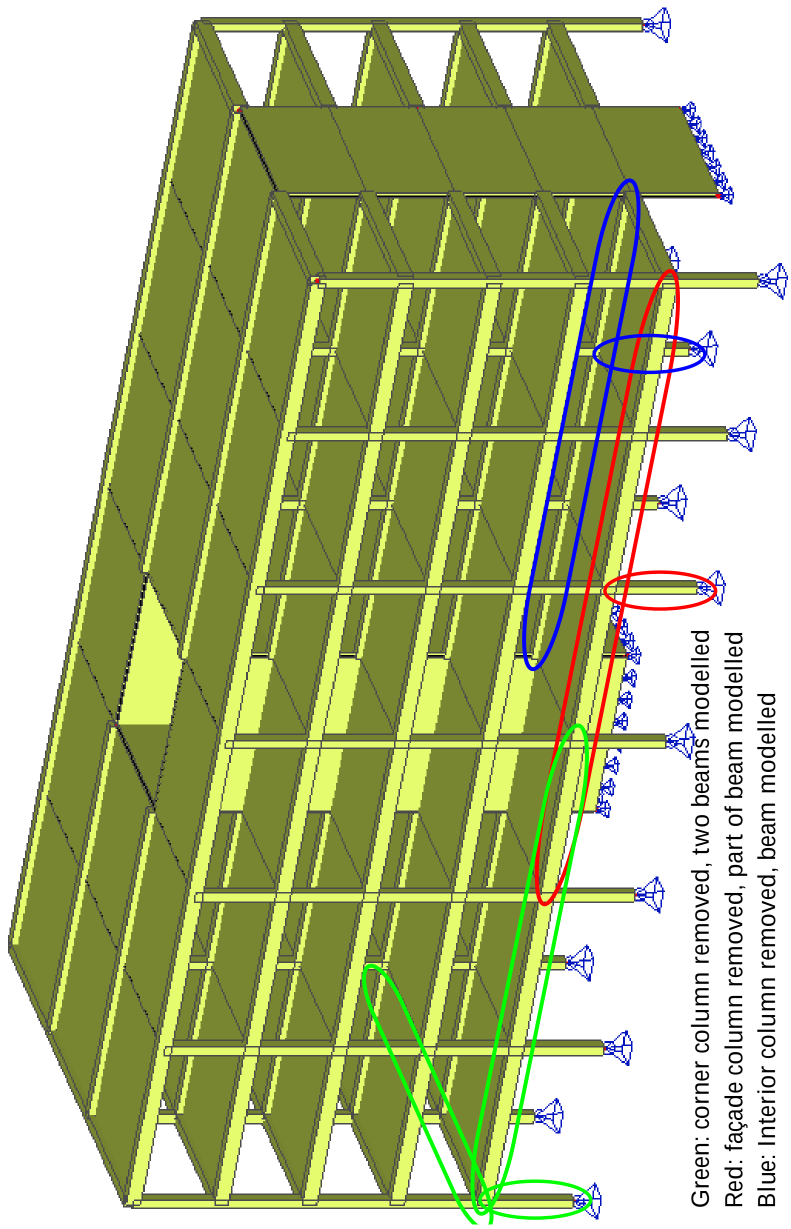

Figure H.1: Object model of office building

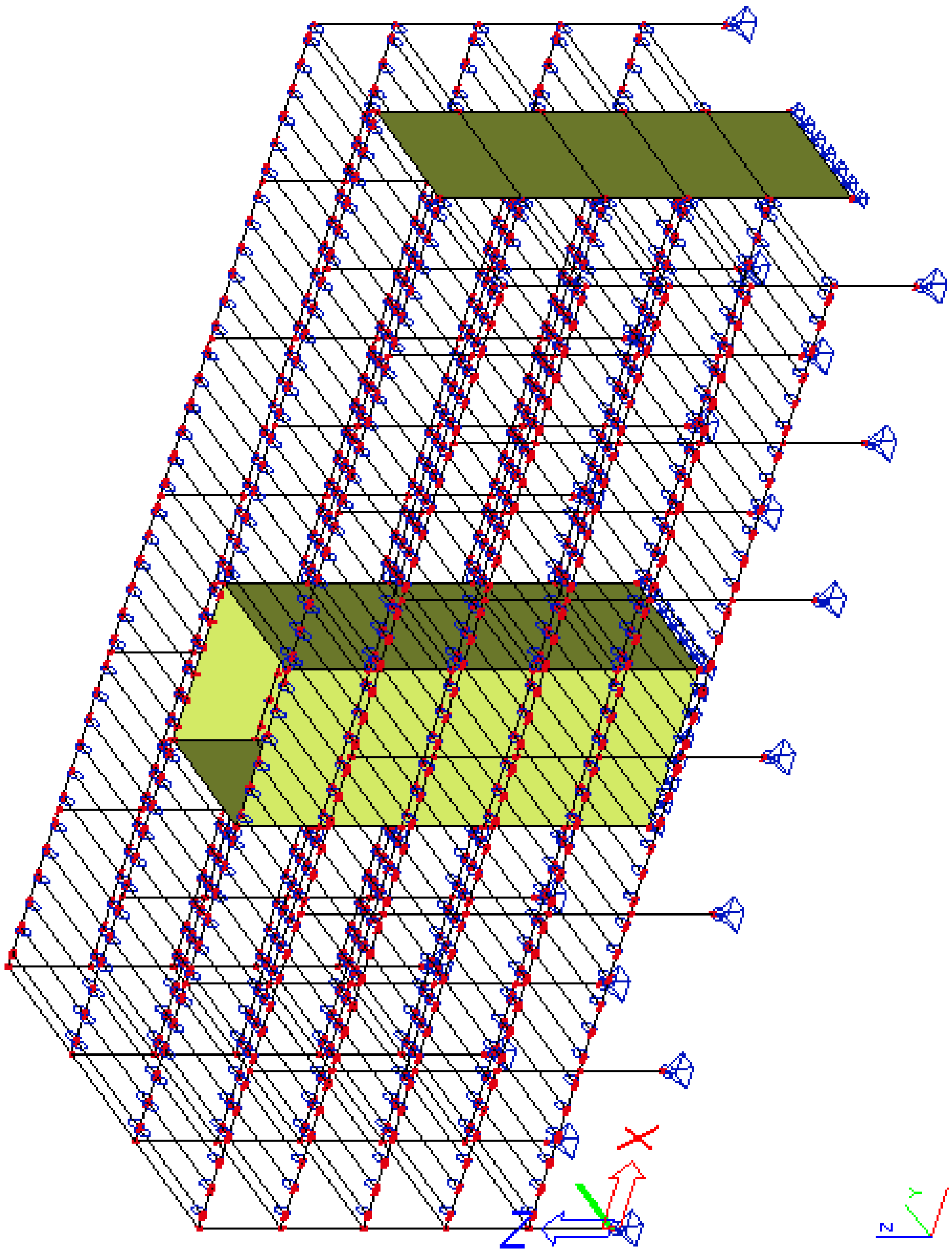

Figure H.2: Calculation model of office building. The hollow core slabs are modeled as members.

Appendix I

Torsional Capacity of Hollow Core Slabs

The hollow core slab was modeled as a hollow box girder with a wall thickness t of 40 mm (Figure I.1). The concrete has concrete quality C45/55.

The torsional moment capacity $M_{t;u}$ is reached if the ultimate shear strength for torsion is exceeded. The ultimate shear strain is determined per NEN 6720 art. 8.4.1.3 as:

$$\tau_1 = 0.3 f_b = 0.3 \cdot 3.17 = 0.95 MPa$$

where τ_1 ultimate shear strength
f_b is the tensile strength of concrete (calculated with γ_m is 1.2)

For thin walled cross sections the maximum shear strain can be calculated from the torsional moment by the formula of Bredt:

$$\tau_{max} = \frac{M_t}{2 A_h t_{min}}$$

where A_h is the area of the hollow section
t_{min} is the minimum wall thickness

With this formula the torsional moment at ultimate strain is calculated:

$$M_{t;u} = 2\tau_1 A_h t_{min} = 2 \cdot 0.95 \cdot 1120 \cdot 120 \cdot 40 \cdot 10^{-6} = 10.21 kNm$$

Because the wall thickness is relatively small a finite element calculation was used to determine the ultimate torsional moment more precisely (See Figure I.3). From this calculation it followed that the ultimate shear strength is reached at a torsional moment of $11.3kNm$.

In the finite element calculation also the torsional moment of inertia I_t is calculated (Figure I.2). When the moment of inertia is known the rotational constant k can be calculated as follows:

$$k = \frac{M_t}{\phi} = \frac{G I_t}{l} = \frac{15 \cdot 10^3 \cdot 2.18 \cdot 10^9}{6 \cdot 10^3} = 5.45 \cdot 10^9 kNm/rad$$

where G is the shear modulus
I_t is the torsional moment of inertia
l is the length of the member

from which follows that the rotation ϕ_u at ultimate rotation is:

$$\phi_u = \frac{M_{t;u}}{k} = \frac{11.3 \cdot 10^6}{5.45 \cdot 10^9} = 2.1 \cdot 10^{-3} rad$$

The load-displacement diagram of Figure I.4 can be drawn, since plastic behaviour is expected after torsional capacity is reached.

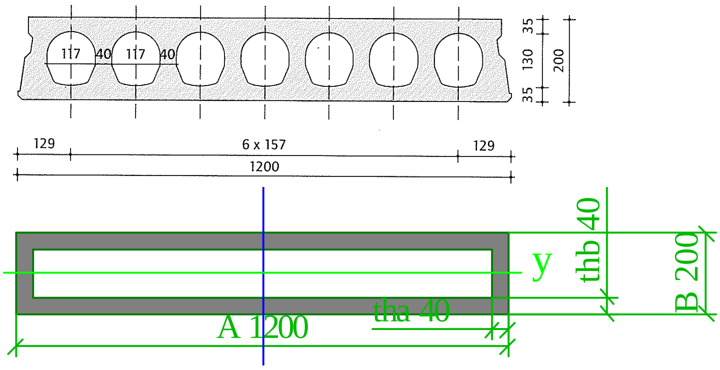

Figure I.1: Actual size of hollow core slab (top) and corresponding model (bottom).

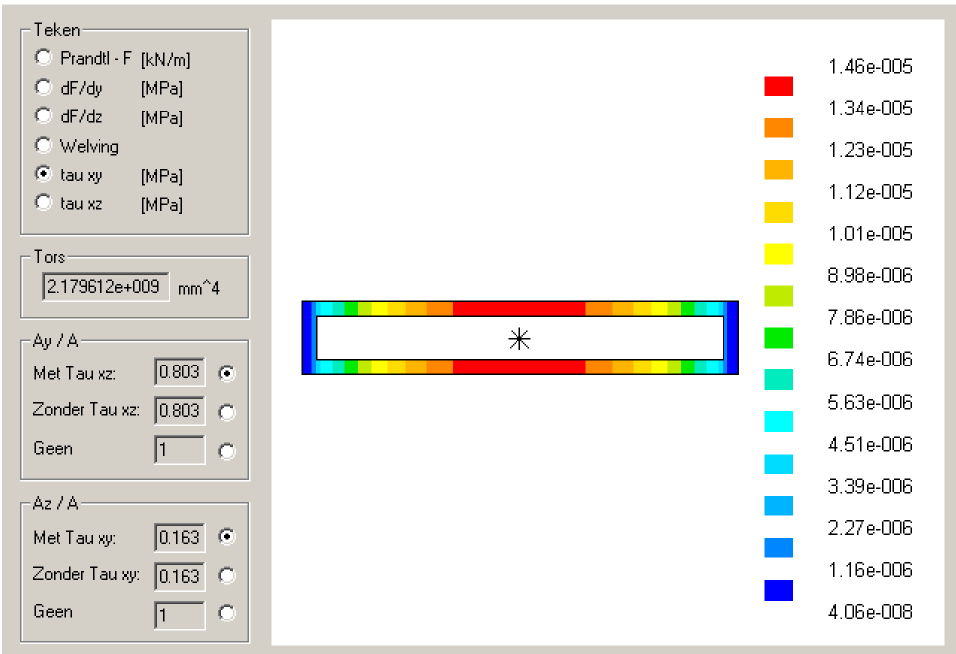

Figure I.2: Finite element calculation of cross-section properties. (FE mesh was set at 1 mm)

1. 1D-Member

Naam	Doorsnede	Lengte [m]	Vorm	Beginknoop	Eindknoop	Type	EEM-type	Laag
S1	CS1 - O (1200, 40, 200, 40)	6,000	Lijn	K1	K2	Algemeen (0)	standaard	Laag1

2. Cross section

Naam	Type	Mater	A [m^2]	A_y [m^2]	A_z [m^2]	I_t [m^4]	I_y [m^4]	I_z [m^4]
CS1	O	B 55	1,0560e-001	8,4805e-002	1,7278e-002	2,1169e-003	6,3872e-004	1,4751e-002

3. Internal Forces

Lineaire berekening, Extreem : Globaal, Systeem : Hoofd
Selectie : Alle
Belastinggevallen : BG1

Staaf	BG	dx [m]	N [kN]	Vy [kN]	Vz [kN]	Mx [kNm]	My [kNm]	Mz [kNm]
S1	BG1	0,000	**0,00**	**0,00**	**0,00**	**11,30**	**0,00**	**0,00**

4. Strain

Lineaire berekening, Extreem : Staaf
Selectie : Alle
Belastinggevallen : BG1

Staaf	BG	dx [m]	Afschuiving [MPa]
S1	BG1	0,000	**0,95**

Figure I.3: Calculation results for hollow core member in torsion.

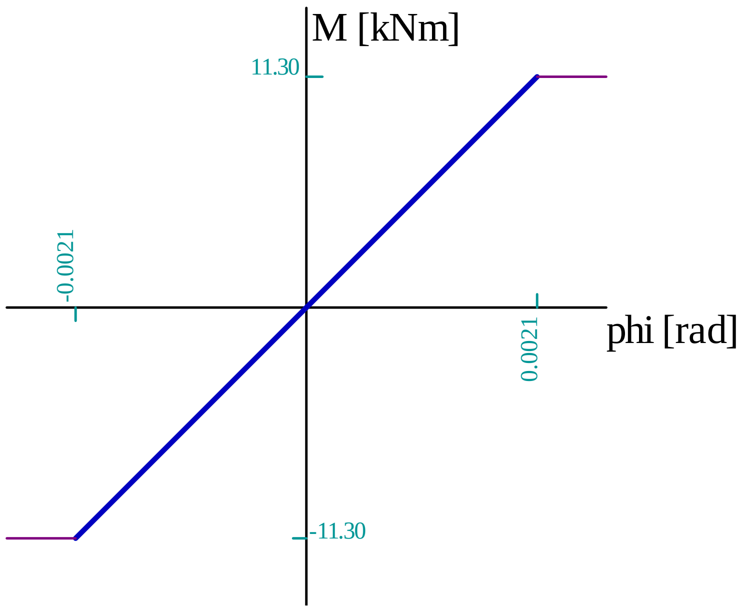

Figure I.4: Assumed torsion rotational characteristics of hollow core slab.

Appendix J

Results of Non-Linear Calculations

J.1 Legend for Tables

Legend	
Uz	Calculated maximum displacement on beam
Fi	Calculated maximum rotation on beam
Md supp	Calculated maximum bending moment at support (for the facade beam this value is taken at a 200 mm offset from the support node
Md span	Calculated maximum bending moment in the span
Md midsp	Calculated maximum bending moment at midspan (this is the critical section for the interior beam)
Md longs	Calculated maximum bending moment at support of facade beam of long side of building (taken at an offset of 200 mm from the support node)
Md shorts	Calculated maximum bending moment at support of facade beam of short side of building (taken at an offset of 200 mm from the support node)
Mu FNL	Ultimate Moment capacity of cross section according to Fysical Non-Linear cross-sectional calculation
Mu Lin	Ultimate Moment capacity of cross section as calculated in Appendix F

The selected limit loadcases are outlined and marked yellow

J.2 Results Facade Beam

Facade Beam w/o floor — Mu FNL: 323.0 197.3 — Mu Lin: 266.5 153.1

Load:	FNL Calculation:				Md/Mu FNL		Linear Calculation:			Md FNL/Md lin		Md lin/Mu lin	
P	Uz	Fi	Md supp	Md span	supp	span	Uz lin	Md supp	Md span	supp	span	supp	span
[kN/m]	[mm]	[mrad]	[kNm]	[kNm]	[-]	[-]	[mm]	[kNm]	[kNm]	[-]	[-]	[-]	[-]
22.5	683.8	108.6	347.2	220.2	1.07	1.12	18.62	302.8	255.6	1.15	0.86	1.14	1.67
22.0	546.4	87.9	331.8	221.4	1.03	1.12	18.20	296.1	249.9	1.12	0.89	1.11	1.63
21.5	343.5	56.8	317.5	221.5	0.98	1.12	17.79	289.3	244.2	1.10	0.91	1.09	1.60
21.0	108.1	19.4	322.9	197.3	1.00	1.00	17.38	282.6	238.5	1.14	0.83	1.06	1.56
20.5	102.5	18.4	314.5	193.2	0.97	0.98	16.96	275.9	232.8	1.14	0.83	1.04	1.52
20.0	97.1	17.5	306.3	189.1	0.95	0.96	16.50	269.2	221.2	1.14	0.86	1.01	1.44
19.5	92.3	16.6	298.1	184.9	0.92	0.94	16.10	262.4	221.5	1.14	0.83	0.98	1.45
19.0	87.9	15.8	290.3	180.3	0.90	0.91	15.70	255.7	215.8	1.14	0.84	0.96	1.41
14.0	56.9	9.9	211.6	135.2	0.66	0.69	11.60	188.4	159.0	1.12	0.85	0.71	1.04
9.0	10.8	2.1	120.5	102.8	0.37	0.52	7.40	121.1	85.2	1.00	1.21	0.45	0.56

Facade Beam with floor — Mu FNL: 323.0 197.3 — Mu Lin: 266.5 153.1

Load:	FNL Calculation:				Md/Mu FNL		Linear Calculation:			Md FNL/Md lin		Md lin/Mu lin	
P	Uz	Fi	Md supp	Md span	supp	span	Uz lin	Md supp	Md span	supp	span	supp	span
[kN/m]	[mm]	[mrad]	[kNm]	[kNm]	[-]	[-]	[mm]	[kNm]	[kNm]	[-]	[-]	[-]	[-]
25.0	922.9	148.7	337.7	218.0	1.05	1.10	20.70	336.4	284.0	1.00	0.77	1.26	1.85
24.0	421.7	70.1	345.2	219.7	1.07	1.11	19.90	323.0	272.6	1.07	0.81	1.21	1.78
23.5	259.9	43.9	329.8	195.9	1.02	0.99	19.40	316.3	266.9	1.04	0.73	1.19	1.74
23.0	131.9	23.5	319.4	190.5	0.99	0.97	19.00	309.5	261.2	1.03	0.73	1.16	1.71
22.5	109.4	19.9	312.1	187.4	0.97	0.95	18.60	302.8	255.6	1.03	0.73	1.14	1.67
22.0	97.3	17.8	304.5	180.6	0.94	0.92	18.20	296.1	249.9	1.03	0.72	1.11	1.63
21.5	88.0	16.1	296.6	176.2	0.92	0.89	17.80	289.3	244.2	1.03	0.72	1.09	1.60
16.0	51.5	9.1	213.1	124.7	0.66	0.63	13.20	215.3	181.7	0.99	0.69	0.81	1.19
10.0	9.3	1.8	116.3	90.9	0.36	0.46	8.30	134.6	113.6	0.86	0.80	0.50	0.74

Figure J.1: Numerical calculation results of facade beam for various loading.

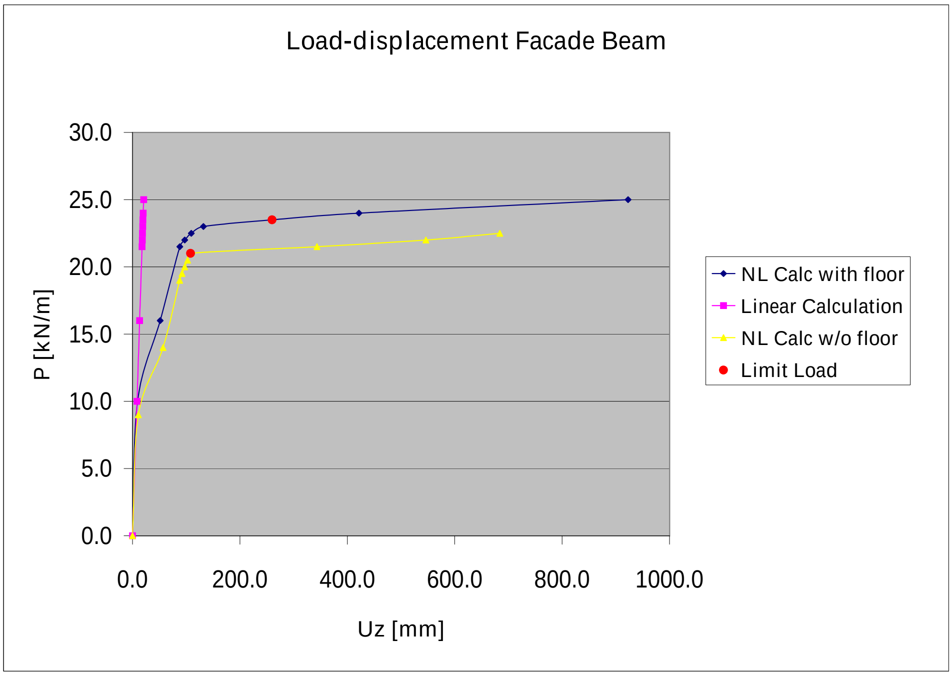

Figure J.2: Load-displacement diagram of facade beam for linear calculation, non-linear calculation without floor action taken into account and non-linear calculation with floor action taken into account.

Facade Beam without floor					
Load [kN/m]	d_x [m]	σ_{cc} [MPa]	ϵ_{cc} $[\cdot 10^{-4}]$	σ_{rt} [MPa]	ϵ_{rt} $[\cdot 10^{-4}]$
21.0	7.0	-35.0	-32.4	556.3	306.5
Facade Beam with floor					
Load [kN/m]	d_x [m]	σ_{cc} [MPa]	ϵ_{cc} $[\cdot 10^{-4}]$	σ_{rt} [MPa]	ϵ_{rt} $[\cdot 10^{-4}]$
23.0	7.0	-35.0	-33.6	559.1	320.3

d_x is position on beam

ϵ_{cc} is concrete compressive strain $\quad$ ϵ_{rt} is reinforcement tensile strain

σ_{cc} is concrete compressive stress $\quad$ σ_{rt} is reinforcement tensile stress

Table J.1: Stresses and strains in the critical cross-section at ultimate load.(See also Figures J.13 and J.14)

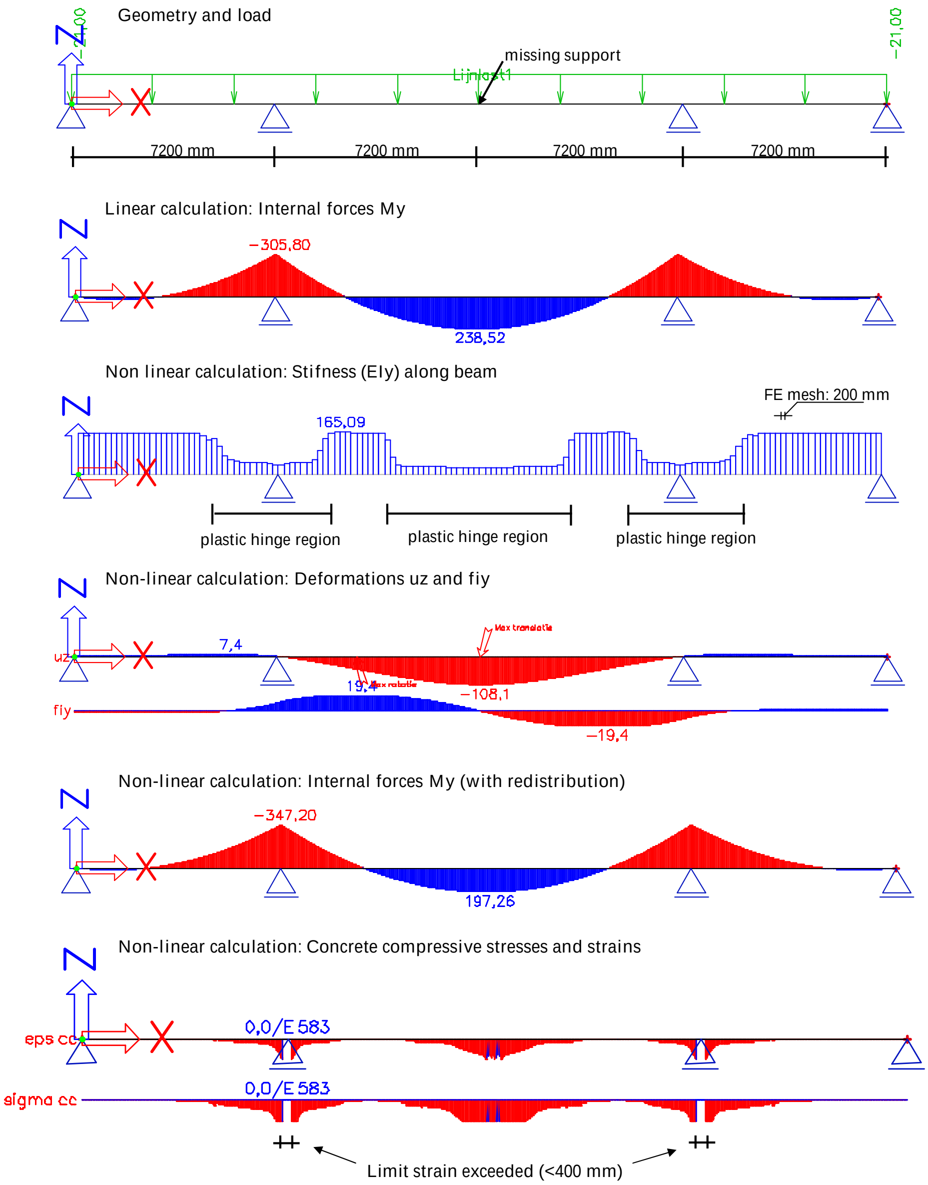

Figure J.3: Graphical representation of results for the limit load case of the facade beam without floor.

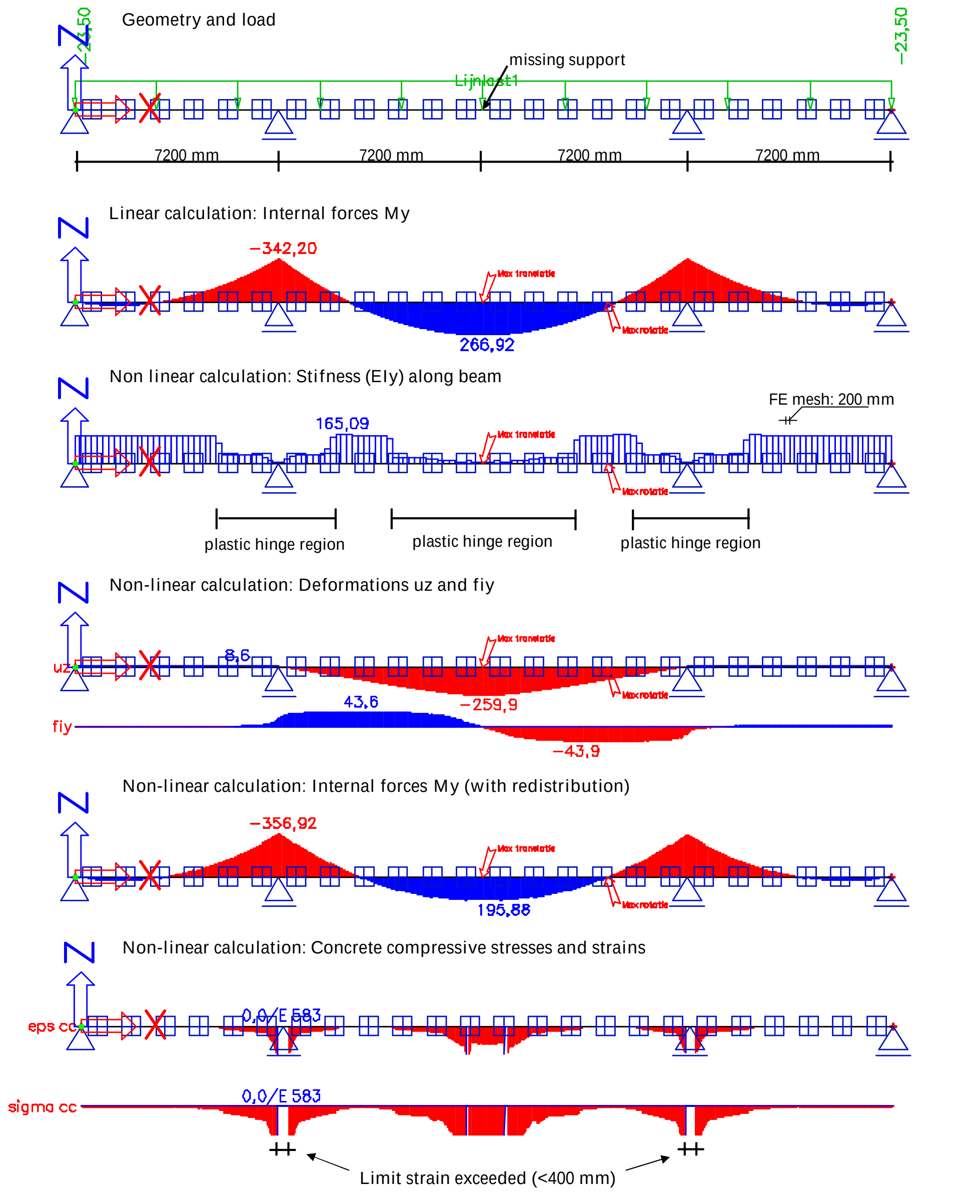

Figure J.4: Graphical representation of results for limit load case of facade beam with floor.

J.3 Results Interior Beam

Interior Beam w/o floor					Mu FNL:	703.2	323.0					Mu Lin:	604.8	266.5
Load:	FNL Calculation:					Md/Mu FNL		Linear Calculation:			Md FNL/Md lin		Md lin/Mu lin	
P	Uz	Fi	Md supp	Md span	Md midsp	supp	midsp	Uz lin	Md supp	Md span	supp	span	supp	span
[kN/m]	[mm]	[mrad]	[kNm]	[kNm]	[kNm]	[-]	[-]	[mm]	[kNm]	[kNm]	[-]	[-]	[-]	[-]
30.0	1187.1	177.5	772.7	410.3	353.9	1.10	1.10	42.3	581.8	512.4	1.33	0.80	0.96	1.92
29.5	732.4	114.5	803.3	405.4	350.1	1.14	1.08	41.6	572.1	505.3	1.40	0.80	0.95	1.90
29.0	218.2	44.2	764.2	417.4	369.0	1.09	1.14	40.9	562.4	495.8	1.36	0.84	0.93	1.86
28.5	173.3	37.7	723.1	421.0	376.9	1.03	1.17	40.2	552.7	488.2	1.31	0.86	0.91	1.83
28.2	159.4	35.6	701.0	422.1	380.2	1.00	1.18	39.8	546.8	483.1	1.28	0.87	0.90	1.81
28.0	156.7	35.1	694.1	419.8	379.7	0.99	1.18	39.5	543.0	479.6	1.28	0.88	0.90	1.80
26.0	125.3	29.5	609.4	403.5	369.2	0.87	1.14	36.7	504.2	445.4	1.21	0.91	0.83	1.67
25.0	118.7	28.1	582.7	389.3	356.6	0.83	1.10	35.3	484.8	428.2	1.20	0.91	0.80	1.61
24.0	112.3	26.7	556.8	374.7	343.6	0.79	1.06	33.8	465.4	410.0	1.20	0.91	0.77	1.54
23.0	106.2	25.3	531.9	359.8	330.2	0.76	1.02	32.4	446.0	392.9	1.19	0.92	0.74	1.47
22.5	103.3	24.6	519.8	352.2	323.3	0.74	1.00	31.7	436.3	384.3	1.19	0.92	0.72	1.44
22.0	100.4	23.9	508.1	344.5	316.2	0.72	0.98	31.0	426.6	375.8	1.19	0.92	0.71	1.41
15.0	63.4	14.8	348.3	234.2	214.7	0.50	0.66	21.1	256.2	290.9	1.36	0.81	0.42	1.09

Interior Beam with floor					Mu FNL:	703.2	323.00					Mu Lin:	604.8	266.5
Load:	FNL Calculation:					Md/Mu FNL		Linear Calculation:			Md FNL/Md lin		Md lin/Mu lin	
P	Uz	Fi	Md supp	Md span	Md midsp	supp	midsp	Uz lin	Md supp	Md span	supp	span	supp	span
[kN/m]	[mm]	[mrad]	[kNm]	[kNm]	[kNm]	[-]	[-]	[mm]	[kNm]	[kNm]	[-]	[-]	[-]	[-]
36.0	967.5	157.5	826.3	451.6	354.6	1.18	1.10	50.8	698.1	616.7	1.18	0.73	1.15	2.31
35.5	748.8	124.9	826.9	449.1	354.3	1.18	1.10	50.1	688.4	608.1	1.20	0.74	1.14	2.28
35.0	379.6	71.3	814.4	451.8	360.9	1.16	1.12	49.4	678.7	599.5	1.20	0.75	1.12	2.25
34.0	170.9	39.0	765.1	448.5	362.8	1.09	1.12	48.0	791.2	698.9	0.97	0.64	1.31	2.62
33.0	141.3	33.6	717.6	440.6	362.8	1.02	1.12	46.6	639.9	561.9	1.12	0.78	1.06	2.11
30.0	114.5	28.0	632.2	394.1	335.5	0.90	1.04	42.3	581.8	512.4	1.09	0.77	0.96	1.92
29.0	108.7	26.6	606.5	378.8	323.4	0.86	1.00	40.9	562.4	496.7	1.08	0.76	0.93	1.86
28.0	103.2	25.3	581.5	363.4	310.7	0.83	0.96	39.5	543.0	476.8	1.07	0.76	0.90	1.79
27.0	97.9	24.0	556.9	347.9	297.6	0.79	0.92	38.1	523.6	461.2	1.06	0.75	0.87	1.73
26.0	92.8	22.8	533.2	332.4	283.9	0.76	0.88	36.7	504.2	445.4	1.06	0.75	0.83	1.67
24.0	82.8	20.3	486.5	301.1	255.6	0.69	0.79	33.8	465.4	410.0	1.05	0.73	0.77	1.54
22.0	72.6	17.7	438.9	270.2	227.8	0.62	0.71	31.0	426.6	376.9	1.03	0.72	0.71	1.41
15.0	36.2	8.7	262.5	168.4	136.6	0.37	0.42	21.1	256.2	290.9	1.02	0.58	0.42	1.09

Figure J.5: Numerical calculation results of interior beam for various loading.

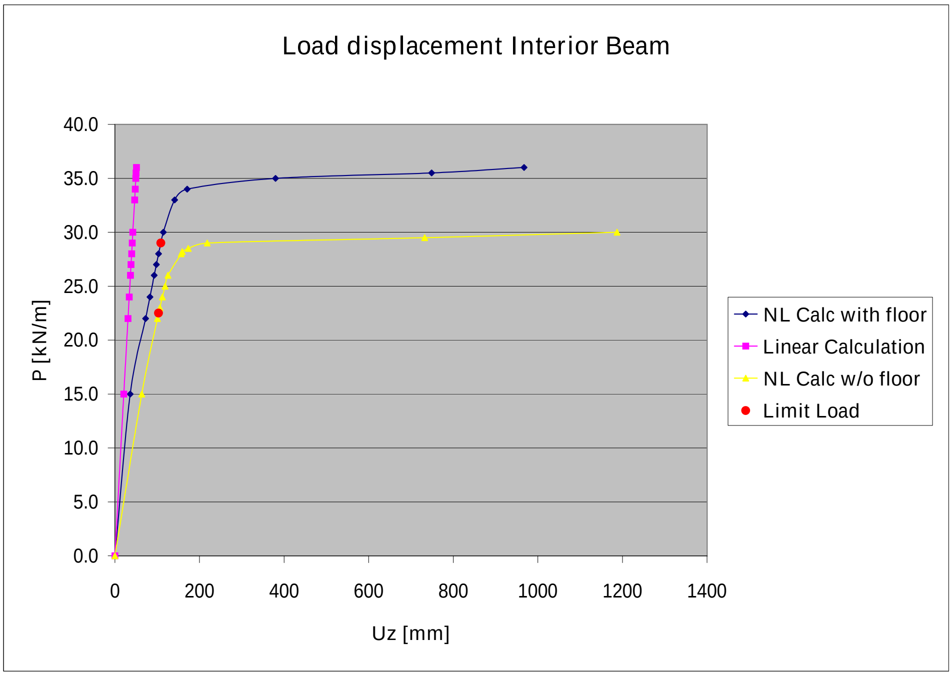

Figure J.6: Load-displacement diagram of interior beam for linear calculation, non-linear calculation without floor action taken into account and non-linear calculation with floor action taken into account.

Interior Beam without floor					
Load [kN/m]	d_x [m]	σ_{cc} [MPa]	ϵ_{cc} $[\cdot 10^{-4}]$	σ_{rt} [MPa]	ϵ_{rt} $[\cdot 10^{-4}]$
22.0	14.4	-35.0	-31.9	559.9	324.6
Interior Beam with floor					
Load [kN/m]	d_x [m]	σ_{cc} [MPa]	ϵ_{cc} $[\cdot 10^{-4}]$	σ_{rt} [MPa]	ϵ_{rt} $[\cdot 10^{-4}]$
29.0	14.4	-35.0	-31.7	322.4	559.5

d_x is position on beam
ϵ_{cc} is concrete compressive strain $\quad$ ϵ_{rt} is reinforcement tensile strain
σ_{cc} is concrete compressive stress $\quad$ σ_{rt} is reinforcement tensile stress

Table J.2: Stresses and strains in the critical cross-section at ultimate load.(See also Figures J.13 and J.14)

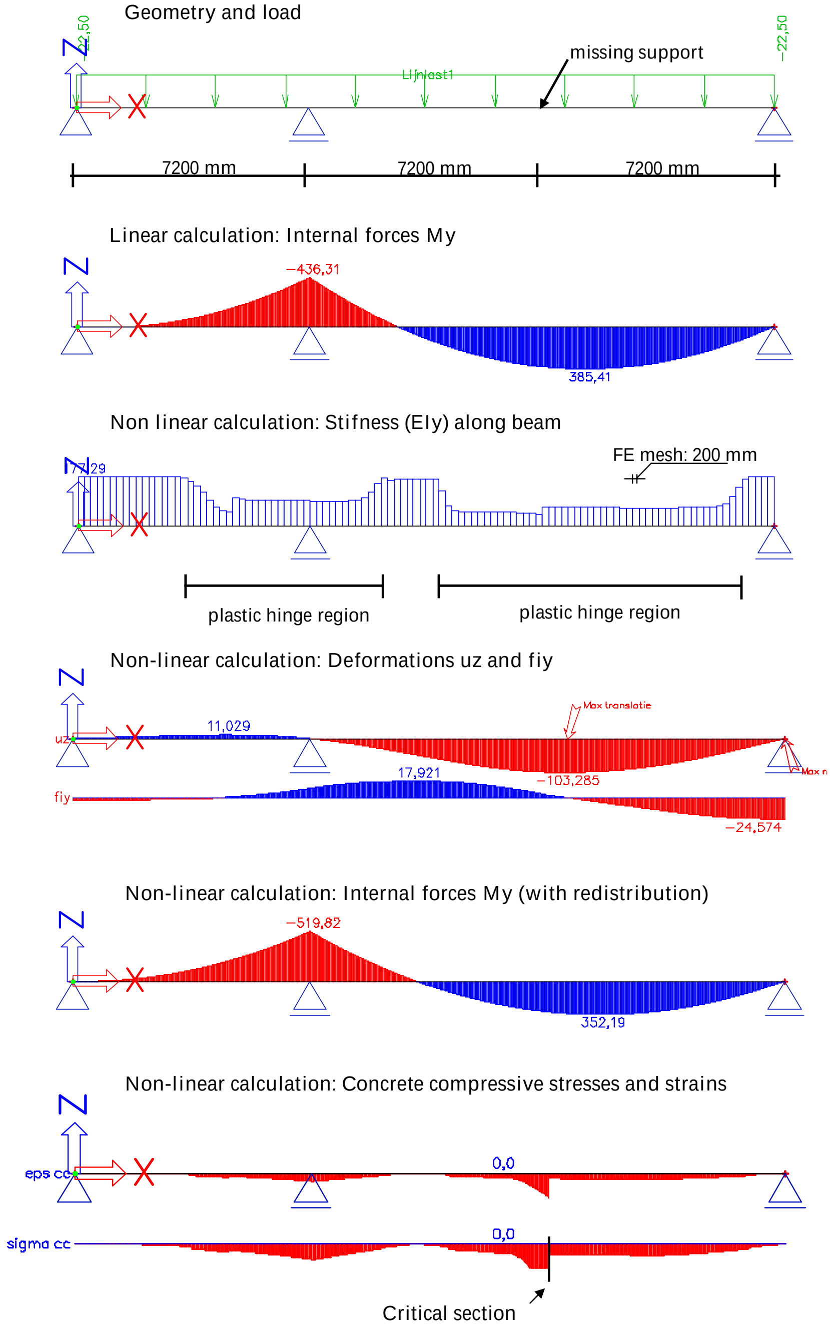

Figure J.7: Graphical representation of results for the limit load case of the interior beam without floor.

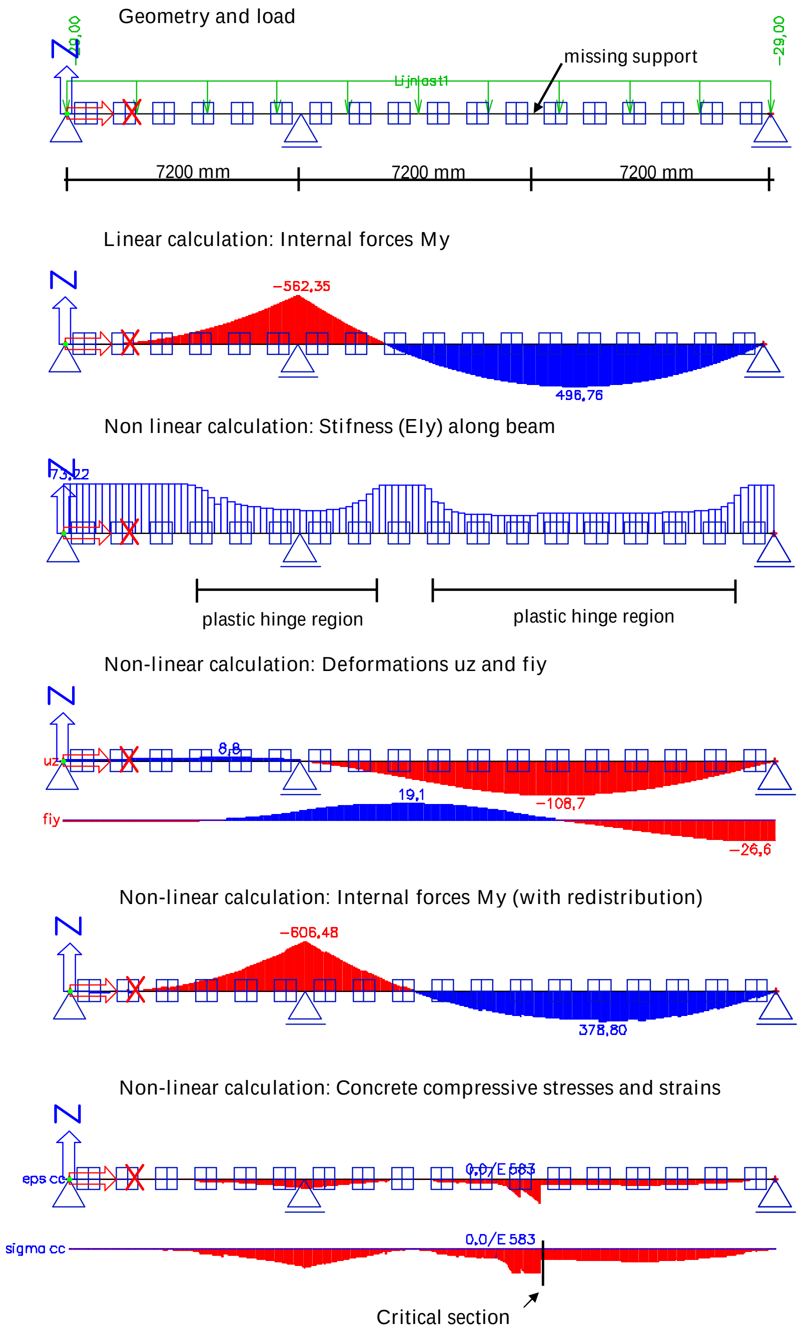

Figure J.8: Graphical representation of results for the limit load case of the interior beam with floor.

J.4 Results Corner Beams

Corner Beams w/o floor			Mu FNL:		323.0	135.0					Mu Lin:	266.5	123.1
Load:	FNL Calculation:				Md/Mu FNL		Linear Calculation:			Md FNL/Md lin		Md lin/Mu lin	
P	Uz	Fi	Md longs	Md shorts	longs	shorts	Uz lin	Md longs	Md shorts	longs	shorts	longs	shorts
[kN/m]	[mm]	[mrad]	[kNm]	[kNm]	[-]	[-]	[mm]	[kNm]	[kNm]	[-]	[-]	[-]	[-]
21.0	244.7	49.7	312.6	166.3	0.97	1.23	23.0	252.2	218.3	1.24	0.76	0.95	1.77
20.0	166.1	33.3	277.7	176.3	0.86	1.31	21.9	240.2	207.9	1.16	0.85	0.90	1.69
19.0	142.8	28.2	291.9	144.2	0.90	1.07	20.8	228.2	197.5	1.28	0.73	0.86	1.60
18.5	138.3	26.6	297.5	129.6	0.92	0.96	20.3	222.2	192.3	1.34	0.67	0.83	1.56
18.0	114.3	21.9	276.7	135.5	0.86	1.00	19.7	216.2	187.1	1.28	0.72	0.81	1.52
17.0	100.5	19.0	255.6	132.7	0.79	0.98	18.6	204.2	176.7	1.25	0.75	0.77	1.44
16.5	94.0	17.7	244.8	131.5	0.76	0.97	18.1	198.2	171.5	1.24	0.77	0.74	1.39
16.0	88.1	16.5	235.2	129.5	0.73	0.96	17.5	192.2	166.3	1.22	0.78	0.72	1.35
15.0	76.9	14.4	217.1	124.2	0.67	0.92	16.4	180.1	155.9	1.21	0.80	0.68	1.27
14.5	73.9	13.8	208.9	121.0	0.65	0.90	15.9	174.1	150.7	1.20	0.80	0.65	1.22
14.0	68.3	12.7	200.3	118.0	0.62	0.87	15.3	168.1	145.5	1.19	0.81	0.63	1.18
13.5	62.7	11.7	191.9	114.9	0.59	0.85	14.8	162.1	140.3	1.18	0.82	0.61	1.14
13.0	56.9	10.6	183.3	111.9	0.57	0.83	14.2	156.1	135.1	1.17	0.83	0.59	1.10
10.5	17.4	3.6	127.0	108.3	0.39	0.80	11.5	126.1	109.1	1.01	0.99	0.47	0.89
10.0	10.9	2.3	120.1	103.9	0.37	0.77	10.9	120.9	103.9	0.99	1.00	0.45	0.84

Corner Beams with floor			Mu FNL:		323.0	135.1					Mu Lin:	266.5	123.1
Load:	FNL Calculation:				Md/Mu FNL		Linear Calculation:			Md FNL/Md lin		Md lin/Mu lin	
P	Uz	Fi	Md longs	Md shorts	longs	shorts	Uz lin	Md longs	Md shorts	longs	shorts	longs	shorts
[kN/m]	[mm]	[mrad]	[kNm]	[kNm]	[-]	[-]	[mm]	[kNm]	[kNm]	[-]	[-]	[-]	[-]
25.0	255.5	50.9	331.1	175.8	1.03	1.30	27.4	300.2	259.8	1.10	0.68	1.13	2.11
24.0	233.9	48.7	284.1	197.4	0.88	1.46	26.3	288.2	249.4	0.99	0.79	1.08	2.03
23.0	130.2	26.0	298.9	164.5	0.93	1.22	25.2	276.2	239.0	1.08	0.69	1.04	1.94
22.5	140.6	28.6	337.7	121.4	1.05	0.90	24.6	270.2	233.8	1.25	0.52	1.01	1.90
22.0	134.3	26.3	308.4	136.2	0.95	1.01	24.1	264.2	228.6	1.17	0.60	0.99	1.86
21.5	132.8	25.7	298.8	134.7	0.93	1.00	23.5	258.2	223.4	1.16	0.60	0.97	1.82
21.0	110.8	21.2	285.5	134.7	0.88	1.00	23.0	252.2	218.3	1.13	0.62	0.95	1.77
20.5	103.8	19.7	275.7	132.8	0.85	0.98	22.4	246.2	213.1	1.12	0.62	0.92	1.73
19.5	90.6	17.1	255.4	129.5	0.79	0.96	21.3	234.2	202.7	1.09	0.64	0.88	1.65
19.0	85.1	16.0	246.0	127.1	0.76	0.94	20.80	228.2	197.5	1.08	0.64	0.86	1.60
18.5	79.9	15.0	236.9	124.6	0.73	0.92	20.30	222.2	192.3	1.07	0.65	0.83	1.56
18.0	74.7	14.0	228.1	121.8	0.71	0.90	19.70	216.2	187.1	1.06	0.65	0.81	1.52
17.5	69.6	13.0	219.3	119.0	0.68	0.88	19.20	210.2	181.9	1.04	0.65	0.79	1.48
17.0	66.6	12.4	211.0	115.8	0.65	0.86	18.60	204.2	176.7	1.03	0.66	0.77	1.44
16.0	53.1	10.4	193.0	110.4	0.60	0.82	17.50	192.2	166.3	1.00	0.66	0.72	1.35
15.0	46.8	8.7	174.9	105.3	0.54	0.78	16.40	180.1	155.9	0.97	0.68	0.68	1.27
13.5	17.1	3.6	137.1	107.4	0.42	0.80	14.80	162.1	140.3	0.85	0.77	0.61	1.14
12.0	14.2	3.0	122.4	92.5	0.38	0.69	13.10	144.1	124.7	0.85	0.74	0.54	1.01
7.5	8.5	1.8	79.0	56.6	0.24	0.42	8.20	90.1	77.9	0.88	0.73	0.34	0.63

Figure J.9: Numerical calculation results of corner beams for various loading.

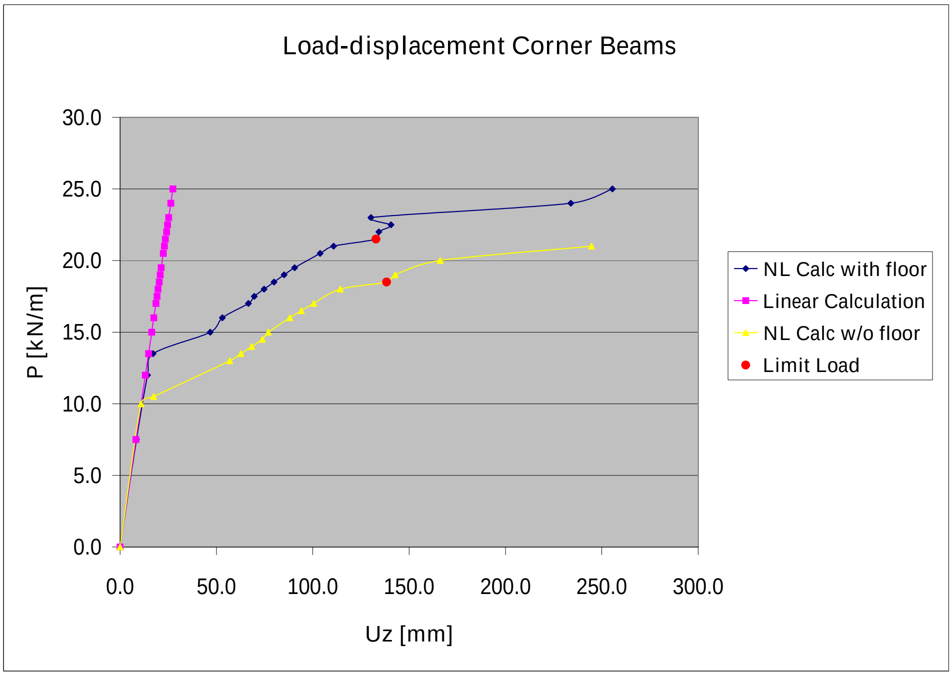

Figure J.10: Load-displacement diagram of corner beams for linear calculation, non-linear calculation without floor action taken into account and non-linear calculation with floor action taken into account.

Corner Beam without floor (short side)					
Load [kN/m]	d_x [m]	σ_{cc} [MPa]	ϵ_{cc} [$\cdot 10^{-4}$]	σ_{rt} [MPa]	ϵ_{rt} [$\cdot 10^{-4}$]
18.5	5.8	-28.5	-14.3	521.5	132.4
Corner Beam with floor (short side)					
Load [kN/m]	d_x [m]	σ_{cc} [MPa]	ϵ_{cc} [$\cdot 10^{-4}$]	σ_{rt} [MPa]	ϵ_{rt} [$\cdot 10^{-4}$]
21.5	5.8	-35.8	-18.8	538.8	218.8

d_x is position on beam
ϵ_{cc} is concrete compressive strain ϵ_{rt} is reinforcement tensile strain
σ_{cc} is concrete compressive stress σ_{rt} is reinforcement tensile stress

Table J.3: Stresses and strains in the critical cross-section at ultimate load. (See also Figures J.13 and J.14)

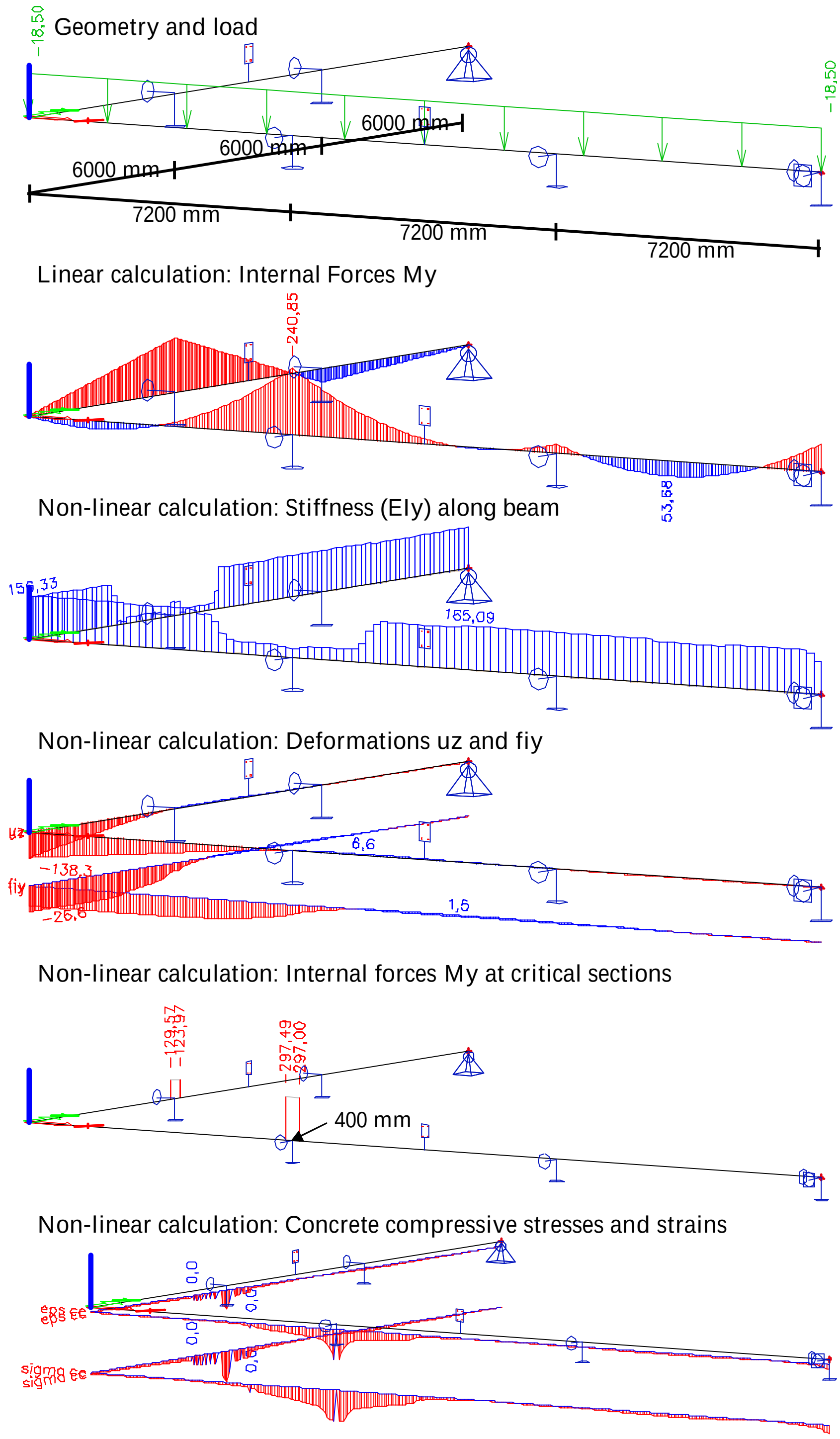

Figure J.11: Graphical representation of results for the limit load case of the corner beams without floor.

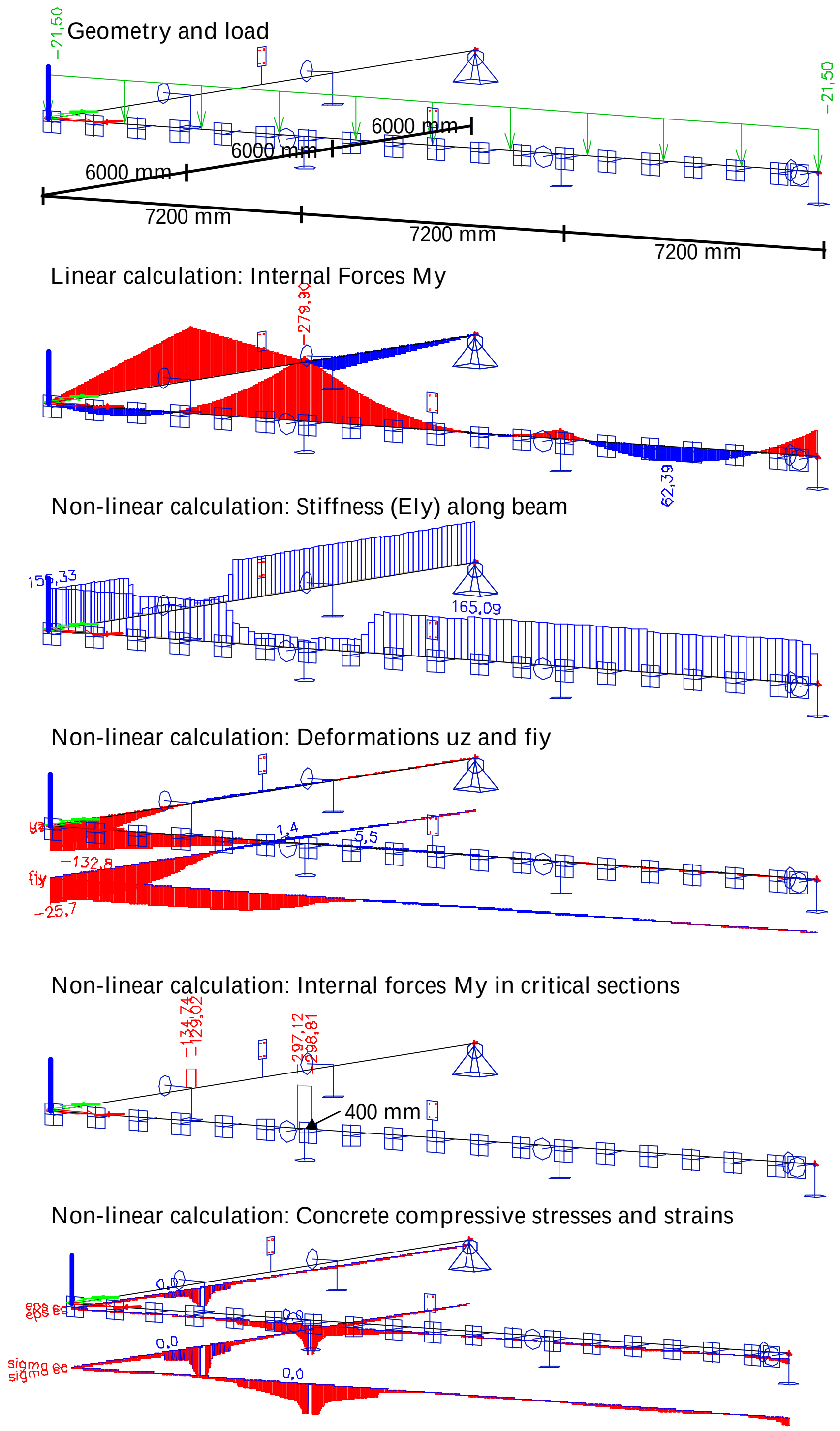

Figure J.12: Graphical representation of results for the limit load case of the corner beams with floor.

J.5 Stresses and Strains in Cross-Sections

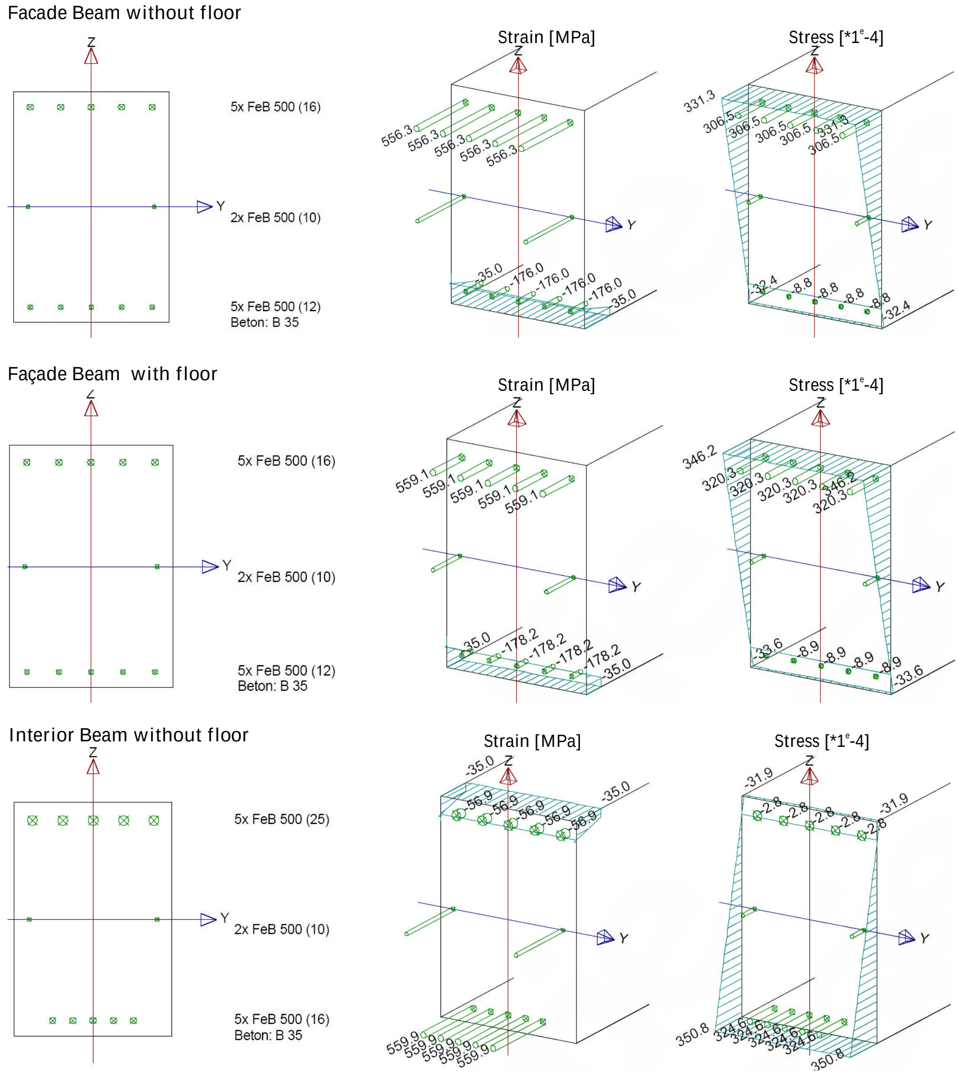

Figure J.13: Graphical representation of stresses and strains in the critical cross-sections for ultimate limit load.

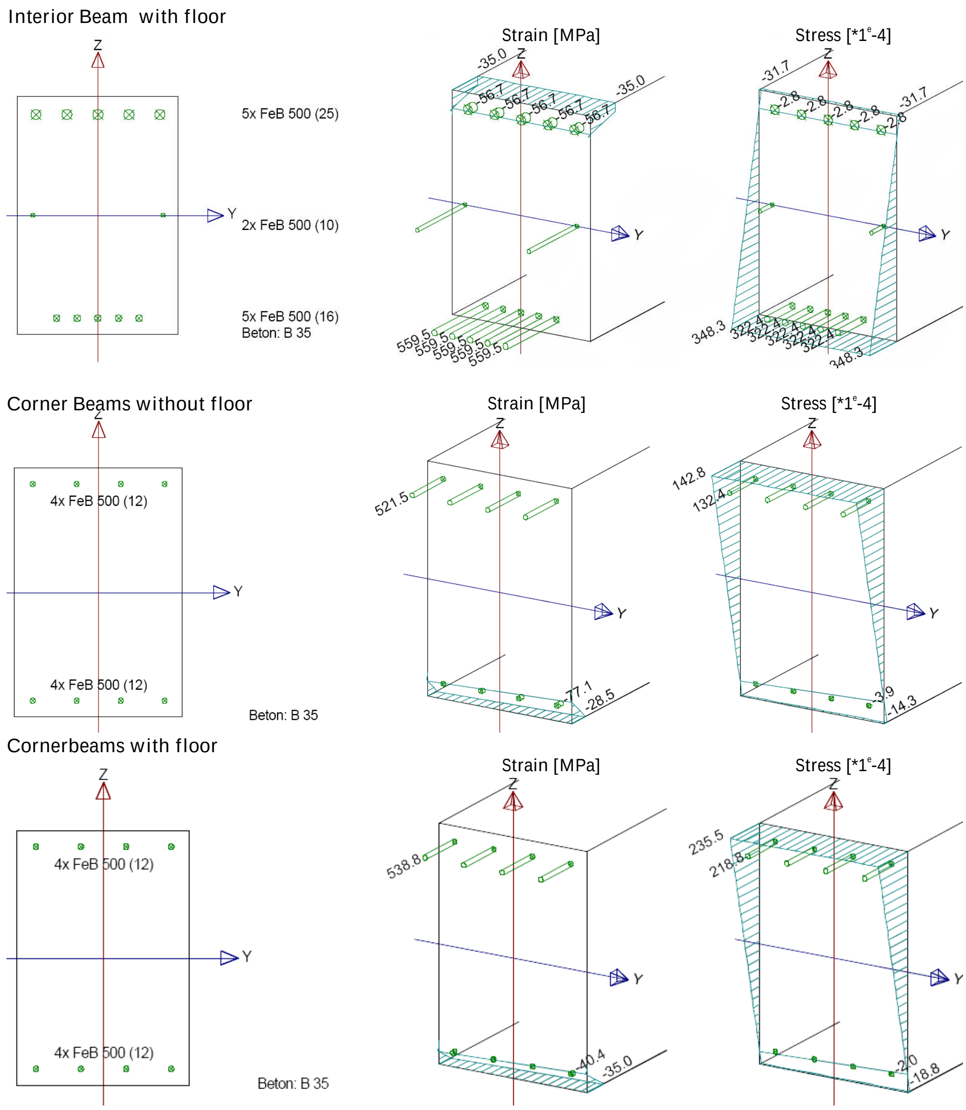

Figure J.14: Graphical representation of stresses and strains in the critical cross-sections for ultimate limit load.

Appendix K

Extended Models

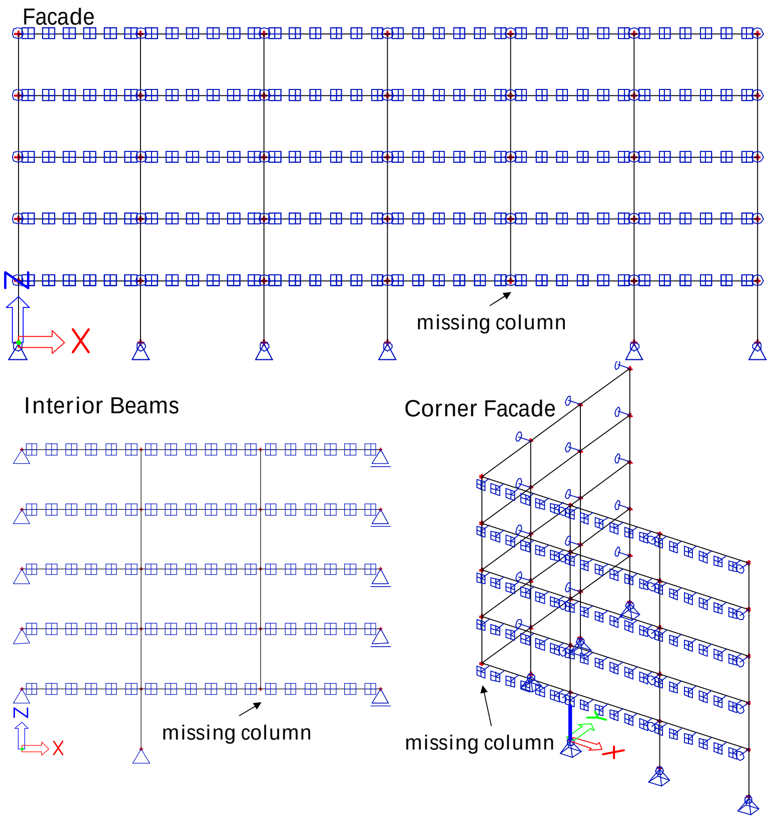

Figure K.1: Extended models for facade beams, interior beams and corner of the building.

Appendix L

Acceptance Criteria FEMA 356

Table 6-7 Modeling Parameters and Numerical Acceptance Criteria for Nonlinear Procedures—Reinforced Concrete Beams

Conditions			Modeling Parameters[3]			Acceptance Criteria[3]				
						Plastic Rotation Angle, radians				
						Performance Level				
							Component Type			
			Plastic Rotation Angle, radians		Residual Strength Ratio		Primary		Secondary	
			a	b	c	IO	LS	CP	LS	CP
i. Beams controlled by flexure[1]										
$\frac{\rho - \rho'}{\rho_{bal}}$	Trans. Reinf.[2]	$\frac{V}{b_w d \sqrt{f'_c}}$								
≤ 0.0	C	≤ 3	0.025	0.05	0.2	0.010	0.02	0.025	0.02	0.05
≤ 0.0	C	≥ 6	0.02	0.04	0.2	0.005	0.01	0.02	0.02	0.04
≥ 0.5	C	≤ 3	0.02	0.03	0.2	0.005	0.01	0.02	0.02	0.03
≥ 0.5	C	≥ 6	0.015	0.02	0.2	0.005	0.005	0.015	0.015	0.02
≤ 0.0	NC	≤ 3	0.02	0.03	0.2	0.005	0.01	0.02	0.02	0.03
≤ 0.0	NC	≥ 6	0.01	0.015	0.2	0.0015	0.005	0.01	0.01	0.015
≥ 0.5	NC	≤ 3	0.01	0.015	0.2	0.005	0.01	0.01	0.01	0.015
≥ 0.5	NC	≥ 6	0.005	0.01	0.2	0.0015	0.005	0.005	0.005	0.01
ii. Beams controlled by shear[1]										
Stirrup spacing ≤ d/2			0.0030	0.02	0.2	0.0015	0.0020	0.0030	0.01	0.02
Stirrup spacing > d/2			0.0030	0.01	0.2	0.0015	0.0020	0.0030	0.005	0.01
iii. Beams controlled by inadequate development or splicing along the span[1]										
Stirrup spacing ≤ d/2			0.0030	0.02	0.0	0.0015	0.0020	0.0030	0.01	0.02
Stirrup spacing > d/2			0.0030	0.01	0.0	0.0015	0.0020	0.0030	0.005	0.01
iv. Beams controlled by inadequate embedment into beam-column joint[1]										
			0.015	0.03	0.2	0.01	0.01	0.015	0.02	0.03

Figure L.1: Deformation Limits for Reinforced Concrete Beams as presented in FEMA 356 (p. 6-21). (source: [FEMA & ASCE, 2000])

Notes:

IO = Immediate Occupancy Performance

LS = Life Safety Performance

CP = Collapse Prevention Performance

1. When more than one of the conditions i, ii, iii, and iv occurs for a given component, use the minimum appropriate numerical value from the table.

2. 'C' and 'NC' are abbreviations for conforming and nonconforming transverse reinforcement. A component is conforming if, within the flexural plastic hinge region, hoops are spaced at $\leq$ d/3, and if, for components of moderate and high ductility demand, the strength provided by the hoops (Vs) is at least three-fourth of the design shear. Otherwise, the component is considered nonconforming.

3.Linear interpolation between values listed in the table shall be permitted.

Table 6-11 Numerical Acceptance Criteria for Linear Procedures—Reinforced Concrete Beams

Conditions			m-factors[3]				
			Performance Level				
				Component Type			
				Primary		Secondary	
			IO	LS	CP	LS	CP
i. Beams controlled by flexure[1]							
$\frac{\rho - \rho'}{\rho_{bal}}$	Trans. Reinf.[2]	$\frac{V}{b_w d \sqrt{f_c'}}$					
≤ 0.0	C	≤ 3	3	6	7	6	10
≤ 0.0	C	≥ 6	2	3	4	3	5
≥ 0.5	C	≤ 3	2	3	4	3	5
≥ 0.5	C	≥ 6	2	2	3	2	4
≤ 0.0	NC	≤ 3	2	3	4	3	5
≤ 0.0	NC	≥ 6	1.25	2	3	2	4
≥ 0.5	NC	≤ 3	2	3	3	3	4
≥ 0.5	NC	≥ 6	1.25	2	2	2	3
ii. Beams controlled by shear[1]							
Stirrup spacing ≤ d/2			1.25	1.5	1.75	3	4
Stirrup spacing > d/2			1.25	1.5	1.75	2	3
iii. Beams controlled by inadequate development or splicing along the span[1]							
Stirrup spacing ≤ d/2			1.25	1.5	1.75	3	4
Stirrup spacing > d/2			1.25	1.5	1.75	2	3
iv. Beams controlled by inadequate embedment into beam-column joint[1]							
			2	2	3	3	4

Figure L.2: Modification factors for Reinforced Concrete Beams as presented in FEMA 356 (p. 6-26). (source: [FEMA & ASCE, 2000])
Notes:
IO = Immediate Occupancy Performance
LS = Life Safety Performance
CP = Collapse Prevention Performance
1. When more than one of the conditions i, ii, iii, and iv occurs for a given component, use the minimum appropriate numerical value from the table.
2. 'C' and 'NC' are abbreviations for conforming and nonconforming transverse reinforcement. A component is conforming if, within the flexural plastic hinge region, hoops are spaced at $\leq d/3$, and if, for components of moderate and high ductility demand, the strength provided by the hoops (Vs) is at least three-fourth of the design shear. Otherwise, the component is considered nonconforming.
3.Linear interpolation between values listed in the table shall be permitted.

Appendix M

Acceptance Criteria GSA/UFC

Table 2.1. Acceptance criteria for nonlinear analysis[1].

COMPONENT	DUCTILITY (μ)[3]	ROTATION Degrees (θ)[4]	ROTATION %Radians (θ)[4]
Reinforced Concrete (R/C) Beam[5]		6	10.5
R/C One-way Slabs w/o tension membrane[5]		6	10.5
R/C One-way Slabs w/ tension membrane[5]		12	21
R/C Two-way slabs w/o tension membrane[5]		6	10.5
R/C Two-way Slabs w/ tension membrane[5]		12	21
R/C Columns (tension controls)[5]		6	10.5
R/C Columns (compression controls)	1		
R/C Frames		2	3.5
Prestressed Beams	2		
Steel Beams	20	12	21

1. COTR approval must be obtained for the use of updated tables.
2. Ductility is defined as the ratio of ultimate deflection to elastic deflection (Xu/Xe).
3. Rotation for members or frames can be determined using Figures 2.2 and 2.3 provided below.
4. Concrete having more than 2-degrees rotation must include shear stirrups per requirements of DAHSCWE Manual (See Reference 3, Page 6-1).
5. Proprietary connections must have documented test results justifying the use of higher rotational limits.

Figure M.1: Deformation limits for RC structures from GSA Guidelines (partial). (source: [GSA, 2003])

Table 4-4 Deformation Limits for Reinforced Concrete

Component	AP for Low LOP		AP for Medium and High LOP	
	Ductility (μ)	Rotation, Degrees (θ)	Ductility (μ)	Rotation, Degrees (θ)
Slab and Beam Without Tension Membrane[A]				
Single-Reinforced or Double-Reinforced w/o Shear Reinforcing[B]	-	3	-	2
Double-Reinforced w/ Shear Reinforcing[C]	-	6	-	4
Slab and Beam With Tension Membrane[A]				
Normal Proportions (L/h ≥ 5)	-	20	-	12
Deep Proportions (L/h < 5)	-	12	-	8
Compression Members				
Walls and Seismic Columns[D,E]	3	-	2	-
Non-Seismic Columns[E]	1	-	0.9	-

[A] Requirements for developing tension membrane response are provided in Park and Gamble 1999 and UFC 3-340-01; the tension membrane effect is an extension of the yield line theory of slabs and it increases the ultimate resistance. It cannot be developed when the slab has a free edge.
[B] Single-reinforced members have flexural bars in one face or mid-depth only. Double-reinforced members have flexural reinforcing in both faces.
[C] Stirrups or ties meeting ACI 318-02 minimums must enclose the flexural bars in both faces, otherwise use the response limits for Double-Reinforced w/o shear reinforcing.
[D] Seismic columns have ties or spirals in accordance with ACI 318-02 Chapter 21 seismic design provisions for special moment frames.
[E] Ductility of compression members is the ratio of total axial shortening to axial shortening at the elastic limit.

Figure M.2: Deformation limits for RC structures from UFC Guidelines. (source: [DoD, 2001])

Bibliography

ASCE, American Society of Civil Engineers. 2002. *ANSI A58.1-1982: Minimum Design Loads in Buildings and Other Structures*.

Bigaj, A.J. 1999. *Structural Dependence of Rotation Capacity of Plastic Hinges in RC Beams and Slabs*. Ph.D. thesis, Delft University of Technology, http://www.darenet.nl.

Booth, E., & Key, D. 2006. *Earthquake Design Practice for Buildings*. 2nd edn. Thomas Telford.

CEN, European Committee for Standardization. 2005a (September). *prEN 1991-1-7: Eurocode 1 - Actions on structures - Part 1-7: General actions - Accidental actions*. Final Draft.

CEN, European Committee for Standardization. 2005b (September). *prEN 1991-1-7: Eurocode 1 - Actions on structures - Part 1-7: General actions - Accidental actions*. Annex A.

Cesare, M.A., & Sues, R.H. 1999. ProFES Probabilistic Finite Element System – Bringing Probabilistic Mechanics To The Desktop. http://www.profes.com.

Coenders, J.L., & Wagemans, L.A.G. 2005. *Proposal for a Quick Building Assessment Tool for Progressive Collapse*.

Corley, W.G. 2002. *Applicability of Seismic Design in Mitigating Progressive Collapse*. Tech. rept. NIBS Multi-hazard Mitigation Council. National Workshop on Prevention of Progressive Collapse.

CUR. 1988. *Ontwerp en Betrouwbaarheid van Demontabele Betonconstructies*. Tech. rept. 88-1. Civieltechnisch Centrum Uitvoering Research en Regelgeving Gouda.

DoD, U.S. Department of Defense. 2001. *Interim Antiterrorism/Force Protection Construction Standards, Guidance on Structural Requirements*. Draft.

DoD, U.S. Department of Defense. 2005 (January). *UFC 4-023-03: Design of Buildings to Resist Progressive Collapse*. https://pdc.usace.army.mil/library/ufc.

Dusenberry, D.O. 2002. *Review of Existing Guidelines and Provisions Related to Progressive Collapse*. Tech. rept. NIBS Multi-hazard Mitigation Council. National Workshop on Prevention of Progressive Collapse.

Ellingwood, B.R. 2002. *Load and Resistance Factor Criteria for Progressive Collapse Design*. Tech. rept. NIBS Multi-hazard Mitigation Council. National Workshop on Prevention of Progressive Collapse.

Engström, B. 1992. *Ductility of Tie Connections in Precast Structures*. Ph.D. thesis, Chalmers University of Technology, Göteborg, Sweden.

FEMA, U.S. Federal Emergency Management Agency. 2000a. *FEMA-350: Recommended Seismic Design Criteria for New Steel Moment-Frame Buildings*. http://www.fema.gov.

FEMA, U.S. Federal Emergency Management Agency. 2000b (September). *FEMA-355D: State of the Art Report on Connection Performance*. http://www.nehrp.gov.

FEMA, U.S. Federal Emergency Management Agency, & ASCE, American Society of Civil Engineers. 2000. *FEMA 356: Prestandard and Commentary for the Seismic Rehabilitation of Buildings*. http://www.nehrp.gov/info/PDF/FEMA356/FEMA356.pdf.

FIP, Commision on Prefabrication. 1988. *Precast Prestressed Hollow Core Floors*. FIP-Recommendations. Thomas Telford.

Gilmour, J.R., & Virdi, K.S. 1998. *Numerical Modelling of the Progressive Collapse of Framed Structures as a Result of Impact or Explosion*. 2nd Int. PhD Symposium in Civil Engineering 1998 Budapest.

GSA, U.S. General Services Administration. 2003 (June). *Progressive Collapse Analysis and Design Guidelines for New Federal Office Buildings and Major Modernization Projects*. http://www.oca.gsa.gov.

Hamburger, R., & Whittaker, A. 2004. *Design of Steel Structures for Blast-Related Progressive Collapse Resistance*. Presented at the 2003 AISC and Steel Institute of New York Steel Building Symposium: Blast and Progressive Collapse Resistance (symposium proceedings), American Institute of Steel Construction.

HMSO, U.K. Statutory Instrument. 1991. *Buildings and Buildings. The Building Regulations 1991*. London.

Hoogenboom, P.C.J. 2004 (May). *Non Linear Mechanics*. lecture notes.

Krauthammer, T., Hall, R.L., Woodson, S. C., Baylot, J. T., Hayes, J. R., & Sohn, Y. 2002. *Development of Progressive Collapse Analysis Procedure and Condition Assessment for Structures*. Tech. rept. NIBS Multi-hazard Mitigation Council. National Workshop on Prevention of Progressive Collapse.

Lewis, W.J. 2003. *Tension Structures - Form and Behaviour*. Thomas Telford.

Leyendecker, E.V., & Burnett, E.F.P. 1976. *The Incidence of Abnormal Loading in Residential Buildings*. Building Science Series 89. National Bureau of Standards, Washington, D.C.

Marchand, K.A., & Alfawakhiri, F. 2005. *Facts for Steel Buildings 2: Blast and Progressive Collapse*. American Institute of Steel Construction, Inc. http://www.aisc.org.

MMC, Multihazard Mitigation Council NIBS. 2002. *Prevention of Progressive Collapse, Report on the July 2002 national workshop and recommendations for future efforts*. http://www.nibs.org/MMC.

NNI, Dutch Normalisation Institute. 1991. *NEN 6700 General Requirements for Building Structures*.

NNI, Dutch Normalisation Institute. 1995. *NEN 6720 Regulations for concrete Structural requirements and calculation methods TGB 1990*. Wijzigingsblad A3:2004.

NNI, Dutch Normalisation Institute. 2001. *NEN 6702 Technical Principles for Building Structures - TGB 1990 - Loadings and Deformations*. Wijzigingsblad A1:2005.

NRCC, National Research Council of Canada. 1998. *National Building Code of Canada 1977*.

SCIA Groep nv, Herk de Stad, Belgium. 2006. *SCIA.ESA PT Release 2006*. student version.

Siersma, R.C. 2006. *Progressive Collapse of Building Structures*. M.Sc. thesis, Delft University of Technology.

Starossek, U. 2006. Progressive Collapse of Structures: Nomenclature and Procedures. *Structural Engineering International*, **16**(2), 113–117.

Stufib, study cell 2. 2005. *Constructieve Samenhang van Bouwconstructies*. Draft.

VROM-Inspectie, regio Zuid. 2003. *Patio Sevilla Onderzoek naar het Instorten van Balkons, Ceramique blok 29*. Tech. rept. Dutch Ministry of Housing, Spatial Planing and the Environment.